MODELING NEURAL CREST INDUCTION, MELANOCYTE SPECIFICATION AND DISEASE-RELATED PIGMENTATION DEFECTS IN hESCS AND PATIENT-SPECIFIC iPSCS

by

Yvonne Gruber Mica

A Dissertation

Presented to the Faculty of the Louis V. Gerstner, Jr.

Graduate School of Biomedical Sciences,

Memorial Sloan-Kettering Cancer Center

in Partial Fulfillment of the Requirements for the Degree of

Doctor of Philosophy

New York, NY

May, 2013

_____ _____

Lorenz Studer, MD Date

Dissertation Mentor

DEDICATION

To my mother, who inspired me.

To my father, who gave me strength.

And to my husband, who stands by me.

ABSTRACT

Melanocytes are pigment-producing cells of neural crest origin responsible for protecting the skin against UV-irradiation. Melanocyte dysfunction leads to pigmentation defects including albinism, vitiligo, and piebaldism and is a key feature of systemic pathologies such as Hermansky-Pudlak (**HP**) and Chediak-Higashi (**CH**) Syndromes. Yet, while the developmental biology of melanocytes has been well studied in avian and murine models, the processes underlying melanocyte development in the human system remain poorly understood. We hypothesized that basic developmental insights could be applied to model progressive and selective specification of human pluripotent cell lines along the melanocytic lineage through a neural crest intermediate.

Here we report that timed exposure to activators of WNT, BMP and EDN3 signaling triggers the sequential induction of neural crest and melanocyte precursor fates under dual-SMAD inhibition conditions. Using a *SOX10::GFP* hESC reporter line, we demonstrate that the temporal onset of WNT activation is particularly critical for human neural crest induction. Surprisingly, suppression of BMP signaling does not reduce neural crest yield. Subsequent differentiation of hESC-derived melanocyte precursors under defined conditions yields pure populations of pigmented cells matching the molecular and functional properties of adult melanocytes.

Pluripotent stem cell technology offers a novel approach for human disorders. As a proof-of-principle we also derive melanocytes from HP- and CH patient-specific induced pluripotent stem cells and demonstrate that our system is able to faithfully recapitulate known disease associated pigmentation defects.

BIOGRAPHICAL SKETCH

Yvonne Gruber Mica was born in Austria. Her father's work for the Austrian government took her from Russia, to the Czech Republic, to Canada and back to Austria before finally bringing her to New York in 1999. There, Yvonne attended the United Nations International School in New York, NY where she met her husband, George.

Yvonne completed her undergraduate studies at Wellesley College, from which she graduated magna cum laude with a concentration in Biological Sciences. Her first exposure to laboratory research came during the summer after her freshman year at Wellesley when she joined Dr. Dennis Smith's lab to work on a project investigating the effects of xamoterol hemifumarate on the rat lung. She continued her work in the Smith lab, eventually writing an honors thesis titled "Lung Morphology in a Mouse Model of Rett Syndrome." Two seminar courses taken during her senior year, "Cancer Genomics" and "The Biology of Stem Cells," sparked Yvonne's interest in both cancer and stem cell research.

It was therefore with great enthusiasm that Yvonne returned to New York to pursue her graduate studies at the Louis V. Gerstner, Jr. Graduate School of Biomedical Sciences. In 2008 Yvonne joined Dr. Lorenz Studer's laboratory to study the generation of melanocytes from human embryonic stem cells, with the goal of one day using this system as a novel model for malignant melanoma. During the course of her study, Yvonne was awarded the Joanna M. Nicolay Melanoma Foundation Research Award.

ACKNOWLEDGEMENTS

First and foremost I would like to express my gratitude to my mentor, Dr. Lorenz Studer, who has given me the opportunity to work under his guidance and with the support of a wonderful group of talented individuals. His passion and dedication to his work have been an inspiration and I cannot express enough my appreciation for the experiences I have made under his wing.

I would like to thank my thesis committee Dr. Michel Sadelain and Dr. Neal Rosen for their insights and encouragement during my graduate work. I would also like to thank Dr. Anna-Katerina Hadjantonakis for serving as my thesis defense chairperson and Dr. Richard White for joining my defense committee.

I would also like to acknowledge Dr. Jan Hendrkx of the SKI Flow Cytometry Core, Dr. Agnes Viale of the SKI Genomics Core, Dr. Katia Manova-Todorova of the SKI Molecular Cytology Core, the Rockefeller University Electron Microscopy Center and their staff for their excellent technical support. I also owe a sincere and earnest gratitude to the Joanna M. Nicolay Melanoma Foundation for their recognition and generous financial support of my work.

Without Dr. Ken Marians there would be no Gerstner Sloan-Kettering Graduate School and I am grateful for the tireless efforts of Dr. Marians and all the members of GSK who keep the graduate program running smoothly. In particular I would like to thank Maria Torres, without whom I would quite literally not be here due to a visa mishap that almost left me stranded in Prague. Also, Iwona Abramek who was my guiding light during the

preparation of this thesis and who responded to my questions at all hours of the day and night.

Dr. Mark Tomishima is the person who has most impacted my graduate career, in ways that are too numerous to fully list here. From first recruiting me to the lab, to providing me with a space to work, to supporting me with patient guidance and advice. I wouldn't be here without him.

I am also deeply indebted to Dr. Gabsang Lee, without whose expertise the neural crest would still be a great mystery and who has been a role model for what mentorship in science can and should be. My thanks also go to Dr. Stuart Chambers who served as my voice of reason and who taught me to never bet on an experiment unless I already knew the outcome. Dr. Jason Tchieu brought fresh eyes and infinite patience to my project and I am thankful for that.

To the ladies in the lab, Liz, Justine, Inna, and Sarah: without their company and humor late nights in lab would not have been the same. To them and the other members of the Studer Lab, both past and present, I say: they are my inspiration!

Many thanks to Nick Gauthier, a fellow Gerstner graduate student, who has been a dear friend and lent a patient ear throughout our graduate careers.

Lastly, I would like to thank my family and friends for their continued encouragement. This dissertation would not have been possible without the patience and unwavering love of my husband, George Mica, who has supported me at every step throughout

these last six years. I also thank his parents, George and Alena Mica, who welcomed me into their family twelve years ago and who have given me a home away from home.

I would also like to acknowledge the role my sister, Sandra Steininger, has played in shaping who I am today and for teaching me perseverance. And finally, I am infinitely grateful to my parents, Johann and Helga Gruber, for their love and support and for instilling in me the belief that I could do anything I set my mind to.

TABLE OF CONTENTS

LIST OF TABLES

LIST OF FIGURES

LIST OF ABBREVIATIONS

α-MSH: α-melanocyte-stimulating hormone

ACTH: Adrenocorticotropic hormone

AP: Anterior-posterior

BE: BMP4-Endothelin 3 (A promelanocytic differentiation condition)

BMP: Bone morphogenetic protein

cAMP: cyclic adenosine monophosphate

CHS: Chediak-Higashi Syndrome

CNS: Central nervous system

CREB: cAMP responsive-element-binding protein

DSi: Dual SMAD inhibitioni

EB: Embryoid body

EDN: Endothelin

EDNRB: Endothelin receptor B

EMT: Epithelial-to-mesenchymal transition

ESCs: Embryonic stem cells

FD: Familial Dysautonomia

FGF: Fibroblast growth factor

GFP: Green fluorescent protein

hESCs: Human embryonic stem cells

HPS: Hermansky-Pudlak Syndrome

iPSCs: Induced pluripotent stem cells

LRO: Lysosome-related organelle

mESCs: Mouse embryonic stem cells

MC1R: Melanocortin-1 receptor

MITF: Microphthalmia-associated transcription factor

MSA: Migration staging area

MSC: Melanocyte stem cell

NC: Neural crest

NCSC: Neural crest stem cell

OCA: Oculocutaneous albinism

PNS: Peripheral nervous system

PSCs: Pluripotent stem cells

RPE: Retinal pigment epithelium

SCF: Steel factor or stem cell factor

SCNT: Somatic cell nuclear transfer

TS: Tietz Syndrome

Tyrp1: Tyrosinase-related protein 1

UVR: Ultraviolet radiation

WS: Waardenburg Syndrome

CHAPTER ONE

Introduction

Human Embryonic Stem Cells

Definition, Characteristics, Derivation

Embryonic stem cells (ESCs) are a unique population of cells derived from the inner cell mass of the blastocyst. ESCs are characterized by their ability to self-renew and by their pluripotency. Self-renewal is the capacity of ESCs to be propagated in their undifferentiated state. ESCs can however also give rise to the different specialized cell types of the embryo through a series of increasingly fate-restricted epigenetic events, in a process known as differentiation. The ability of ESCs to differentiate into any cell type of the embryo is known as pluripotency.

Experimentally, the pluripotency of ESCs can be assayed by demonstrating differentiation into all three germ layers of the embryo (ectoderm, mesoderm, and endoderm). This can be achieved through embryoid body formation, in which cells are grown in a non-adherent spherical structure that supports the spontaneous differentiation into different lineages (Itskovitz-Eldor et al., 2000). ESCs can also be spontaneously differentiated through sub-cutaneous implantation into immunocompromised mice, where they will give rise to tumors known as teratomas that contain derivatives of all three germ layers (Thomson et al., 1998). More elegantly, ESCs can be led to differentiate along specific lineages through co-culture with supporting feeder cells or exposure to signaling factors and small molecules known to support the induction of different cell fates. Universal contribution of ESCs to all tissues in the embryo and adult can be demonstrated in the mouse through chimera formation by injecting ESCs into the blastocyst cavity of the embryo (Zhao et al., 2010). The

embryos that form after subsequent transplantation into pseudopregnant mice will display integration of ESC-derived cells into all organs to varying degrees. This is most commonly visualized through mosaic-patterning of coat color or green fluorescent protein (GFP) expression by ESC progeny. The most stringent assay for pluripotency is known as tetraploid complementation (Eakin and Hadjantonakis, 2006). In this approach, a tetraploid embryo is generated at the two cell stage through exposure to an electric current . The tetraploid embryo can develop normally to the blastocyst stage however the tetraploid cells are unable to contribute to the embryo proper and are restricted to the extraembryonic lineage (Zhao et al., 2009). When regular diploid ESCs are therefore injected into the tetraploid blastocyst, the resulting embryo will be entirely derived from the ESCs. Both the chimera formation and tetraploid complementation assays are uniquely possible in the mouse. The assessment of human ESC pluripotency is therefore generally restricted to directed differentiation and teratoma formation.

Murine ESCs were first derived in 1981 by two independent groups (Evans and Kaufman, 1981; Martin, 1981) while human ESCs (hESCs) were isolated a few years later by Jamie Thomson's group (Thomson et al., 1998). While mESCs and hESCs share many features of pluripotency, including the regulation by a pluripotency network of transcription factors including Oct4, Sox2, and Nanog, a number of differences involving their morphology and signaling requirements have also been noted. While these differences were previously thought to reflect species-specific differences, it has now been demonstrated that hESCs more closely resemble murine pluripotent stem cells isolated from the post-implantation embryo, a later embryonic stage than the inner cell mass (Brons et al., 2007; Tesar et al., 2007). A review of the differences between these different pluripotent populations can be found in (Nichols and Smith, 2009).

Using hESCs to Model Embryonic Development

Species-specific differences in the signaling requirements for lineage specification, maturation, and maintenance of different cell types have highlighted the continued need for the direct study of human development and differentiation. In the absence of other technically and ethically viable approaches, hESCs have been widely used as an experimental tool for studying early development in the human system. However, findings from the study of embryonic development in other model organisms, including Xenopus, chick, mouse, and zebrafish have informed approaches for the directed differentiation of hESCs *in vitro* and have led to testable hypotheses for the generation of cells from hESCs.

ESCs have provided an experimental platform for investigating the requirements for both signaling pathways and genetic components in a number of different lineages using multiple approaches. The defined conditions of directed differentiation protocols are highly amenable to evaluating the contribution of exogenous signaling molecules (and their antagonists) to lineage specification and maturation (Idelson et al., 2009; Kriks et al., 2011). Similarly the roles of various genes, particularly transcription factors in lineage specification have been investigated through knockdown and overexpression studies (Fasano et al., 2010). The temporal regulation of such factors has further been explored through the use of lineage-specific reporters, which in turn have also been instrumental in the optimization of induction protocols (Placantonakis et al., 2009) while lineage tracing experiments have shed light on the contribution of different populations to different lineages (Mascré et al., 2012).

These methods, along with gene expression studies using immunofluorescence, qRT-PCR, and microarray, have confirmed that in many systems the step-wise activation of

genes during directed differentiation recapitulates events observed during embryogenesis, with early genes expressing before later, more mature markers (Chambers et al., 2012b; Ganat et al., 2012; Green et al., 2003). Similarly, the derivation of various mature cell types from hESCs has been found to proceed through developmentally relevant intermediate or progenitor stages. Striking examples of this phenomenon include the sequential changes in fate potential of hESC-derived neural progenitor cells which first give rise to neurons before becoming gliogenic as they age *in vitro* (Gaspard and Vanderhaeghen, 2010) and the derivation of nociceptors which proceed through a neural crest intermediate (Chambers et al., 2012b).

However, while it is tempting to present these anecdotes as evidence that the requirements for the derivation of a given cell type from hESCs *in vitro* will faithfully recapitulate the requirements observed in the embryo, reports of experiments, particularly of transdifferentiation, highlight that it is possible to manipulate cell fates *in vitro* in ways that are not always reflective of developmental events. Findings regarding the signaling requirements of hESC differentiation to a given cell type should be validated *in vivo* whenever possible.

Using hESCs to Derive Mature Cell Types

In addition to recapitulating the progressive differentiation that occurs during embryogenesis, hESCs can be used to derive a virtually limitless pool of specialized, terminally differentiated cells. To date the cell types that have successfully been derived from hESCs include, but are not limited to, keratinocytes (Green et al., 2003), cardiomyocytes (Kehat et al., 2001; Mummery et al., 2003; Xu et al., 2002a), myoblasts (Barberi et al., 2007), neural crest (Pomp et al., 2005), neural progenitors (Elkabetz et al., 2008), neurons (including dopamine (Kriks et al., 2011), motorneurons (Li et al.,

2005), and interneurons (Maroof et al., 2010)), oligodendrocytes (Wang et al., 2013), hematopoietic precursors (Chadwick et al., 2003; Kaufman et al., 2001), melanocytes (Fang et al., 2006), nociceptors (Chambers et al., 2012b), osteogenic cells (Sottile et al., 2003), insulin producing cells (Assady et al., 2001), adipocytes (Xiong et al., 2005) hepatocytes (Rambhatla et al., 2003), trophoblast cells (Xu et al., 2002b), endothelial cells (Gerecht-Nir et al., 2003; Levenberg et al., 2002), and retinal pigment epithelium (RPE) (Idelson et al., 2009).

The properties of *in vitro* hESC-derived cell types should always be compared to their *in vivo* counterparts. The distinctive morphology of some cell types, such as the cobblestone-like organization of RPE or the inclusion of lipid droplets in the cytoplasm of adipocytes, can provide an initial, although not definitive, indication of cell type (Idelson et al., 2009; Xiong et al., 2005). Gene expression analysis, both at the single gene level with qRT-PCR and at the global level through microarray analysis, can provide further confirmation of cell type, particularly if compared with primary cells when available (Chadwick et al., 2003; Chambers et al., 2012b). The *in vivo* survival, migration, and integration into the appropriate tissue can be assayed through transplantation into embryonic or adult model organisms such as chick or mouse (Idelson et al., 2009; Kriks et al., 2011). Finally, the functionality of hESC-derived cells can be analyzed in cell type-specific manners such as electrophysiology for neurons, beating for cardiomyocytes, insulin production by pancreatic beta cells, and pigmentation for RPE and melanocytes (Assady et al., 2001; Idelson et al., 2009; Li et al., 2005; Mummery et al., 2003).

Through the application of such stringent criteria one can arrive with confidence at a cell type that closely resembles its naturally-occurring counterpart and which will be suitable

for various downstream applications such as high throughput screening and disease-modeling.

Using hESCs for Disease-Modeling

The ability to derive virtually any cell type from hESCs, provides a platform through which ES-derived cells can be used to model diseases in the disease relevant cell type. Disease modeling in hESC-derived cells offers the advantage of potentially obtaining the large numbers of relatively pure populations that are necessary for drug screening purposes and which might not be readily expandable from primary cell sources (Crook and Kobayashi, 2008). Furthermore, it is possible to derive cells from hESCs that might not otherwise be accessible, for example neural cell types. To date, disease-specific hESCs have been established for a number of different disorders including Huntington's Disorder (Niclis et al., 2009; Verlinsky et al., 2005), Fragile X Syndrome (Eiges et al., 2007; Verlinsky et al., 2005), Lesch-Nyhan disease (Urbach et al., 2004), Cystic fibrosis (Pickering et al., 2005), Duchenne and Becker muscular dystrophy, Fanconi anaemia, Marfan syndrome, and thalassaemia (Verlinsky et al., 2005). For the most part these lines have been established either as transgenic lines through methods such as homologous recombination or were derived from preimplantation genetic diagnosis (PGD) embryos that were found to carry the disease-relevant mutation. Neither of these approaches is currently readily scalable as homologous recombination in hESCs is highly inefficient (Zwaka and Thomson, 2003) (although newer tools such as zinc finger (Hockemeyer et al., 2009) and TALEN-mediated (Hockemeyer et al., 2011) recombination offer improved efficiencies) and the derivation of disease-specific PGD embryos requires the use of a scarce resource. However a novel experimental system, induced pluripotent stem cells which will be discussed in greater detail in the following

section, overcomes many of these limitations and are now widely used as an alternative to hESCs for disease-modeling purposes.

The Limitations of hESCs

Another challenge to the advancement of disease modeling using hESCs, has been the ethical controversies surrounding their derivation and use. The isolation of the inner cell mass results in the destruction of the fertilized human embryo, although a proof-of-principle report in 2006 demonstrated that hESCs can be derived from a single blastomere which in turn can be isolated without the destruction of an embryo (Klimanskaya et al., 2006). This raises a number of ethical questions, including whether or not human life is thought to begin at conception and whether a human embryo should therefore be granted the moral status of a human being. As a result, legislation regarding the use hESCs in research, and in particular the application of federal funding to such research, has undergone a number of changes in recent decades. Currently, the use of federal funding for hESC research is restricted to hESC lines listed on the NIH Human Embryonic Stem Cell Registry and cannot be applied for the derivation of novel hESC lines. However a landmark discovery, which we will explore in the following section, has drastically changed the landscape of human stem cell research and the use of hESCs in disease modeling.

Human Induced Pluripotent Stem Cells

Nuclear Reprogramming

The process of differentiation has been famously compared to a valleyed landscape (**Figure 1.1**) (Waddington, 1957). A marble (i.e. the cell) begins at the top of the hill and begins to roll down the slope. At each juncture of two valleys the marble is committed to choosing only one path (a lineage choice), which in turn will determine which

progressively more restricted choices remain open to it. At the end of its travels the marble finds itself resting at the bottom of the incline (i.e. the terminally differentiated state of a specialized cell type).

For a long time it was not understood, whether this progressive commitment of differentiation was the result of genetic events, in which the DNA associated with other lineages was gradually shed and which would make differentiation an irreversible process, other whether differentiation was in fact an epigenetic process. Half a century ago, this question was tested in a seminal paper in which the nucleus of a somatic cell was transplanted into an enucleated oocyte, in a process termed somatic cell nuclear transfer (SCNT) (Briggs and King, 1952; Gurdon, 1962). In this experiment, 10 normal tadpoles were produced following SCNT of intestinal epithelium cell nuclei into enucleated *Xenopus* oocytes, confirming not only that the genome remained intact during the process of differentiation, but also that the epigenetic changes associated with differentiation were reversible.

Subsequent studies have shown that similar changes in cell fate can be achieved by the overexpression of transcription factors. It was found that overexpression of MyoD in fibroblasts was sufficient to convert cells to a muscle cell (Davis et al., 1987) while GATA-1 causes transdifferentiation of hematopoietic lineages (Kulessa et al., 1995).

Together these studies suggested that it might be possible to reprogram a cell to an ES-like pluripotent state through the overexpression of ES cell specific transcription factors.

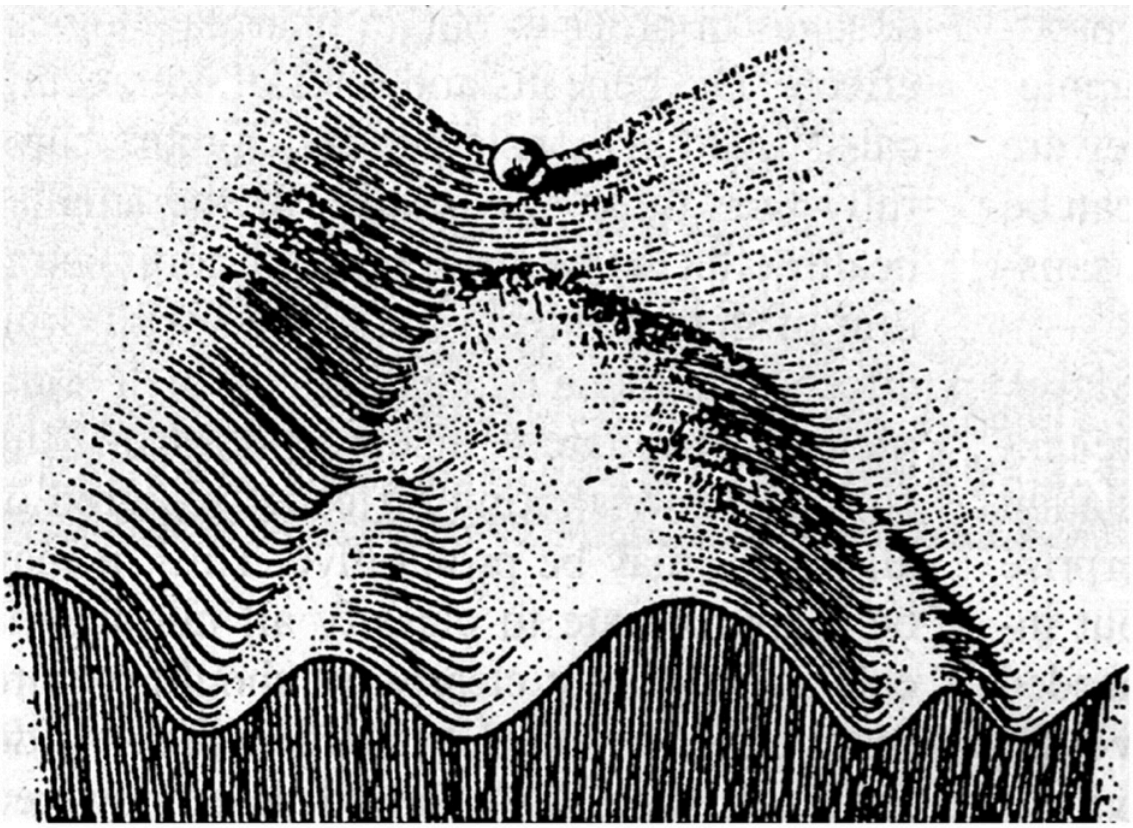

Figure 1.1. <u>Waddington's Epigenetic Landscape</u>. The fate choices of a differentiating stem cell, represented by the marble at the top of a valleyed landscape, are compared to the bifurcations in the valleys as the marble rolls down the incline. Waddington, C. H. (1957). *The strategy of the genes; a discussion of some aspects of theoretical biology.* New York: Macmillan with kind permission from Taylor and Francis.

These studies recently culminated in a landmark finding by Shinya Yamanaka in 2006 (Takahashi and Yamanaka, 2006). In an elegant demonstration Yamanka and colleagues found that four transcription factors (Oct4, Klf4, Sox2, c-Myc) were sufficient to revert a mouse fibroblast back to a pluripotent state that exhibited ES-like morphology and expression of pluripotency factors Nanog and Oct4 . He termed the resulting cells induced pluripotent stem cells (iPSCs). Subsequent refinement of the method for the derivation of iPSCs led to the establishment of germline competent iPSCs (Maherali et al., 2007; Okita et al., 2007; Wernig et al., 2007). This second generation of iPSCs, which were drug-selected based on their expression of the pluripotency markers *Oct4* or *Nanog*, exhibited gene expression and methylation patterns that were highly similar to ESCs (Maherali et al., 2007). Not long after Yamanaka's initial finding, the same cocktail of transcription factors (Lowry et al., 2008; Park et al., 2008b; Takahashi et al., 2007) as well as an alternative combination of Oct4, Sox2, Lin28, and Nanog (Yu et al., 2007) were found to support the induction of human iPSCs. Since then, there has been an explosion of iPSC-based papers, investigating not only the mechanism of iPSC induction but also demonstrating the broad range of applications for iPSCs in disease-modeling.

Using iPSCs in Disease Modeling

While iPSCs share with ESCs the ability to expand large, pure populations of a given cell of interest for disease modeling applications, iPSCs have the additional advantage of being readily derived in a desired genetic background. By establishing iPSCs directly from patient cells, one can establish model systems in any disease background, something that had been particularly problematic for polygenic disorders or diseases in which the causal mutation had not yet been identified. This approach however does require careful consideration of appropriate controls. Ideally healthy cells from a patient could be used in the case of somatic mutations while gene corrected cells could be used

to establish syngeneic controls in the case germ line mutations. Alternatively a healthy sibling or family member might minimize variability in genetic background however often, out of practical considerations, non-familial, age-matched donors are used as controls.

To date, a iPSC models for a variety of neurodegenerative diseases (Dimos et al., 2008; Lee et al., 2009; Park et al., 2008a; Soldner et al., 2009), hematopoietic disorders (Raya et al., 2009; Ye et al., 2009), metabolic conditions (Maehr et al., 2009; Park et al., 2008a; Rashid et al., 2010) and cardiovascular pathologies (Carvajal-Vergara et al., 2010; Moretti et al., 2010) have been established (for a more comprehensive review of currently published iPS disease models see (Cherry and Daley, 2012; Unternaehrer and Daley, 2011)).

However it has been surprisingly difficult to identify disease-relevant phenotypes even when the appropriate cell type is generated from patient-specific iPSCs. It is thought that the emergence of disease-related phenotypes may require exposure to stress stimuli or, in the case of age-related phenotypes, may only become apparent *in vitro* after additional aging of iPS-derived cells, which by default exhibit fetal characteristics. The first successful demonstration of disease phenotype in iPS-derived cells was achieved in our own lab when it was shown that neural crest cells established from Familial Dysautonomia (FD) patient iPSCs exhibited a tissue-specific splicing defect as well as neurogenic differentiation and migration defects associated with disease pathology (Lee et al., 2009). This experimental system was subsequently used by the authors in a high throughput screen to identify novel therapeutic targets to ameliorate the disease phenotype (Lee et al., 2012).

Beyond the application in disease modeling, iPSCs also hold great promise for future roles in cell replacement therapies, in which cell types of interest are generated from a patient's own fibroblasts, genetically corrected if necessary, and then are reintroduced back into the patient. This approach would completely eliminate any risk of immune rejection. The therapeutic utility of iPSCs in such a setting has already been demonstrated in an elegant proof-of-principle experiment in which fibroblasts from a sickle cell mouse were reprogrammed and the resulting iPSCs subjected to genetic correction of the causal mutation (Hanna et al., 2007). The corrected iPSCs were differentiated into hematopoietic cells and reintroduced into the sickle mouse where they were able to ameliorate the disease phenotype. However, a number of obstacles remain to be overcome before we can expect iPSCs to be routinely used in the clinical setting.

Limitations/Challenges of iPSCs

The first generation of iPSCs were established using retro- and lentiviral vectors to express the cocktail of exogenous transcription factors necessary to revert cells to a pluripotent state (Takahashi and Yamanaka, 2006). However, the residual expression or reactivation of the factors, particularly of oncogenes Klf4 and Myc, has been shown to increase tumorigenesis in mouse models (Nakagawa et al., 2008), while insertional mutagenesis has been shown to have tragic deleterious effects in previous non-iPSC applications (Hacein-Bey-Abina et al., 2003). Several viral-free alternative approaches for the derivation of iPSCs have since been developed including transposon (Woltjen et al., 2009), DNA plasmid (Okita et al., 2008), RNA (Warren et al., 2010), and protein (Zhou et al., 2009) delivery methods (for a comprehensive review of reprogramming methods see (González et al., 2011)).

While iPSCs were initially heralded as a replacement for ESCs, a body of evidence has since accumulated suggesting that there may be inherent differences between iPSCs and ESCs, ranging from methylation status of certain genes (Doi et al., 2009) to differentiation efficiency along different lineages (Löhle et al., 2012) (Bilic and Izpisua Belmonte, 2012). It is not entirely clear however how many of these differences can be attributed to incomplete reprogramming and whether many if not all of these differences are eliminated in high quality iPSCs. Regardless, there will continue to be a complementary need for both ESC- and iPSC-based work as we continue to improve our understanding and technology for iPSC derivation. In the end, we can expect that most, if not all, of these limitations will eventually be overcome as our understanding of iPSC derivation improves. Perhaps the greatest challenge that will however remain in applying iPSC technology to the clinic will be our ability to derive the disease-relevant cell types and to define disease states that can be effectively treated using a cell based therapeutic approach.

Neural Crest

Definition

The neural crest (NC) is a transient, highly migratory population of cells unique to vertebrates. It arises early during development at the neural plate border, where it is specified by converging signals from the neural plate, the adjacent non-neural ectoderm, and the underlying mesoderm. The prospective neural crest progenitors subsequently under go an epithelial-to-mesenchymal transition (EMT), delaminate, and migrate extensively throughout the embryo where they then differentiate into a wide range of derivatives, determined, in part, by their anterior-posterior (AP) axial level. These derivatives include, but are not limited to cells of the peripheral nervous system (PNS), facial cartilage and bone, smooth muscle cells, and melanocytes. In light of this

multipotent nature, the neural crest has sometimes been referred to as “fourth germ layer” (Hall, 2000).

In light of the contribution of NC to so many tissues and organs, it is not surprising that defects in NC specification, development, migration, or maintenance can result in a broad range of disorders. This diverse class of pathologies, collectively referred to as neurocristopathies, includes, among others, Familial Dysautonomia, Hirschsprung disease, piebaldism, Waardenburg Syndrome, neurofibromatosis type I, CHARGE syndrome, congenital insensitivity to pain and anhydrosis, and malignant melanoma.

The NC has been an attractive model for the study of embryonic induction, specification, lineage commitment, and migratory behavior. As a result, an extensive body of literature has been accumulated in *Xenopus*, zebrafish, and mouse regarding the signaling requirements underlying these events in NC (Betancur et al., 2010; Stuhlmiller and García-Castro, 2012). It is now understood that the development of NC is a multi-step process that occurs over a timeframe that spans from the beginning of gastrulation to late organogenesis. It begins with the convergence of multiple inductive signals at the presumptive neural plate border between the neighboring neural and non-neural ectoderm (**Figure 1.2**). With the onset of neurulation, the specified NC precursors are found in the developing neural folds and dorsal neural tube. The NC cells begin to acquire a migratory phenotype and undergo an EMT that eventually, after neural tube closure, allows them to delaminate, migrate extensively throughout the embryo, and eventually, upon arrival at their final destination, terminally differentiate into a variety of cell types (Betancur et al., 2010; Sauka-Spengler and Bronner-Fraser, 2008; Stuhlmiller and García-Castro, 2012).

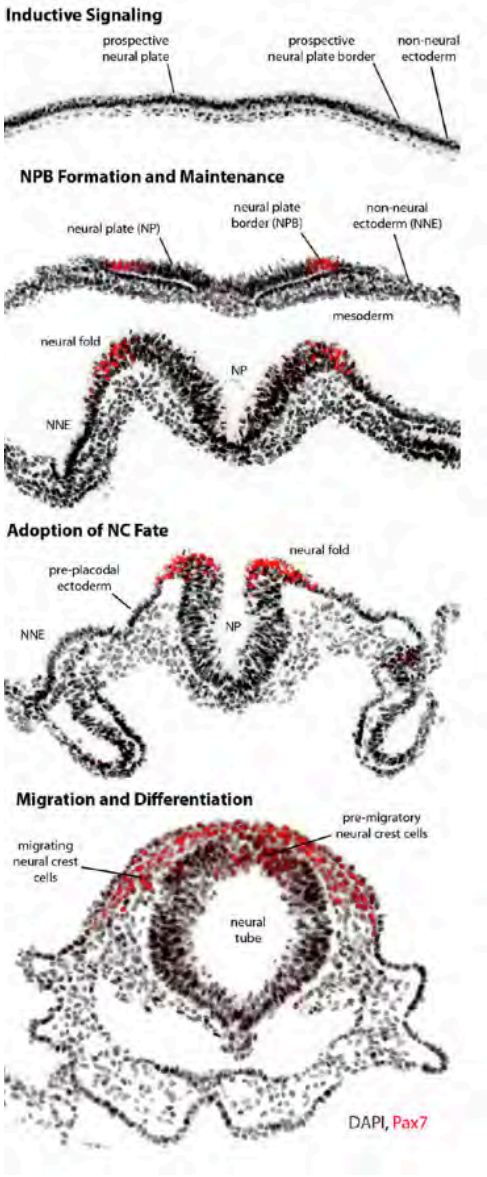

Figure 1.2. Morphogenetic changes during NC induction. The chick embryo is used as an example of morphogenetic events that occur during NC development from gastrulation to neurulation. Pax7 expression, in red, marks the neural plate border and later NC progenitors. NC is specified at the neural plate border, which is found between the neural plate and non-neural ectoderm, during the gastrula stage. As the neural plate thickens and rises, the expression of NC specifier genes can be detected in the neural folds. After formation of the neural tube, NC cells undergo an epithelial-to-mesenchymal transition and migrate throughout the embryo to differentiate into a range of derivatives. "Springer and Cellular and Molecular Life Sciences, vol. 69, 2012, pp. 3715-37, Current perspectives of the signaling pathways directing neural crest induction, Stuhlmiller TJ, García-Castro MI., Figure 1, with kind permission from Springer Science and Business Media."

Specification - Signaling

Specification of NC occurs as a result of converging signals arising from the neural plate and neighboring tissues that are integrated at the neural plate border. This process begins during gastrulation however despite studies across multiple model organisms it has been difficult to separate the processes of NC and neural induction. The latter represents the initial step during which the neural plate, from which the future nervous system will form, is specified as a subregion of the embryonic ectoderm. Historically, studies using cell lineage mapping and transplantation of neural plate adjacent to non-neural ectoderm have demonstrated that neural plate cells can also give rise to NC (Selleck and Bronner-Fraser, 1996). More recently it has been suggested that BMP signaling may play stage-specific events in neural plate and NC specification such that these may be independent events (Wawersik et al., 2005). The nature of the signals directing NC specification have been thoroughly investigated across a range of model systems and it is now understood that NC induction is largely driven by a combination of BMP, Wnt, and FGF signals.

Bone morphogenetic protein (**BMP**) signaling is active throughout the entire ectoderm prior to gastrulation in *Xenopus* and zebrafish embryos (Fainsod et al., 1994; Hemmati-Brivanlou and Thomsen, 1995). At gastrulation the dorsal mesoderm releases BMP antagonists including noggin, chordin, cerberus, nodal, and follistatin, which are found in the underlying paraxial mesoderm (Barth et al., 1999; Dick et al., 2000; Fürthauer et al., 1999; Marchant et al., 1998; Mayor et al., 1995; Morgan and Sargent, 1997; Nguyen et al., 1998; Schmid et al., 2000; Willot et al., 2002). This, along with the BMP-inhibitory activity of co-existing Wnt signals, establishes a BMP gradient that patterns the neural plate, including prospective NC (Baker et al., 1999). The resulting intermediate levels of BMP signaling at the neural plate border are required for NC specification (LaBonne and

Bronner-Fraser, 1998; Marchant et al., 1998; Morgan and Sargent, 1997; Nguyen et al., 1998). In contrast, higher levels of BMP will give rise to non-neural ectoderm (epidermis), while lower levels result in the specification of neural plate. However BMP signaling alone is not sufficient to induce NC. Rather additional Wnt, RA, and FGF signals are required (Delaune et al., 2005; LaBonne and Bronner-Fraser, 1998; Villanueva et al., 2002). There also remains some discussion about whether BMP is needed at this most early timepoint or later for the maintenance of the newly induced NC, although inconsistencies in findings may simply reflect species-specific differences (Linker and Stern, 2004).

The **Wnt** pathway functions in multiple reiterative roles during NC development. It has been found to be both necessary and sufficient for NC induction in both *Xenopus* (Bang et al., 1999; Deardorff et al., 2001; LaBonne and Bronner-Fraser, 1998; Saint-Jeannet et al., 1997; Wu et al., 2005) and chick models (García-Castro et al., 2002). Wnt signaling also appears to required for NC induction in zebrafish (Lewis et al., 2004). However in the mouse the primary role of Wnt signaling may be in NC lineage specification as mutants with conditional inactivation of Wnts or Wnt pathway components exhibit severe defects in the development of NC derivatives such as cranial and trunk ganglia, melanocytes, and craniofacial skeletal elements (Jones and Trainor, 2005). However a role of Wnt in NC specification cannot be ruled out as detailed analyses at early stages of mouse embryonic development have not been conducted. Interestingly, recent data also suggest that early neural crest induction may require an initial inhibition of Wnt signals (Steventon and Mayor, 2012).

Species specific differences have also been documented both in the Wnt family members driving NC induction and the source of Wnt molecules in different models

systems. While in the chick, NC specification requires Wnt pathway activation by Wnt6 secreted by the non-neural ectoderm (García-Castro et al., 2002), Wnt8 has been found necessary for NC induction in Zebrafish (Lewis et al., 2004).

Fibroblast growth factor (**FGF**) signaling has been shown to play an important role in NC induction. Exposure of *Xenopus* naïve ectoderm to Fgf2 in combination with BMP antagonists is sufficient to induce upregulation of NC markers such as *Slug* (LaBonne and Bronner-Fraser, 1998; Mayor et al., 1997; Mayor et al., 1995). In fact, exposure to Fgf8 alone is necessary and sufficient to support a transient induction of NC (Monsoro-Burq et al., 2003).

Evidence for a role for **Notch** signaling in NC specification has largely been obtained from studies in avian and Xenopus models (reviewed in (Cornell and Eisen, 2005)). In particular, Notch signaling was found to function upstream of BMP signaling during specification of NC in the cranial neural folds. Studies in Xenopus for example have shown that activation of Notch signaling by overexpression of the downstream effector *Hairy2* is sufficient to induce expression of *Snail2*-expressing NC (Glavic et al., 2004). However while Notch has also been found to play a role in later lineage specification of NC derivatives, the role of Notch signaling in early NC induction may not be conserved in mammalian systems. Thus, no early NC defects are observed in Delta 1 null mouse mutants even though expression of several Notch pathway genes can be detected in cranial NC (Betancur et al., 2010).

The convergence at the neural plate border of the signaling pathways outlined here triggers a temporally, spatially, and quantitatively highly regulated response from a

battery of transcription factors (**Figure 1.3**) (Betancur et al., 2010; Sauka-Spengler and Bronner-Fraser, 2008).

Specification - Genes

A set of genes, referred to sometimes as the neural plate border specifiers, are directly induced by the signaling pathways outlined above **(Figure 1.4**). This group of transcription factors which includes *Msx1*, *Dlx5*, *Pax3*, *Gbx2* , and *Zic* genes have been found to be required for NC specification in mouse, zebrafish, and *Xenopus* by establishing NC competence at the neural plate border (Brewer et al., 2004; Knight et al., 2003; Luo et al., 2003b; Meulemans and Bronner-Fraser, 2002; Sato et al., 2005; Suzuki et al., 1997; Tribulo et al., 2003). Neural plate border specifiers are expressed early during neurulation, being first observed in the non-neural ectoderm before they later become restricted to the neural fold region from which NC will later arise (Davidson, 1995; Luo et al., 2002; Suzuki et al., 1997). This pattern of expression correlates with the gradient of BMP activity discussed above. This, along with the presence of cis-regulatory regions in the promoters of some of these genes, suggests that they might be direct targets of BMP activity (Alvarez Martinez et al., 2002; Park and Morasso, 2002; Suzuki et al., 1997). The exact hierarchical organization and interactions between these factors is however still being investigated.

Msx1 plays a transient role in neural crest development, possibly by acting upstream of *Snail* genes, before being downregulated itself upon the induction of NC (Monsoro-Burq et al., 2005; Sato et al., 2005; Tríbulo et al., 2004). Later expression of Msx1 has been associated with apoptosis of NC (Monsoro-Burq et al., 2005; Tríbulo et al., 2004).

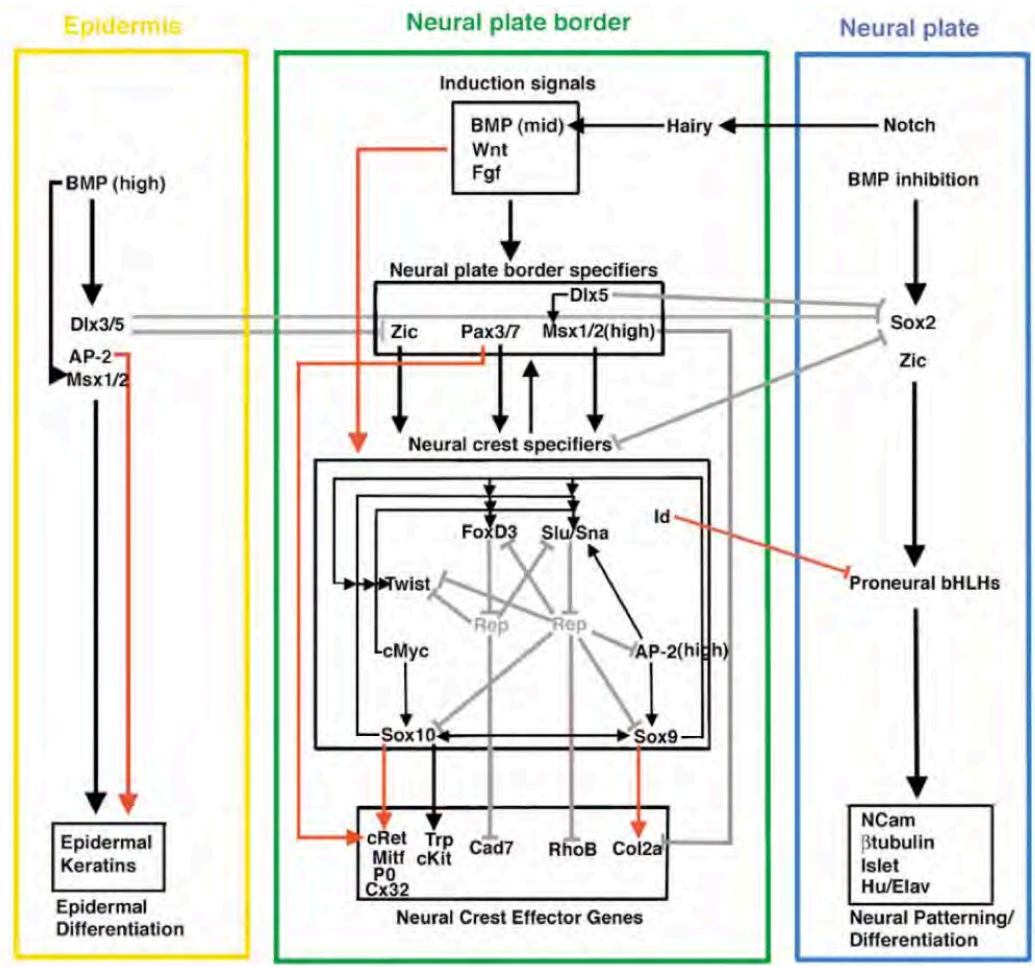

Figure 1.3. Putative Neural Plate Border Gene Network. A representation of putative gene networks acting at the neural plate in vertebrates with red arrows to indicate direct regulatory interactions, black arrows to represent genetic interactions suggested by studes in Xenopus, and gray lines to indicate repressive regulation. "Reprinted from Developmental Cell, 7(3), Meulemans D, Bronner-Fraser M., Gene-regulatory interactions in neural crest evolution and development, 291-9, Copyright 2004, with permission from Elsevier."

Dlx genes appear to play a broader role in the positioning and patterning of the neural plate border, including not just NC but also placodal cells and may function partly by expanding the region of Msx1 expression (McLarren et al., 2003; Woda et al., 2003). Of the *Dlx* family members, *Dlx5* appears to play a more specific role in NC specification (Luo et al., 2001)

Expression of ***Pax3*** can be observed in the neural fold region early in embryonic development. Loss of function experiments in both mouse and *Xenopus* have established the critical contribution of *Pax3* to NC (Borycki et al., 1999; Mansouri et al., 2001; Monsoro-Burq et al., 2005; Sato et al., 2005; Wiggan et al., 2002). *Pax3* appears to function downstream of *Msx1* (Monsoro-Burq et al., 2005) and cooperatively with *Zic1* (Sato et al., 2005). Simultaneous expression of both *Pax3* and *Zic1* is required to specify NC fate, as expression of either individually will promote alternative neural plate border fates (Hong and Saint-Jeannet, 2007). *Pax3* may also act as a mediator of Wnt and FGF signaling in NC specification (Monsoro-Burq et al., 2005).

In mouse, ***Zic*** knockdown has been shown to disrupt the development of NC and multiple NC derivatives (Aruga et al., 1998; Inoue et al., 2004; Nagai et al., 2000), while in xenopus overexpression of *Zic* has been shown to promote neural plate and NC formation (Brewster et al., 1998; Kuo et al., 1998; Mizuseki et al., 1998; Nakata et al., 2000; Nakata et al., 1997, 1998; Sato et al., 2005)

Gbx2**,** a gene previously associated with anteriorposterior (AP) patterning, has recently also been shown to be expressed in the ectodermal where the NC is formed (Li et al., 2009). It was found that not only does *Gbx2* act upstream of other neural plate border specifiers such as *Msx1* and *Pax3*, but it is also a direct downstream target of Wnt

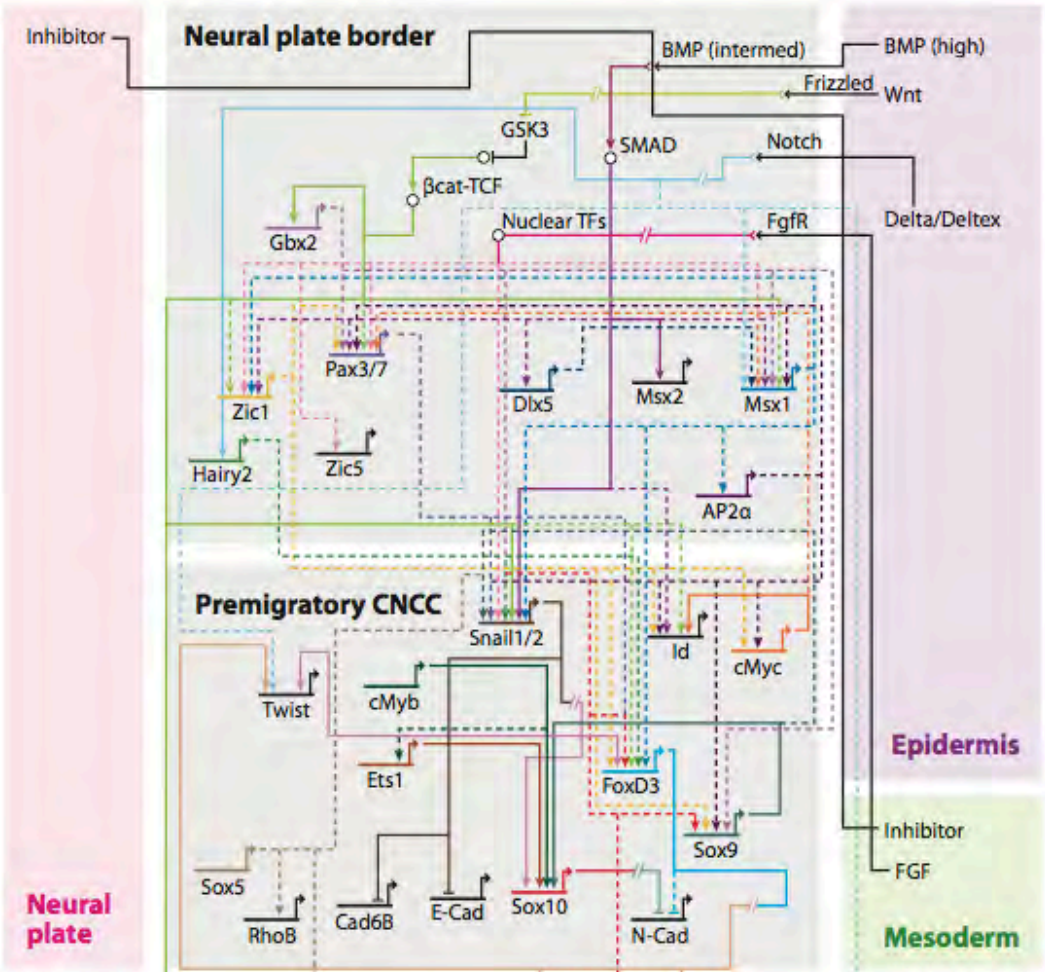

Figure 1.4. A putative gene regulatory network during cranial NC specification. Hierarchical gene regulatory interactions during the induction and specification of cranial NC as inferred from gene perturbation data in Xenopus, chick, mouse, and zebrafish models. Solid lines indicate direct regulatory interactions. Dashed lines indicate potential direct regulatory interactions. Broken lines indicate potential indirect interactions. "Republished with permission from: Assembling neural crest regulatory circuits into a gene regulatory network, Betancur P, Bronner-Fraser M, Sauka-Spengler T., 26, 581-603, 2010; permission conveyed through Copyright Clearance Center, Inc."

signaling, suggesting that *Gbx2* might act as the earliest mediator of Wnt inductive signals specifying NC fate.

The initial specification of NC by the gene regulatory network described above, induces the expression of a subsequent group of genes specific to the NC population (termed NC specifiers) which are required for NC survival. Accordingly, several of these genes, in addition to upregulating further downstream NC-specific gene networks also function to inhibit pro-apoptotic pathways. The expression of a subgroup of these genes (AP2α, Snail1/2, Id, c-Myc, and Twist) however precedes the emergence of NC progenitors, raising the possibility that they may function as a regulatory link between the establishment of NC competence at the neural plate border and the actual lineage specification of bona fide NC. Interpretation of these interactions is somewhat complicated by species-specific differences in the timing of expression onset and maintenance within the neural plate border.

AP2α is a gene that plays a dual role first in the specification and later in the apoptosis of neural crest. A requirement for *AP2α* in the early specification of NC has been demonstrated in *Xenopus* using morpholino mediated knockdown (Luo et al., 2003b), while in zebrafish the *AP2α* mutant, *mont blanc*, exhibits defects not only in early NC specification, but also in the establishment of NC derivatives (Barrallo-Gimeno et al., 2004; Knight et al., 2004; Knight et al., 2003; O'Brien et al., 2004). The role of *AP2α* therefore does not appear to be just restricted to the early specification of NC but also extends into later NC development.

While ***c-Myc*** is expressed at the neural plate border in a broader expression pattern than many specific NC genes it is also expressed simultaneously and in the same cells

as *Msx1* and *Pax3*, suggesting that interactions between these factors may be required in early NC specification (Bellmeyer et al., 2003), Independent of its interactions with other genes, morpholino knockdown as well as overexpression studies in *Xenopus* have confirmed a requirement for *c-Myc* in NC development and it may further function in maintaining NC precursors in a multipotent state (Bellmeyer et al., 2003). Interestingly, and perhaps unexpectedly, c-Myc's function appears to be independent of its effects on cell proliferation or cell death (Bellmeyer et al., 2003).

Snail and ***Slug*** (*Snai2)* are members of the *Snail* family of transcription factors. *Snail* expression can be observed in *Xenopus* in prospective neural folds slightly prior to *Slug* expression and appears to function upstream of *Slug* (Aybar et al., 2003; Linker et al., 2000). Both genes also contribute to the survival of NC cells by controlling the expression of Bcl-xL and specific caspases (Tríbulo et al., 2004; Vega et al., 2004). Knock-down experiments in *Xenopus* have established a role for *Slug* in the induction of *Slug*, *Sox9*, *Twist*, *Ets-1*, *FoxD3* and *Sox10 (Aybar et al., 2003; Honoré et al., 2003; LaBonne and Bronner-Fraser, 2000; Sasai et al., 2001).* Overexpression studies have shown that *Slug* can induce the expansion of a HNK-1, RhoB, and *Pax3* expressing population in the embryo (Cheung et al., 2005). Both genes are also associated with EMT, which will be discussed in following section.

Twist expression has been observed in pre-migratory NC in both *Xenopus* (Linker et al., 2000) and mouse embryos (Gitelman, 1997; Soo et al., 2002). *Twist* has a well established role in promoting EMT, which is also reflected in the NC cell migration deficiency that is observed in addition to a neural tube closure defect in *Twist* mutant mice (Soo et al., 2002).

Like *Snail* and *Slug,* ***Id3*** has been shown to prevent the apoptosis of NC cells. *Id3* functions downstream of myc and also appears to be involved in the maintenance of NC gene expression as knockdown of *Id3* resulted in downregulation of NC genes *Slug*, *Sox10*, *FoxD3* and *Twist* (Kee and Bronner-Fraser, 2005; Light et al., 2005). Like c-Myc, *Id3* also appears to be involved in the maintenance of multipotent NC progenitors, as loss of *Id3* leads to a loss of NC progenitors (Kee and Bronner-Fraser, 2005; Light et al., 2005).

The activation of this network of NC specifier genes is followed by the induction of bona fide NC-associated genes, many of which function by promoting NC survival.

Several members of the ***Sox*** gene family of transcription factors are expressed in the NC at different points during embryonic development (Hong and Saint-Jeannet, 2005). Of these, *Sox9* and ***Sox10*** have been found to be play particularly critical roles in the survival of NC cells. In null mouse strains of either *Sox9* or *Sox10*, the NC population undergoes massive cell death either prior to delamination or before differentiation, respectively (Kapur, 1999; Sonnenberg-Riethmacher et al., 2001; Southard-Smith et al., 1998). In the *Sox10* zebrafish mutant (*colorless*) NC cells similarly exhibit a defect in migration and then undergo cell death (Dutton et al., 2001). While Sox9 is expressed before Sox10, it is quickly downregulated after initiation of NC migration (McKeown et al., 2005). In contrast, Sox10 expression is first detected before NC exit the neural tube and is maintained in migrating NC populations and persists in some NC derivatives including Schwann cells and melanocytes. Ectopic expression of Sox10 is in fact sufficient to induce an HNK-1 expressing population of undifferentiated NC in chick (McKeown et al., 2005).

Effects of ***FoxD3*** expression may be dose-dependent as overexpression of *FoxD3* at high levels has been found to enhance the expansion of the neural plate at the expense of neighboring NC (Linker et al., 2000), while injection of low levels of *FoxD3* mRNA induced expression of *Slug*, *AP-2*, *FoxD3*, *Ets-1*, *Twist* and *Sox 2* (Sasai et al., 2001). *FoxD3* has also been shown to increase the presence of migratory NC from the dorsal neural tube in the chick embryo (Cheung et al., 2005; Dottori et al., 2001; Kos et al., 2001).

While endothelin (**EDN**) has long been implicated in the differentiation of NC derivatives, it has recently been shown that expression of the EDN receptor, EDNRA, can be observed in *Xenopus* neural folds beginning at the gastrula stage (Bonano et al., 2008). Through gain- and loss-of-function experiments the authors demonstrate that EDN1/EDNRA signaling downstream of *Msx1* is required for NC progenitor maintenance and survival. EDN signaling was further found to be upstream of pro-NC factors Sox9 and Sox10.

In summary, intermediate levels of BMP signaling at the neural plate border cooperate with Wnt, FGF, RA, and Notch activity to activate a genetic cascade of early neural plate and NC specifiers (*Msx1, Dlx, Zic, Pax3, c-Myc*) which subsequently activate a pro-NC gene network (*AP2α , Snail/Slug, Id3, Sox, Twist, FoxD3*). The resulting NC progenitors can be identified at the dorsal neural tube on account of their expression of NC-associated factors including Sox10, FoxD3, EDNRA, and HNK-1.

EMT and Delamination

Premigratory NC resides within the dorsal neural tube in a polarized epithelial layer bound by adherens junctions and tight junctions (Sauka-Spengler and Bronner-Fraser,

2008). In order to migrate, NC precursors must first delaminate and undergo an EMT in order to decrease adhesiveness and increase cell motility. This process involves major cytoskeletal rearrangements and changes to cell junctions and adhesion properties, including a switch from type I to type II cadherins, a transition from tight junctions to gap junctions, and the induced expression of matrix metalloproteases to facilitate invasion and movement through the extracellular matrix (Sauka-Spengler and Bronner-Fraser, 2008). Many of these processes are regulated by Snail family members and FoxD3. Transcription from the promoter of E-cadherin, a type I cadherin, has for example been shown to be inhibited by binding of Snail family members while expression of N-cadherin is regulated by FoxD3 activity (Sauka-Spengler and Bronner-Fraser, 2008).

Migration

NC migration occurs in a highly regulated fashion along segmentally organized pathways. In the trunk, NC migration is organized metamerically with repeating streams of cells migrating through the anterior portions of somites. This migration is guided by interactions with other cells and the environment, although much of the signaling cues appear to prevent NC from responding to cell types and pathways prior to arriving at the final destination. Repulsive interactions between ephrin-expressing cells in the posterior halves of somites and trunk NC expressing the cognate Eph receptors for example, restrict the movement of the latter to the anterior portion of the somite. Similarly in avian models, early migrating trunk NC are repelled from the ephrin-ligand expressing dorsolateral migration pathway by their expression of ephB receptors. NC migration is further tightly regulated by additional cues including semaphoring-neuropilin and Slit-Robo signaling interactions. The upstream factors regulating expression of these signals are however still under investigation. Reviewed in (Sauka-Spengler and Bronner-Fraser, 2008).

Terminal Differentiation

How cells switch from a migratory phenotype and differentiate once they reach their destination is less well understood. Typically, the arrival of NC cells at their final destination is accompanied by a downregulation of early NC-associated genes including Snail, Slug, FoxD3, Id, AP2α (Betancur et al., 2010). The expression of some NC factors is however notably maintained in a subset of lineages. FoxD3 expression continues to be expressed in glial and neural precursors where it serves to inhibit differentiation along the melanocyte lineage by inhibiting binding of Pax3 to the MITF promoter (Thomas and Erickson, 2009) while Sox10 expression persists in the melanocyte and glial populations.

Human NC

Much has been learned about the events governing NC induction, migration, and differentiation from numerous animal models and many signaling requirements are conserved among different model systems. However the existence of some species-specific differences highlight the need to study human NC biology directly.

Some knowledge about the roles of different NC-associated genes in the human system has been gained from the identification of causal mutations in numerous neurocristopathies. Mutations in Pax3 and Sox10 have been found to underlie Waardenburg Syndrome (Pingault et al., 1998; Tassabehji et al., 1992), piebaldism can be caused by mutations in Slug (Sánchez-Martín et al., 2003), defects in Msx1 cause tooth agenesis/orofacial cleft, while Hirschsprung disease can be attributed to mutations in EDNRB (Amiel et al., 1996; Svensson et al., 1999).

Recently, direct studies of human embryonic tissues have provided novel information about human NC behavior. A histological analysis of human embryo sections has

established a detailed insight into NC structures in the human system (O'Rahilly and Müller, 2007). Extensive molecular profiling of presumptive NC cells isolated from human embryonic dorsal neural tube explants has confirmed conservation of NC traits with chick and mouse but has also identified molecular cascades unique to the human system (Thomas et al., 2008). Global molecular analysis further revealed that human NCs are highly similar to hESCs, including expression of Nanog, Oct4, and Sox2. This finding, along with the observation that the isolated NC cells were able to self-renew *in vitro*, suggests that the authors may have isolated a NC stem cell population that may or may not have a corresponding counterpart *in vivo*. A recent immunohistochemical study of Carnegie Stage 12 to 18 embryos confirms expression of Pax3, Sox9, and Sox10 in pre-migratory trunk NC, while AP2, Pax7, Sox9, and Sox10 were identified in more anterior sections (Betters et al., 2010). Notably, HNK-1 was found to only label a small subset of migrating NC cells. p75 was found to label more of the migrating NC population, but was also broadly expressed in non-NC cells. This is of particular importance as HNK-1 and p75 expression has (Lee et al., 2007) and continues to be used (Menendez et al., 2011) to identify NC populations derived from hESCs.

The Derivation of NC from hPSCs

In light of the technical and ethical limitations of studying early human development directly, hESCs offer a viable alternative approach to investigate human NC biology. While it may be difficult to evaluate how closely this system recapitulates embryonic development, it is possible to test different signaling pathway and molecule requirements and compare these with findings in other animal systems. To date, hESC-derived NC cells have been established using multiple different approaches (Milet and Monsoro-Burq, 2012).

Early approaches for the derivation of NC from hESCs relied on stromal coculture (Jiang et al., 2009; Lee et al., 2007; Pomp et al., 2005). In one case, NC were found to migrate from a rosette-like structure that appeared to replicate the neural tube (Lee et al., 2007), further supporting the hypothesis that ESC differentiation recapitulate events during embryonic development. However the presence of feeder cells in these conditions makes the evaluation of signaling events governing NC induction difficult while the lengthy duration and low yield of the differentiation can make this approach technically challenging. Later studies required intermediates steps of embryoid body (Fang et al., 2006; Zhou and Snead, 2008) or neurosphere formation (Bajpai et al., 2010; Cimadamore et al., 2011; Curchoe et al., 2010). More recently several defined protocols for the rapid derivation of NC from hESCs have been reported (Chambers et al., 2009; Lee et al., 2010; Menendez et al., 2011). However, these approaches have relied on the use of HNK-1/p75 has markers for presumptive NC. As mentioned above, studies in human embryos have not validated the expression of these markers in human NC (Betters et al., 2010) and at least one study has found this isolation strategy to be ineffective in differentiating between NC from non-NC in a hESC differentiation context (Curchoe et al., 2010). It has therefore been suggested that Sox10 may be a more suitable marker for human NC induction (Betters et al., 2010). However it should nevertheless be noted that HNK-1 and p75 expression have been successfully applied to isolate cells from hESC differentiations that were able to generate a range of NC derivatives. Recently, these cells have also been used in NC disease modeling applications (Lee et al., 2009; Lee et al., 2012).

A novel approach for the neural conversion of hESCs was reported by our group in 2009 (Chambers et al.). It was found that treatment with two small molecules to inhibit both arms of SMAD signaling was sufficient to promote rapid and efficient induction of a Pax6

expressing neurectodermal population. Interestingly, the same approach was found to support the spontaneous induction of a small subpopulation of NC, identified by the co-expression of HNK-1 and p75. In this dual SMAD inhibition (DSi) protocol, BMP signaling was originally inhibited with recombinant Noggin, however comparable effects have now been achieved more cost efficiently with the small molecules Dorsomorphin or LDN-193189 (LDN). Treatment with the small molecule SB431542 (SB) is used to inhibit TGF-β, Activin, and Nodal signaling. Inhibition of both arms of SMAD signaling is required to trigger exit from the pluripotent state, prevent trophectoderm formation and block the formation of mesendoderm and non-neural ectoderm (Chambers et al., 2009). The basic dual SMAD protocol has now been modified to support induction of human midbrain dopamine neurons (Kriks et al., 2011), nociceptors (Chambers et al., 2012b), and placode cells (in review). As NC competence of DSi derived cells had been demonstrated by the spontaneous induction of NC contaminants during CNS derivation, we hypothesized that DSi would provide a highly suitable platform for investigating the signaling requirements to further optimize NC specification.

Melanocytes

Definition

Melanocytes are the pigment-producing cells found in the skin, iris, hair follicles, and inner ear. However, for the purposes of this discussion, we will focus nearly exclusively on epidermal melanocytes. In humans, epidermal melanocytes reside at the basement membrane between the dermal and epidermal layers. There, they establish themselves in close proximity with neighboring keratinocytes, which actually make up the bulk of the epidermis. Due to their highly dendritic morphology, each melanocyte is able to associate with up to 36 keratinocytes, in what is termed the “epidermal melanin unit” (Reviewed in (Nordlund, 2007)). The synthesis of the pigment melanin occurs in the

melanocyte within specialized lysosome-related organelles, known as melanosomes. Melanosomes are subsequently transferred to neighboring keratinocytes, where they establish a photoprotective barrier by forming cap-like structures that shield the keratinocyte nuclei from incoming UV irradiation (UVR) (Byers et al., 2003). Given the pivotal role of melanocytes in establishing pigmentation, it is not surprising that defects in melanocyte development, maintenance, and function are associated with a number of different disorders including piebaldism, vitiligo, and oculocutaneous albinism, while transformation of melanocytes causes malignant melanoma.

Melanin

Melanins are complex biopolymers synthesized through a multistep, tyrosinase-dependent pathway (Slominski et al., 2004). They exist in two different forms, the yellow-red **pheomelanin**, and the black-brown **eumelanin**, and while all individuals produce both forms, their variable relative abundance contributes in part to the wide range in human pigmentation. Both pheomelanin and eumelanin are synthesized through the hydroxylation of tyrosine to dopaquinone (through an L-DOPA intermediate) by the enzyme tyrosinase. The further processing of dopaquinone differs for the synthesis of pheomelanin and eumelanin. While the formation of pheomelanin requires at least one cysteine-dependent reduction step, the processing of eumelanin requires successive hydroxylation, oxidation, and carboxylation reactions that involve the additional activity of enzymes dopachrome tautomerase (Dct or Trp2) and Trp1. The melanin intermediates are subsequently polymerized onto protein scaffolds to produce fully pigmented melanins (Hearing, 1999).

Pheomelanin and eumelanin differ not only in their color, but also in the size, shape, and packing of their granules, which further impacts their properties and function *in vivo*. The

lighter-colored pheomelanin is reactive to UVR exposure (Lin and Fisher, 2007). The DNA damage than can result from these factors may contribute to the increased risk for melanoma in fair-skinned individuals, as they have higher proportion of pheomelanin compared to darker-skinned individuals.

Regulation of Pigmentation

The switch between pheomelanin and eumelanin expression is regulated at multiple levels, however a key regulatory node is found at the melanocortin-1 receptor (**MC1R**) in a cyclic adenosine monophosphate (**cAMP**) dependent manner.

The seven-transmembrane G-protein coupled receptor encoded by the *MC1R* gene was first identified on account of altered coat color in mice (Lin and Fisher, 2007). While wild-type mice exhibited black/brown eumelanotic hair, recessive mutants displayed yellow pheomelanotic hair. The *MC1R* mutation has been highly conserved across evolution and has been found to correlate with coat color in species ranging from mammoths to dogs.

When MC1R is bound by its agonists α-melanocyte-stimulating hormone (α-MSH) and adrenocorticotropic hormone (ACTH), adenylyl cyclase is activated which in turn induces production of cAMP. This leads to the phosphorylation of cAMP responsive-element-binding protein (CREB) transcription factor family members, which in turn transcriptionally activate target genes including the transcription factor MITF. MITF, which will be discussed in greater detail below, is upstream of numerous melanin production enzymes and melanocyte differentiation factors. The MITF transcriptional activity results in increased eumelanin production (Lin and Fisher, 2007).

The agouti (*Asip*) gene encodes a MC1R antagonist. Inactivating mutations in this gene cause black fur in mice, while recent evidence also suggests that similar effects may contribute to dark eye and hair in some humans. However a larger part of human pigmentation variability in humans can be attributed to MC1R polymorphism. More than 30 allelic variants of MC1R have been identified, most of which result from a single amino acid substitution. Hypomorphic alleles that either lack the ability to bind the MC1R ligand or have reduced cAMP activation activity result in a 'red-head' phenotype that includes red hair color, fair skin, an inability to tan, and a propensity to freckle (Ringholm et al., 2004). Due to the higher proportion of pheomelanin, these individuals also frequently experience higher susceptibility to developing skin cancers. However additional factors further control skin pigmentation, as can be deduced from individuals who exhibit dark hair and fair skin.

Epidemiological studies support the hypothesis that high levels of pigmentation have been evolutionarily selected for in regions with high sun exposure, although it is still unclear whether this is a result of requirements for vitamin D production or protection against UVR-induced DNA damage (Lin and Fisher, 2007). Populations that left the sun-rich African continent were no longer under this restraint and may have developed lower levels of pigmentation to obtain sufficient levels of vitamin D.

Melanin fulfills a UV protective role in the skin by absorbing, scattering and photo-oxidizing incident UVR to reduce penetration of UVR through the epidermis while also scavenging free radicals to prevent DNA damage (Costin and Hearing, 2007). It has been well established that pigmentation levels are increased in response to UVR exposure and that this can be attributed to increases in melanin production, melanosome number, and melanocyte dendricity resulting in increased melanosome

transfer to neighboring keratinocytes (Friedmann and Gilchrest, 1987). It has now been shown that UVR promotes pigmentation via multiple mechanisms. Activation of p53 in keratinocytes following sun exposure increases their production of α-MSH. Binding of α-MSH to MC1R on neighboring melanocytes activates MITF and results in increased melanin production (Cui et al., 2007). More recently it has been found that UVR also represses TGF-β production in keratinocytes which in turn upregulates PAX3 expression in melanocytes. PAX3 cooperates with Sox10 in a cAMP-dependent manner to again activate transcription of MITF (Yang et al., 2008).

Melanosome Biogenesis and Maturation

Melanin is synthesized within melanosome structures, which are membrane bound intracellular organelles unique to pigment cells. The sequestration of melanin within melanosomes not only creates the specialized local environment of factors and acidic intraluminal pH necessary for melanin synthesis, but also enables the efficient transfer of melanosomes to keratinocytes by epidermal melanocytes (Raposo and Marks, 2007).

Melanosome biogenesis occurs through a series of four morphologically defined stages. The first two stages are unpigmented and are defined by the presence of intraluminal proteinaceous fibrils, which begin to form during stage I and are completed by stage II (Raposo and Marks, 2007). The maturation from stage I to stage II melanosome is further accompanied by a morphological shift from a spherical to an ellipsoid shape. Once fibril formation is complete, melanin synthesis can be initiated. As melanin is deposited onto the fibril scaffold in stage III melanosomes, the fibrils become progressively thicker and blacker until the lamellar structure is completely obscured by melanin in stage IV melanosomes. At this point the melanosomes can essentially be thought of as a membrane-enclosed bag of melanin (Hearing, 1999). In epidermal

melanocytes, stage IV melanosomes subsequently translocate outward from the perinuclear region along a microtubule network to the dendrites, where the melanosomes continue their migration along actin filaments (Introne et al., 1999).

Melanocytes belong to a group of vesicles known as lysosome-related organelles (LROs), although recent evidence suggests that melanosomes actually arise from endosomal intermediates (Raposo and Marks, 2007). While much of the cellular machinery involved in melanosome formation is shared with other LROs, the specific targeting of melanin enzymatic factors such as tyrosinase and Tyrp1 suggests that mechanisms specifying the sorting of melanosomal macromolecules must also be present in melanocytes.

PMEL (PMEL17/gp100/silver) is the main constituent of the intraluminal proteinaceous fibrils found in stage I and II premelanosomes (Raposo and Marks, 2007). In the absence of PMEL, melanosomes in *silver* mouse strain do not form fibrillar structure and maintain enlarged, rounded appearance (Theos et al., 2006). In contrast, exogenous expression of PMEL is sufficient to induce formation of similar fibrils in non-melanocyte cells, suggesting that PMEL is both necessary and sufficient for formation of fibrils and melanosome structure (Berson et al., 2001). Stage I melanosomes, in which PMEL fibril formation is initiated, morphologically resemble vacuolar domains of early endosomes and evidence has accumulated that PMEL processing requires endosome intermediate (Raposo and Marks, 2007).

In contrast to PMEL, which is present in early melanosomes, melanin biosynthetic enzymes, **tyrosinase** and **Tyrp1**, are only present in stage III and IV melanosomes. While there is some conflicting evidence regarding whether tyrosinase and Tyrp1 are

delivered to late melanosomes via the trans-Golgi network or early endosome-derived vesicles, the need for melanin synthesis to initiate only after fibril formation has been completed requires strict temporal regulation of enzyme delivery (Raposo and Marks, 2007).

Significant insights into the sorting machinery regulating melanosome cargo trafficking has been learned from the study of human and mouse models of Hermansky-Pudlak Syndrome (HPS), in which the formation and/or function of LROs, including melanosomes, is defective (**Figures 1.5, 1.6**). HPS can arise from mutations in multiple genes, most of which encode subunits of multimeric protein complexes.

The protein complex **AP-3**, which is mutated in HPS2, has been implicated in the trafficking of tyrosinase. AP-3 binds to tyrosinase via a di-leucine based sorting motif in its cytoplasmic domain and traffics it out of the endosome (Theos et al., 2005). In the absence of functional AP-3, tyrosinase accumulates in early endosomes, resulting in pigment dilution. However some mature pigmented melanosomes with tyrosinase activity can be identified even in melanocytes from *pearl* mice or HPS2 patients, suggesting the presence of additional AP-3 independent tyrosinase targeting pathway. One possible candidate is another heterotetrameric adaptor complex, **AP-1** which has been shown to bind tyrosinase, particularly in the absence of AP-3 (Theos et al., 2005). AP-1 has also been found to be exclusively required for the targeting of another melanin biosynthetic enzyme, Tyrp1.

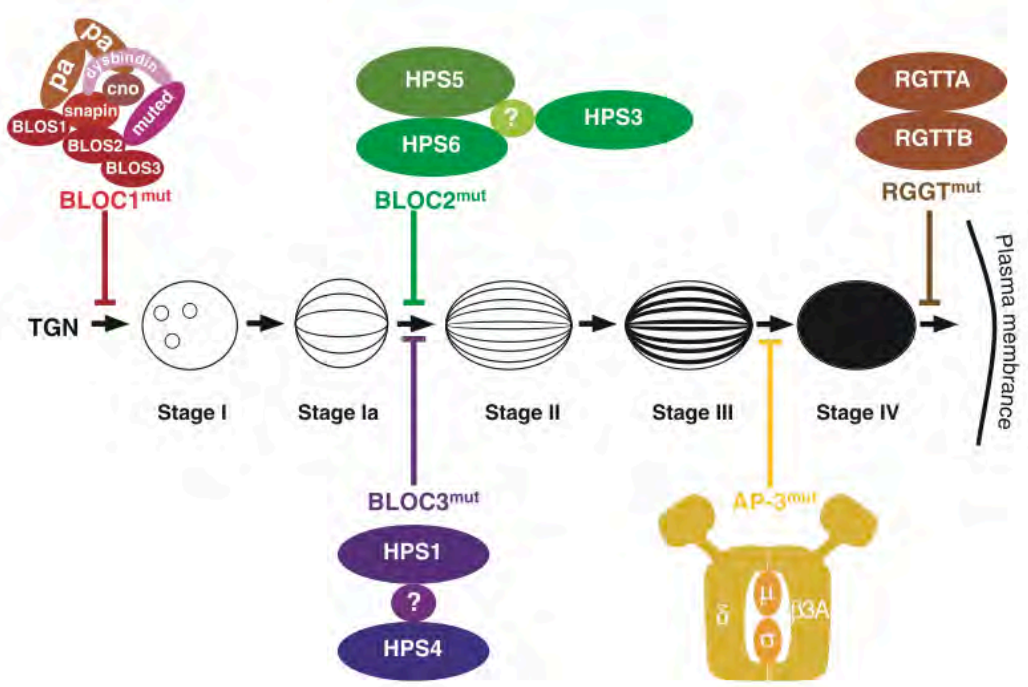

Figure 1.5. <u>Role of HPS protein complexes at different stages of melanosome biogenesis.</u> Mutations in the members of the multiprotein BLOC and AP-3 complexes cause defects at different stages in the formation of melanosomes and other lysosome-related organelles. “Adapted by permission from John Wiley and Sons: Pigment Cell Research, 19(1), 19-42, copyright 2006.”

Mutations in any of the subunits of the **BLOC-1** complex result in the most severely hypopigmented HPS phenotype in both mouse and human (HPS7, HPS8) due to a near complete loss of melanosomes in the eyes and skin (Di Pietro and Dell'Angelica, 2005). In BLOC-1 mutants, tyrosinase is only partially mislocalized, while targeting of Tyrp1 is strongly affected, with increased accumulation of Tyrp1 observed in early endosomal vesicles and at the cell surface (Setty et al., 2007). Evidence suggests that BLOC-1 is required for cargo exit from the early endosome (Raposo and Marks, 2007).

Hypopigmentation observed following mutation to any of the subunits that make up the **BLOC-2** complex (HPS3, HPS5, HPS6), is less severe than that observed in BLOC-1 mutants. BLOC-2 deficient mice exhibit accumulation of Tyrp1 in endosomal compartments that are distinct and downstream from the endosomal vacuoles observed in BLOC-1 mutants (Setty et al., 2007). This suggests a role for BLOC-2 in regulating targeting of endosome-derived membranes to maturing melanosomes.

In non-melanocytic cells, members of the **BLOC-3** complex (HPS1 and HPS4) regulate late endosome and lysosome motility and distribution (Raposo and Marks, 2007). However melanocytes from HPS1 patients demonstrate increased autophagy, and in particular an accumulation of melanosomes in compartments resembling autophagic vacuoles (Smith et al., 2005). Further studies will be needed to define the exact role of BLOC-3 in regulating melanosomal cargo and biogenesis.

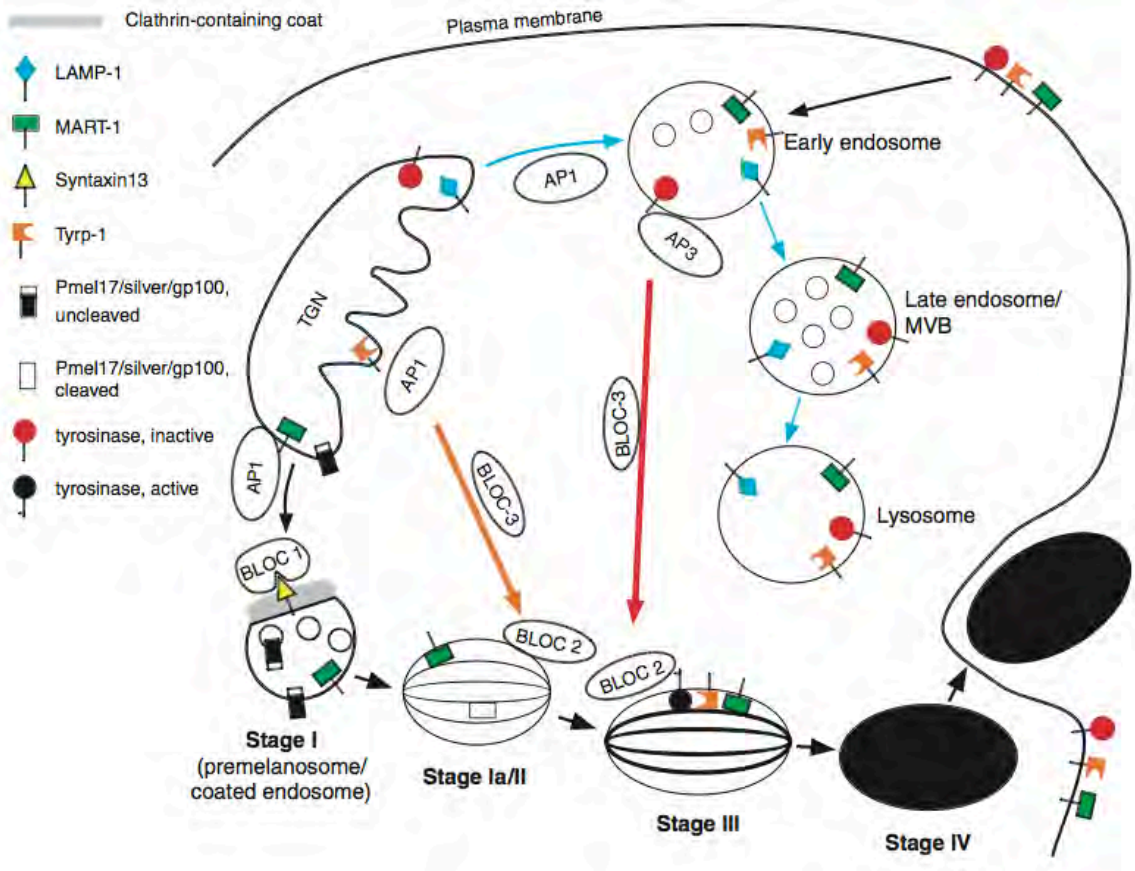

Figure 1.6. <u>The role of different HPS proteins in the trafficking of melanosomal proteins.</u> The trafficking of various melanosome structural and melanin biosynthetic enzymes to different stages of melanosomes is coordinated by multiple HPS-associated complexes. “Adapted by permission from John Wiley and Sons: Pigment Cell Research, 19(1), 19-42, copyright 2006.”

Additional factors are required for full melanosome function. The membrane transporter OCA2/P, mutation of which results in a form of oculocutaneous albinism, appears to play a role in cargo targeting to melanosomes as mutation results in mislocalization of tyrosinase and Tyrp1 (Brilliant, 2001). OCA2/P may also additional function in regulating intraluminal pH of melanosomes (Brilliant, 2001). Another gene of unknown function which as been associated with oculocutaneous albinism, OA1, encodes a transmembrane domain protein with homology to G-protein coupled receptors that localizes to mature melanosomes and late endosomes (Raposo and Marks, 2007).

To summarize, in the current model of melanosome biogenesis a sequential delivery of cargo via distinct endosomal compartments contribute to organelle maturation. However future studies will be required to establish a deeper understanding of how different pathways and complexes are coordinated and how melanosomal specificity of cargo targeting is achieved.

Melanosome Transfer

Mature melanosomes are moved by kinesin along microtubules to the dendritic tips of melanocytes (Hara et al., 2000). At the dendrite tips, melanosomes are captured onto actin filaments by myosin Va via a process that involves Rab27a (Wu et al., 1997; Wu et al., 2001). Accordingly, mutations in Myo-5 or Rab27a result in the hypopigmented disorder Griscelli Syndrome due to disrupted translocation and/or capture of melanosomes at the dendritic tips (Ménasché et al., 2000; Pastural et al., 1997). After aggregation at the dendritic tips, melanosomes are expelled and incorporated into neighboring keratinocytes. Until recently several mechanisms had been proposed via which melanosomes might be transferred to keratinocytes (reviewed in (Boissy, 2003; Van Den Bossche et al., 2006)). Possible mechanism included: i) melanocytes release

melanosomes which are then engulfed by keratinocytes via endocytosis ii) keratinocytes actively engulf the dendritic tips of melanocytes by phagocytosis iii) the active transfer or injection of melanosomes directly into keratinocytes iv) formation of a continuous pore between melanocytes and keratinocytes. While melanosome transfer is likely to occur in multiple ways, recent data now suggests that it might predominantly occur via the first postulated mechanism, as discussed below.

Pigment containing globules have been identified adhering to melanocyte dendrites in association with filipodia (Ando et al., 2011; Wu et al., 2012). The membrane-bound globules contain multiple tightly packed melanosomes. The 2-7μm structures strongly resemble shedding vesicles, which are also single membrane bound and have been found to transport a variety of cargo including DNA, mRNA, and lipids. Further studies indicate that the pigment globules are captured by keratinocyte microvilli in a PAR-2 dependent process (Ando et al., 2012). Keratinocytes had previously been shown to regulate melanosome transfer via PAR-2 (Seiberg et al., 2000). Following transfer melanosomes dispersed over several days to establish protective caps above keratinocyte nucleus (Ando et al., 2012).

While much has been learned about the function of melanocytes, an even greater body of literature has been accumulated about their developmental origins, in part because of the readily apparent phenotype arising from defects in melanocyte specification, proliferation, and survival.

Specification

Melanocytes are one of the many cell types derived from the multipotent NC. The fate choice of NC is determined in part by its axial level (Le Douarin et al., 2008; Lwigale et

al., 2004; Santagati and Rijli, 2003), whereby cranial NC from the mid/hindbrain region gives rise to jaw cartilage and glia, vagal and sacral NC differentiate into the enteric nervous system, while trunk NC derivatives include adrenal cells and sensory ganglia . While melanocytes were traditionally thought to emerge from the trunk NC (NIU, 1947), more recent studies in avian models have established a greater degree of plasticity than originally thought and have shown that melanocytes can also emerge from cranial NC (Baker et al., 1997).

The progressive lineage restriction of the multipotent NC population has been well studied, particularly in avian systems, and it has been established that melanocytes can arise from either multipotent or bipotent glial-melanocyte progenitors (Dupin et al., 2000) at both the cranial and trunk level (Baroffio et al., 1988, 1991; Bronner-Fraser and Fraser, 1989; Bronner-Fraser and Fraser, 1988; Cohen and Konigsberg, 1975; Sieber-Blum, 1989; Sieber-Blum and Cohen, 1980). Similar multipotent and bipotent NC progenitors have also been identified in mammalian studies (Ito et al., 1993). Specification subsequently proceeds through an unpigmented, melanocyte lineage committed cell known as a melanoblast. Depending on the specie, this lineage restriction can occur either premigration in the neural tube or after migration has commenced.

In addition to the presence of bipotent glial-melanocyte progenitors, a close relationship has also been established between glial and melanocyte fates on other fronts. It has been shown that exposure to endothelin (EDN) can revert melanocytes back to the bipotent progenitor state (Dupin et al., 2000). A recent study has further demonstrated that epidermal melanocytes can arise from Schwann cell precursors in nerve innervations (Adameyko et al., 2009).

Together these data suggest that, while during normal embryonic development, melanocyte specification proceeds through a progressively restricted series of progenitors, NC derivatives remain lineally associated and retain multipotency even after differentiation. Therefore specific environmental cues must be present to restrict melanocyte-fated cells to their lineage *in vivo*.

The microphthalmia-associated transcription factor, **MITF**, has been referred to as the "melanocyte master regulator" and its expression is often viewed as a hallmark of the melanocyte lineage (Reviewed in (Steingrímsson et al., 2004)). It is first expressed in melanoblasts shortly after neural crest emigration from the neural tube and in the migration staging area (MSA, discussed in greater detail below). In concert with its downstream target dopachrome tautomerase (Dct), it is frequently used to identify early melanoblasts *in vivo*. There are multiple isoforms of MITF, differing in their 5' first exons. Expression is controlled in a cell type specific manner by multiple promoters (reviewed in (Steingrímsson et al., 2004)). While the melanocyte-specific isoform, MITF-M, is uniquely expressed in melanocytes, other MITF isoforms are also detected in melanocytes. At least some of these alternate isoforms are however unable to transactivate melanocyte gene targets such as tyrosinase (Takemoto et al., 2002).

MITF acts to serves as a focal point integrating melanocyte specification signals and coordinating activation of downstream pathways regulating pigmentation (Dct, tyrosinase, Trp1) and later melanocyte survival (Bcl2) (Opdecamp et al., 1997). In fact, ectopic expression of MITF is sufficient to cause pigmentation and morphological changes in fibroblasts and RPE (Planque et al., 2004; Tachibana et al., 1996). While the reduction in cells expressing Dct in mice homozygous for severe MITF mutations (Opdecamp et al., 1997) and loss of melanophores in zebrafish lacking MITF (Lister et

al., 1999) suggest a role for MITF in early melanocyte development, Dct-expressing cells can in fact be transiently detected in the MSA in MITF-mutant embryos (Hornyak et al., 2001). Thus, while MITF appears to be critical for melanoblast development and survival, other upstream environmental cues may be responsible for actual melanocyte specification.

Wnt signaling has been shown to play a critical role in the specification of the melanocyte lineage in zebrafish (Dorsky et al., 1998), avian (Jin et al., 2001), and mouse (Dunn et al., 2000) embryos. In zebrafish, Wnt activation was found to promote melanocyte differentiation at the expense of neurons and glia, while inhibiton of the Wnt pathway increased neuronal fates (Dorsky et al., 1998). Wnt signaling promotes melanocyte specification through its effects on MITF. Wnt3a expression precedes MITF expression (Nakayama et al., 1998; Takada et al., 1994) and both treatment with exogenous Wnt3a (Takeda et al., 2000) and overexpression of β-catenin (Widlund et al., 2002) increase levels of MITF. Three highly conserved Tcf/Lef binding sites have been identified in the zebrafish, mouse, and human MITF-M promoter that have further been shown to be actively bound by the Tcf/Lef/β-catenin complex and which are required for MITF transcription (Dorsky et al., 2000; Saito et al., 2002; Takeda et al., 2000; Widlund et al., 2002). Following MITF induction, the Wnt pathway further cooperates with MITF itself to further regulate the MITF and Dct promoters (Saito et al., 2002; Yasumoto et al., 2002).

It has recently been suggested that Wnt signaling promotes melanocyte lineage within a very narrow window of time (Hari et al., 2012). Conditional activation of β-catenin was found to promote the formation of ectopic melanoblasts only when timed with migration of NC. Activation in premigratory NC was found to enhance differentiation of sensory

neurons while later activation did not expand the melanocyte population. However this is in contrast to findings in zebrafish were activation in premigratory NC, promoted melanocyte fate (Dorsky et al., 1998). Again, this is likely due to species specific differences in the timing of melanocyte specification.

Antagonistic roles for Wnt and BMP signaling in promoting a NC lineage fate switch have been observed in quail embryos (Jin et al., 2001). While Wnt expression is observed in the trunk dorsal neural tube at the time of NC migration, neuronal and glial precursors also express the Wnt inhibitor cfrzb-1 while melanoblasts do not. *In vitro* exposure of quail NC to Wnt enhanced the yield of melanocytes at the expense of neurons and glia, independently of proliferation. In contrast to Wnt, **BMP** is expressed throughout dorsal neural tube during NC migration, but is downregulated at the time of melanocyte migration, which, in avian models, occurs after the migration of other NC lineages. Exposure to exogenous BMP4 *in vitro*, promoted expansion of neurons and glial cells while reducing the number of pigmented cells, again independently of proliferation (Jin et al., 2001).

In contrast to these findings, a recently published protocol for the derivation of melanocytes from human embryonic stem cells through a neural crest progenitor state, found that pigmented cells could be established in the presence of an intermediate level of BMP4 (Nissan et al., 2011). While BMP4 was originally included for the purpose of supporting NC induction, it was not removed from culture conditions until after pigmented colonies had been established. However, populations established under these conditions included contaminating cell types, including CNS-derived RPE, and the authors did not investigate whether earlier withdrawal of BMP4 would have enhanced melanocyte yield.

While not strictly required for melanocyte lineage specification, **endothelin** signaling has been shown to be important for the expansion of the melanoblast pool. Mice lacking either the endothelin-B receptor (EDNRB) or its ligand, endothelin-3 (EDN3) exhibit pigmentation defects (Baynash et al., 1994). In the mouse, EDNRB expression is observed in a subpopulation of premigratory and migrating NC and has been found to play an indispensible role in melanocyte development during a narrow window between embryonic day (E) 10.5 to E12.5 (Shin et al., 1999). However EDN signaling has also been implicated in distinct roles in later stages of melanocyte differentiation when it promotes expansion and survival of the melanocyte progenitor pool (Lahav et al., 1996). The observation that zebrafish express EDNRB early in migratory NC populations while pigmentation defects are not observed until later in development has led to the suggestion that the involvement of EDN signaling in melanocyte differentiation may be species specific while its role in early melanocyte precursor expansion and migration appears to be universal (White and Zon, 2008). In vitro, addition of exogenous EDN3 has been found to promote expansion of a glial-melanocyte bipotent progenitor and can support reversion of differentiated melanocytes back to this bipotent state (Dupin et al., 2000). The EDN pathways appears to signal through both the phosphorylation of MITF and enhanced expression of MITF (Sato-Jin et al., 2008).

While Wnt and EDN signaling have been shown to directly affect MITF levels, additional factors are involved in the regulation of MITF expression.

The MITF promoter is directly bound by the transcription factors **Sox10** and **Pax3** (Bondurand et al., 2000) However loss of Pax3 merely results in reduced expansion of the melanocyte progenitor population (Hornyak et al., 2001). Loss of Sox10 on the other

hand results in a complete absence of MITF and Dct expressing cells migrating from the neural tube in mouse embryos (Bondurand et al., 2000; Britsch et al., 2001). This result is also born out in zebrafish and xenopus, where it was further demonstrated that Sox10 overexpression expands the pigment cell population (Aoki et al., 2003; Dutton et al., 2001; Elworthy et al., 2003).

Some species-specific differences regarding the role of Sox10 in melanocyte specification and development have been reported. In zebrafish, not only is Sox10 downregulated after early differentiation (Dutton et al., 2001) but the pigmentation loss observed in Sox10-mutant embryos can be fully rescued by MITF overexpression, suggesting that the primary function of Sox10 in zebrafish is the transcriptional activation of MITF (Elworthy et al., 2003). In contrast, Sox10 expression is maintained in the melanocytic lineage in mice (Wong et al., 2006) and MITF gain-of-function is insufficient to rescue melanocyte defects in Sox10-mutant mice (Hou et al., 2006), suggesting that Sox10 may fulfill additional functions in mammalian melanocytes. This is additionally supported by the observation that MITF, Sox10 double mutant mice exhibit more extensive hypopigmentation than either mutant alone (Potterf et al., 2000). It appears that in mice Sox10 is required to synergistically transactivate the Dct promoter with MITF, as MITF alone is not sufficient to do so (Britsch et al., 2001; Jiao et al., 2004; Potterf et al., 2001).

However, Sox10 and Pax3 (as well as Wnt3a, which will be discussed in the following section) are all expressed in the neural tube prior to melanoblast migration and MITF expression (Bondurand et al., 1998; Cheng et al., 2000; Jin et al., 2001; Kuhlbrodt et al., 1998; McKeown et al., 2005; Otto et al., 2006). This suggests that either additional factors are required for the activation of MITF or that an inhibitor prevents the induction

of MITF in early-migrating NC. A recent study has implicated **FoxD3** as a transcriptional repressor fulfilling this role (Thomas and Erickson, 2009). The winged-helix transcription factor, FoxD3, has been shown to be expressed in all NC except for late migrating presumptive melanoblasts (Kos et al., 2001). *In vitro* and *in vivo* knockdown in avian models results in expansion of melanoblast lineage while overexpression prevents melanoblast development (Kos et al., 2001). The authors were subsequently able to demonstrate that FoxD3 does not directly inhibit transcription from the MITF-M promoter, but rather interacts with Pax3 to prevent its activation of MITF (Thomas and Erickson, 2009). Overexpression of Pax3 was therefore sufficient to rescue FoxD3-mediated repression of MITF transcription. However, in mice FoxD3 expression was observed in all NC populations including presumptive melanoblasts migrating along the dorsolateral pathway (Dottori et al., 2001). This may reflect a species specific difference in the timing of melanoblast specification, as melanoblasts in mice also migrate concurrently with other NC populations, as opposed to the chick where melanoblasts migrate later. In mice, FoxD3 downregulation was observed as melanocytes began to differentiate in the epidermis, further suggesting that FoxD3 inactivation may be required for melanocyte differentiation. FoxD3 therefore appears fulfills a critical role in regulating the lineage switch between NC fates, in particular between glia and melanocyte.

To summarize, specification of the melanocyte lineage from multipotent NC progenitors requires Wnt signaling which, in concert with Sox10 and Pax3, activate MITF and downregulate inhibitory FoxD3 (**Figure 1.7**). This in turn triggers the activation of a melanocyte-specific battery of factors involved in pigmentation and cell survival. Endothelin signaling is required for further expansion of the melanoblast progenitor pool. As already noted, the actual timing of melanocyte specification appears to vary between

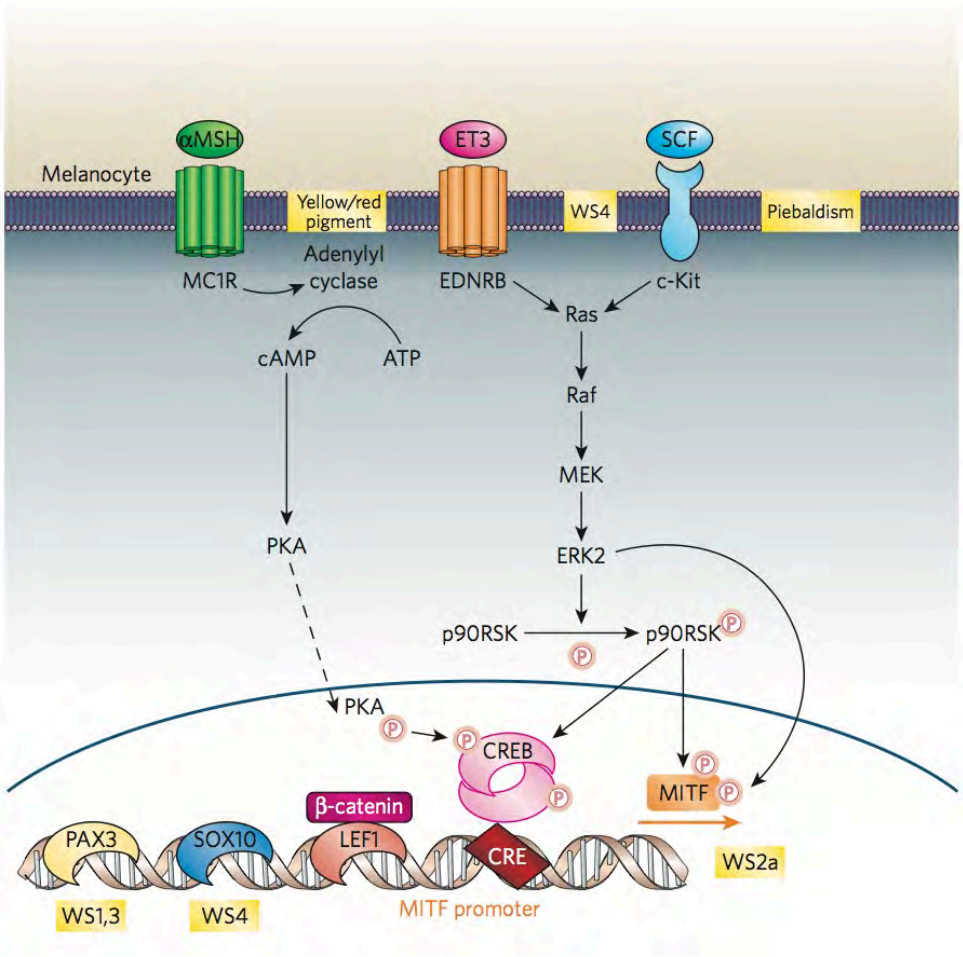

Figure 1.7. Multiple signaling pathways converge on the regulation of the MITF promoter. The transcription factors PAX3, SOX10, LEF-1/TCF and CREB directly regulate the MITF promoter during melanocyte development. The stability of MITF is additionally controlled by post-translationally modifications affected SCF/KIT signaling through the mitogen-activated protein kinase (Ras/Raf/MEK/ERK) pathway. “Adapted by permission from Macmillan Publishers Ltd: NATURE, 445(7130), 843-50, copyright 2007.”

avian and mammalian models, with melanocyte specification occurring in the premigratory NC in avian models and in postmigratory NC in mouse embryos.

Migration

Species specific differences also exist for melanocyte migration. Traditionally, NC migration had been thought to occur in two, both spatially and temporally segregated, waves. Non-melanocyte NC lineages were thought to migrate first along a ventromedial pathway through the anterior part of the somites to eventually give rise to components of the PNS (Teillet and Le Douarin, 1970). In contrast, migration of melanocyte progenitors, was thought to occur a day later, with cells temporarily accumulating between the dorsal neural tube and adjacent somites, in an area known as the migration staging area (MSA) (Erickson et al., 1992; Weston, 1991). Upon migration, melanocyte progenitors then followed a dorsolateral pathway, between the ectoderm and somites (Serbedzija et al., 1989; Tosney, 1978). It was originally thought that early- and late-migrating NC populations differed in their melanogenic potential, with only late-migrating NC exhibiting melanogenic competence (Kitamura et al., 1992). More recent work has clarified that while early migrating NC possess the competence to form melanocytes, for example if exposed to appropriate environmental cues following heterochronic transplantation into older embryos (Baker et al., 1997), they do not typically encounter these signals during normal development due to their active exclusion from these environments during migration (Erickson and Goins, 1995). Moreover, it has now been shown that the spatial and temporal segregation of melanocyte migration observed in the chick *in vivo* may only occur in the avian trunk since subectodermal migration of more rostral NC populations can be observed early in the chick (Thiery et al., 1982).

In zebrafish, cells expressing melanocyte-associated markers were identified within both the dorsolateral and ventromedial pathways (Camp and Lardelli, 2001) while in mouse embryos migration of melanocyte progenitors is not temporally segregated from the migration of non-melanocyte lineages and migration along the dorsolateral pathway commences concomitantly with migration along the ventromedial pathway (Serbedzija et al., 1990). Nevertheless, while melanocytes may not migrate exclusively along the dorsolateral pathway, it does still appear that the melanocyte progenitors are the only NC subpopulation to migrate along the dorsolateral pathway while non-melanocyte lineages are actively excluded from this pathway. Additionally, the recent observation that some melanocytes may arise from Schwann cell precursors has now opened investigations into an additional much later stream of migration along the nerve fibers (Adameyko et al., 2009).

The control of melanoblast migration is at least partially controlled by Eph/ephrin signaling. In chick embryos, the expression of ephrin-B ligands in the dorsolateral pathway was found to actively repel the migration of early migrating NC cells (Santiago and Erickson, 2002). Transmembrane ephrins however continue to be expressed along the dorsolateral pathway and act as bifunctional guidance cues, actively stimulating the entry of later-migrating melanoblasts.

While the additional molecular mechanisms regulating migration are still under investigation, a key player identified in melanoblast migration is KIT. The study of mouse spotting mutants has revealed a particular role for signaling through the c-kit receptor in melanocyte migration, as well as other melanocyte functions (Baxter et al., 2004; Jackson, 1994). Both the genes for the **c-kit** receptor and ligand (steel factor or stem cell factor, **SCF**) are embryonic lethal as homozygotes, but show lineage restricted defects

of melanocytes, hematopoietic cells, germ cells and gut interstitial cells of Cajal in heterozygotes (Williams et al., 1992). The roles of c-kit and SCF signaling in melanocyte development have been investigated extensively (reviewed in (Yoshida et al., 2001)).

The requirement for c-kit at different stages of melanocyte development has been carefully examined through the injection of c-kit blocking antibody ACK2 *in utero* (Yoshida et al., 1996). It was found that c-kit is required, in combination with EDN3, for migration into the dermis. This is followed by a c-kit independent stage during which melanocytes establish themselves in the epidermis. Subsequent melanocyte proliferation in the epidermal layer is again c-kit dependent and also requires endothelin receptor B, although not EDN3. In mice, which largely lack epidermal pigmentation, this is again followed by a c-kit independent step during which melanocytes integrate into developing hair follicles.

Consistent with these inferences, studies of mouse and avian NC melanogenesis in vitro suggest that SCF promote survival and moderate proliferation of melanocytes and their precursors (Murphy et al., 1992; Morrison- Graham and Weston, 1993; Lahav et al., 1994; Reid et al., 1995).

Distinct roles for soluble and membrane bound SCF ligand in promoting melanocyte survival have also been identified, with the former being required for early melanoblast survival, while the latter is required later in the dermis (Wehrle-Haller and Weston, 1995). Notably, transgenic expression of SCF in keratinocytes is sufficient to support homing of melanocytes to the basement membrane in mice, which otherwise lack epidermal melanocytes (Kunisada et al., 1998a; Kunisada et al., 1998b).

In the chick embryo, prospective melanocytes have completed their invasion of the epidermis and differentiate into pigment cells in the epidermis by stage 25. In mouse, melanoblasts invade and disperse within the epidermis by E13 (Kelsh et al., 2009). Human melanocytes can be detected in the epidermis as early as 50 days gestation. As gestation progresses, dermal melanocytes decrease in number until they are nearly undetectable by birth. In contrast, epidermal melanocytes that have established themselves at the basement membrane continue to proliferate and mature (Costin and Hearing, 2007).

Melanocyte Stem Cells

In the adult mouse, where the majority of melanocytes reside in the hair follicle, it has been well established that a population of melanocyte stem cells (MSCs) can be found in the bulge region of the hair follicle. These cells can be identified on account of their expression of Dct and are capable of self-renewal (Nishimura et al., 2002). The existence of an MSC population in the hair follicle is not surprising, as melanocytes associated with the hair follicle must proliferate and differentiate in close coordination with the hair regeneration cycle (Slominski and Paus, 1993). A gene expression profile of isolated and purified MSCs using single cell cDNA amplification found that while MSCs do express Dct and Pax3, they do not express Sox10, MITF, or c-kit, all markers associated with the melanocyte progenitor stage during embryonic development (Osawa et al., 2005). While this may reflect inherent differences between embryonic and adult stem cell populations, another study using a Pax3 reporter system to identify MSCs in the hair follicles did find that MSCs in this expressed both MITF and Sox10 (Lang et al., 2005). In this study Pax3 was found to play a pivotal role in initiating a melanogenic cascade by activating MITF, while simultaneously inhibiting further differentiation.

While these studies have shown the presence of a population of MSCs in the hair follicle bulge that can repopulate the melanocytes contributing to hair pigmentation, these studies did not address whether the progeny of the same MSCs can migrate out of the hair follicle to contribute to epidermal pigmentation. This question is complicated by the inherent differences in mouse and human skin architecture, whereby mice largely lack epidermal melanocytes. However it has been demonstrated that ectopic expression of SCF by keratinocytes can support the establishment of epidermal melanocytes in mice, suggesting that hair follicle bulge MSCs may be competent to contribute to an epidermal melanocyte population as well (Kunisada et al., 1998a; Kunisada et al., 1998b).

There has also been evidence that a multipotent population of NC stem cells with melanocyte competence can be derived from different regions of both mouse and human skin, although it remains to be addressed whether these cells act as bona fide MSCs *in vivo.* In mice, a multipotent population of NC stem cells (NCSCs) residing in the bulge of hair follicles has been identified on account of Wnt1 expression in the epidermis (Sieber-Blum et al., 2004; Sieber-Blum and Hu, 2008). A comparable population of human NCSCs has also been isolated (Clewes et al., 2011). Another study has reported the isolation of a melanocyte-competent, neural crest-derived multipotent stem cell-like population expressing p75 and Sox10 from mouse and human skin (Wong et al., 2006).

Isolation of dermal-derived NCSCs, termed skin-derived precursors (SKPs), has been reported in both mouse (Toma et al., 2001) and human (Toma et al., 2005) systems. Human SKPs were derived from neonatal foreskin and were shown to self-renew *in vitro* in the presence of FGF2 and EGF. While mouse and human SKPs were shown to be multipotent with directed differentiation yielding neurons, glia, and smooth muscles, the authors did not investigate differentiation of SKPs along the melanocyte lineage.

However a more recent study reports the isolation of functional human melanocytes from a similar population of foreskin-derived dermal stem cells, expressing p75, nestin, and Oct4 (Li et al., 2010). As foreskin is comprised of glabrous skin and is devoid of hair follicles, this population of stem cells must be different from hair follicle MSCs described in the mouse. It has however not been demonstrated that this population of NCSCs contribute to the epidermal melanocyte population *in vivo*, and further study will be required to dissect the potential contribution of these different stem cell populations.

Finally, as alluded to in the discussion above, it has been recently established that melanocytes can also arise from Schwann cell progenitors associated with nerve fibers (Adameyko et al., 2009). It is currently unclear whether or not melanocytes in the adult repopulate through this mechanism.

Derivation of Melanocytes from Murine ESCs

Like early neuronal and NC-derivation protocols, the first successful derivation of melanocytes from mouse ESCs required co-culture with a bone marrow-derived stromal cell line, previously shown to support hematopoietic differentiation (Yamane et al., 1999). In the presence of dexamethasone and FGF2 a small but reproducible percentage of melanocytes could be established within 21 days, with early markers of melanoblast specification such as MITF and Dct detected by day 6 of differentiation. While melanocyte specification was found to be dependent on dexamethasone, melanocyte proliferation could be enhanced by addition of exogenous EDN3. Induction was further found to be dependent on SCF production by the ST2 stromal line as treatment with the c-kit blocking antibody ACK2 abolished melanocyte differentiation. This highlights the difficulty in identifying the requirements for melanocyte specification and differentiation in an undefined system where the analysis is inevitably complicated by the contribution of

factors produced by the stromal feeder layer. The authors later found that efficiency of melanocyte induction is highly ES line dependent, with some lines never supporting melanocyte induction (Yamane et al., 2002).

The same group subsequently used genetic tools to further investigate the requirements for melanocyte specification and differentiation in their system. A mESC reporter line established from a *Dct::lacZ* transgenic strain was used to demonstrated that addition of dexamethasone, FGF2, and cholera toxin were sufficient to obtain optimal specification of a Dct expressing melanoblast population (Pla et al., 2004). While EDN3 was found to be dispensable for melanoblast specification, addition of exogenous EDN3 promoted expansion of melanocyte yield (Pla et al., 2004), recapitulating the known role of endothelin signaling observed *in vivo*.

In an elegant demonstration using a EDN3 defective strain the authors later showed that proliferation of melanoblasts in their system was partially promoted by autocrine EDN3 signaling (Aoki et al., 2005). Differentiating cells began producing endogenous EDN3 beginning at day 8 of melanocyte induction. Melanocyte induction in EDN3 null cells could be rescued by the addition of exogenous EDN3. Similarly, melanocyte differentiation was lost when a c-Kit mutant ES line was used, however addition of high amounts of exogenous EDN3 (up to 200ng/ml) could partially rescue melanocyte differentiation in the absence of KIT signaling. These rescue effect of EDN3 were confirmed *in vivo* by crossing a kit mutant strain with a strain conditionally overexpressing EDN3 in the skin (Aoki et al., 2005).

While this system highlighted the requirement for SCF and EDN3 in the establishment of a melanocyte population from ESCs in a stromal coculture system, supplementing the

culture conditions with exogenous recombinant factors was not sufficient to support melanocyte induction in the absence of stromal feeders (Motohashi et al., 2006). Additionally, the authors did not address the requirement for Wnt signaling in melanocyte induction, speculating that it was produced by the ST2 stromal feeder cells (Motohashi et al., 2006). This highlights the difficulty in identifying signaling inputs under non-defined culture systems.

Derivation of Melanocytes from Human ESCs

Wnt signaling was however found to be critical for melanocyte induction from human ESCs (Fang et al., 2006). In this approach, embryoid bodies (EBs) were established from hESCs and subsequently cultured in conditioned media from a Wnt3a producing fibroblast line supplemented with EDN3 and SCF (as well as dexamethasone, cholera toxin, FGF2, ascorbic acid, and TPA). Under these conditions pigmented cells could be established within nine weeks with high efficiency and purity. hESC-derived melanocytes expressed MITF, c-kit, Dct, Tyr, Tyrp1, Sox10, and Pax3 and displayed a stable phenotype both in long term culture and after transplantation. However, recombinant Wnt3a was not sufficient to replace the conditioned media component, while the identification of early signaling events was complicated by the use of a poorly defined embryoid body based differentiation system.

A more recent study adapted a previous protocol for the derivation of keratinocytes that applied high concentrations of BMP4 and ascorbic acid to hESC in coculture with 3T3 stromal cells (Nissan et al., 2011). It was hypothesized that this protocol might be adaptable for the derivation of other ectodermal derivatives by manipulating BMP levels. An intermediate level of BMP was found to support induction of a p75+/HNK1+ NC population with a yield up to 36%. However, pigmented cells established by day 60

included a substantial population of contaminating RPE, as evidenced by the expression of Pax6 and multiple RPE markers. Mechanical dissociation and further expansion in melanocyte media was required to propagate a pure population of melanocytes. The authors did not investigate the further requirements for neural crest or melanocyte lineage specification beyond BMP. Presumably factors such as Wnt, EDN3, and SCF, known to be required for melanocyte induction, proliferation, and survival, were being produced spontaneously by the 3T3 stromal cell line. Neither the kinetics of melanocyte marker induction nor the efficiency of melanocyte derivation were investigated. Additionally, the presence of a large percentage of contaminating cells, including CNS-derived RPE, suggest that the conditions presented here remain far from optimal for both NC and melanocyte induction (Nissan et al., 2011).

While it has been shown that melanocytes can successfully be derived from ESCs, and particularly in the case of mESC-derived melanocytes have confirmed that *in vitro* conditions recapitulate the known roles of signaling pathways reported *in vivo*, many outstanding questions remain untractable in the absence of a defined differentiation system.

Pigmentation Disorders

Pigmentation disorders can arise from defects at multiple points in melanocyte development or melanin production. Hypopigmentation can reflect deficits in melanocyte formation or migration to the skin (Waardenburg syndrome, piebladism, Tietz Syndrome), melanin synthesis within melanosomes (oculocutaneous albinism), melanosome formation in the melanocyte (Hermansky-Pudlak Syndrome, Chediak-Higashi Syndrome), or transfer of mature melanosomes to the tips of dendrites (Griscelli Syndrome Type).

Piebaldism is an autosomal dominant disorder in which depigmented patches of skin, and to a lesser extent hair, completely lacking melanocytes can be found (Boissy and Nordlund, 1997). The severity of the disease can vary drastically, from isolated ventral depigmentation and accompanying white forelock to near complete body depigmentation. However, unlike WS, patients with piebaldism do not present with sensorineural deficits as melanocytes in the eye and ear remain unaffected. Piebaldism has been correlated with mutations in *KIT* and *SLUG*, while mutations in *SCF* cause a piebald-phenotype in the mouse strain, *steel* (Dessinioti et al., 2009).

Waardenburg Syndrome (WS) is an autosomal dominant disorder that is caused by mutations in either the PAX3, MITF, SLUG, SOX10, EDN3, or EDNRB genes (Dessinioti et al., 2009). WS can be classified into four clinical subgroups, depending on symptom presentation. While all patients with WS present with pigmentation defects similar to those observed with piebaldism, patients also experience additional sensorineural deficits, in particular deafness due to loss of melanocytes in the inner ear (Boissy and Nordlund, 1997). Depending on disease subtype, patients may also exhibit craniofacial defects, axial and limb musculoskeletal anomalies, or congenital aganglionic megacolon due to additional involvement of the enteric nervous system (Hornyak, 2006).

Tietz Syndrome arises from a mutation in the DNA binding domain of MITF and combines symptoms of both WS and oculocutaneous albinism (OCA) (Hornyak, 2006). Like patients with WS, Tietz Syndrome patients present with congenital deafness, however they do not exhibit heterochromia irides or patchy pigmentation. Instead, Tietz Syndrome patients display generalized depigmentation like that observed in OCA.

Oculocutaneous albinism (OCA) is the most commonly known hypopigmentation disorder. It results from a defect in melanin production itself, due to complete or partial loss-of-function of tyrosinase or other key pigment enzymes, such as P gene, Tryp1, or MATP depending on OCA subtype (Brilliant, 2001; Dessinioti et al., 2009). Melanocytes themselves develop normally and remain intact. Lack of or significantly reduced pigment is observed in most tissues, including the skin, hair, and eyes and is accompanied by reduced visual acuity with nystagmus and photophobia. However depending on disease subtype, some patients may accumulate some pigment over time or in certain areas of the body.

Hypopigmentation may also arise from defects at discrete steps of melanosome formation, maturation, or trafficking. Griscelli Syndrome, Hermansky-Pudlak Syndrome, and Chediak-Higashi Syndrome all fall into this category of diseases.

Griscelli Syndrome is an autosomal recessive disorder in which genes involved in maintaining the association between melanosomes and the actin network are affected (Dessinioti et al., 2009). Depending on disease subtype, mutations may be found in either myosin 5A, RAB27A, or the melanophilin gene (Van Gele et al., 2009). Griscelli Syndrome patients experience pigmentary dilution of the skin, silver-grey sheen to the hair, large clumps of pigment in the hair shafts, as well as accumulation of large, end-stage melanosomes near the centers of melanocytes (Van Gele et al., 2009). Patients may also exhibit neurological impairment and immune defects.

Hermansky-Pudlak Syndrome

Hermanksy-Pudlak Syndrome (HPS) is a genetically heterogeneous group of related autosomal recessive disorders that share symptoms of OCA and platelet storage

disease while additional symptoms depend on disease subtype (Wei, 2006). To date eight different subtypes of HPS have been described in humans with corresponding mutations in factors involved in membrane and protein trafficking. 16 genes have so far been identified to cause HPS in mice, including 8 orthologous to the known human genes (Li et al., 2004). Presumably additional human HPS subtypes corresponding to the remaining murine strains will be described in time. While all HPS-associated genes are ubiquitously expressed, mutations result in phenotypes restricted to specialized secretory cell types. These defects involve the biogenesis and/or function of lysosome-related organelles (LROs) that affect specialized secretory cells including melanocytes, platelets, T cells, neutrophils, and pulmonary type II epithelial cells (Wei, 2006). All LROs share at least one integral membrane protein with lysosomes and also demonstrate acidic intraluminal pH. The degree of hypopigmentation in HPS patients is extremely variable, ranging from minimal to severe reduction in skin, hair, and ocular pigmentation although the tanning response is almost always impaired (Boissy and Nordlund, 1997).

While the study of mouse models have certainly illuminated the field of HPS, most mouse strains do not harbor the same mutations as are observed in human mutations. Since disease severity can vary significantly with mutational status, the phenotypes observed in mice may not accurately reflect the human condition (Wei, 2006). Furthermore, the low frequency of HPS in humans, in some cases only one to three patients with a given subtype of HPS have been described, makes it difficult to ascertain or attribute mutational consequences and control for background genetic effects. This makes HPS highly suitable for iPS-based disease modeling in which melanocytes derived from patient-specific iPSCs are used to establish a system for further studies of disease mechanism.

The protein complexes affected in a number of HPS subtypes have already been discussed in the previous section describing melanosome formation. To summarize, HPS1 and HPS4 are caused by mutations in members of the BLOC-3 complex, HPS2 is associated with mutations in a AP-3 protein, while HPS3, HPS5, and HPS6 arise from defects in BLOC-2 complex proteins.

We will focus primarily on the clinical features of HPS1 and HPS2 as these will be represented in the disease modeling section of this work.

HPS1 - Clinical Presentation

HPS1 is the most common HPS subtype, and occurs most frequently in the Puerto Rican population. Amongst Puerto Ricans, the most frequent mutation is a 16bp frameshift duplication in exon 15 (Wei, 2006). This mutation is associated with a severe clinical phenotype encompassing restrictive lung disease, hemorrhage, and granulomatous colitis. The symptoms of restrictive lung disease first manifest themselves on average at 35 years of age, with resulting mortality on average at age 37. However disease severity can vary widely between individuals. Patients also frequently experience prolonged bleeding that is however treatable with platelet transfusion. Decreased visual acuity in HPS1 patients is accompanied by hypopigmentation of the iris, choroid, and retina, although these phenotypes do not necessarily correlate directly with skin hypopigmentation. Reduced skin and hair pigmentation is also highly variable among patients, although both hair and skin tend to darken with age. Additional mutations of the HPS1 gene have also been reported, although these are again associated with variable disease severity.

HPS1 - Gene structure and cell biology

The HPS-1 gene is 30.6kb with 20 exons. Both a major (3.0kb) and minor (3.9kb) form of mRNA can be detected due to the use of alternate polyadenylation sites. The 79.2 kDa protein is ubiquitously expressed, and localization primarily observed in the cytoplasm, although a membrane-associated subfraction can also be detected. In HPS1 melanocytes a more perinuclear and granular distribution is observed when compared to control melanocytes (Oh et al., 2000). Immunocytochemical analysis confirms colocalization of HPS1 with tyrosinase and DCT in early melanosomes (Oh et al., 2000). HPS1 appears to be involved in regulating protein trafficking to the melanosomes as melanocytes from HPS1 patients, contain tyrosinase, Tyrp1, and Dct in abnormal large structures in the cell body and dendrites (Richmond et al., 2005). This mislocalization of tyrosinase appears to result in decreased melanin production (Boissy et al., 1998). HPS1 has been shown to associate with HPS4 in the BLOC-3 complex, although results from a yeast-two-hybrid screen suggest that the binding is not direct and at least one other subunit contributes to the BLOC-3 complex (Wei, 2006).

HPS1 - Mouse Model

Murine HPS1 is 81% identical to human HPS1and two mutant allelic strains of the HPS1 model, pale ear (*ep*), have been sequenced (Feng et al., 1997; Gardner et al., 1997). Macromelanosomes can be observed in the choroid of the eye and in cultured melanocytes from HPS1 mutant mice (Gardner et al., 1997), although these enlarged melanosomes are not observed *in vivo* (Nguyen et al., 2002). This reflects observations made in the human system in which enlarged melanosomes can be detected in cultured melanocytes from HPS1 patients, but not always in patient primary skin (Sarangarajan et al., 2001; Toro et al., 1999). Both HPS1 and HPS4 mouse strains differ from other HPS strains in having a coat color that is similar to parental strain, but hypopigmented ears,

tails, and paws due to decreased number of dermal melanocytes at these sites. Whether this reflects defects in melanocyte migration, survival, or proliferation to these areas will require further study (Wei, 2006).

HPS2 - Clinical Presentation

HPS2 can be distinguished from other HPS subtypes by the additional occurrence of immunodeficiency, neutropenia, and susceptibility to recurrent respiratory illness. HPS2 strongly resembles Chediak-Higashi Syndrome (CHS) in these symptoms, however the cells of HPS2 patients lack the large intracellular granules that are a hallmark of CHS (Wei, 2006).

As of 2006 only four patients with HPS2 had been reported in the literature (Clark et al., 2003; Huizing et al., 2002). Two brothers with compound heterozygous mutations in the *AP3B1* gene that resulted in reduced but detectable amounts of β3A protein (Dell'Angelica et al., 1999) have been reported. The patients experienced neutropenia that led to recurrent upper respiratory infections and otitis media. The patients also suffered from hip dysplasia and neurological abnormalities including poor balance. Dermatological symptoms included acanthosis nigricans and hypertrichosis (Shotelersuk et al., 2000).

A young patient with a very severe phenotype resulting from compound heterozygous nonsense mutations at R509X and E659X had no detectable β3A mRNA or protein. The patient required continual oxygen supplementation due to severe respiratory infections, G-CSF administration to treat neutropenia, and platelet transfusions to prevent hemorrhaging. Defects in melanocyte function were reflected in mild conductive hearing

loss and ocular and dermal albinism, although a reduced tanning response was possible (Huizing et al., 2002).

A complete lack of β3A also resulted in symptoms of oculocutaneous albinism and platelet defects, with additional immunodeficiency that required prophylactic treatment with antibiotics and immunoglobulin in a fourth patient (Clark et al., 2003).

HPS2 - Gene structure and cell biology

HPS2 can be attributed to a mutation in the *AP3B1* gene which encodes the β3A subunit of the heterotetrameric adaptor protein complex AP-3 (Wei, 2006). The AP-3 complex has been shown to play a role in the selection of cargo proteins for vesicle transport and trafficking of membrane proteins to the lysosome. This cargo selection / sorting is mediated by the binding of AP-3 to amino acid-encoded sorting signals in the cytoplasmic tails of lysosomally targeted molecules. As a result, loss of β3A in cells of HPS2 patients results in increased cell surface expression of lysosome-targeted molecules (CD63/LAMP-3, LAMP-1, LAMP-2, CD1b) due to impaired trafficking to the lysosome. However this does not appear to centrally contribute to disease pathogenesis. Rather mistargeting of LAMP-1 is reflective of misregulated membrane trafficking while the disease phenotype results from disrupted trafficking to LROs in specialized cell types. For example, in cultured melanocytes from HPS2 patients, tyrosinase is mislocalized to the perinuclear region rather than normal perinuclear and dendritic distribution while the distribution of other melanosome-associated molecules such as Tyrp1 remains unchanged (Huizing et al., 2001b). This suggests that Tyrp1 may be targeted to melanosomes via an AP-3 independent pathway or that a Tyrp1 can be targeted by alternate pathway in absence of AP-3. Melanocytes from HPS2 further contain enlarged multivesicular structures resembling endosomes with intraluminal

tyrosinase enzyme activity that are only observed infrequently in control melanocytes (Huizing et al., 2001b). Interestingly, loss of the β3A subunit, may lead to destabilization of the entire AP-3 complex as other subunits were also undetectable at protein level in some patients with β3A mutation (Clark et al., 2003; Huizing et al., 2002)

HPS2 - Mouse Model

The mouse pearl strain (*pe*) is a model for HPS2. Pearl mice exhibit pigment dilution, kidney impairment, reduced platelet lysosomal enzyme secretion, and prolonged bleeding, the latter of which can be corrected with bone marrow transplant (Swank et al., 1998). Melanocytes from pearl mice also display the mislocalization of tyrosinse observed in human cells.

Other HPS Subtypes

As of 2006, twenty-one patients with **HPS3** had been reported (Wei, 2006). The clinical presentation of HPS3 is much milder than HPS1, with ocular albinism observed as the most significant defect. Melanocytes from HPS3 patients exhibit aberrant targeting of late melanosomes factors tyrosinase and Tyrp1, while the localization of early melanosome targets such as Silver/Pmel17/gp100 and melan-a/MART1 remained unchanged (Boissy et al., 2005). Patients also experience excessive bruising and epistaxis and minimal reduction in pulmonary function. HPS3 disease pathology is reflected in the cocoa mouse strain (*coa*). Cultured melanocytes from cocoa mice show little visible pigmentation and decreased melanin production compared to control melanocytes (Wei, 2006). Examination of dorsal follicular melanocytes by transmission electron microscopy showed abundant immature melanosomes indicative of a block in melanosomes biogenesis at the formation of stage II melanosomes (Nguyen et al., 2002).

HPS4 is often clinically comparable to HPS1 due to the involvement of both molecules in the BLOC-3 complex. Patients suffer from variable degrees of hypopigmentation however all report symptoms of platelet dysfunction (epistaxis and bruising) and have reduced visual acuity. Skin biopsies from HPS4 confirm a normal number of melanocytes in spite of reduced melanin content. The mouse strain light ear (*le*) also exhibits enlarged melanosomes in choroidal melanocytes, while dorsal epidermal melanocytes display small, abnormally shaped immature melanosomes both *in vitro* and *in vivo*.

Patients with **HPS5** experience nystagmus and visual impairment, bruising, an absence of platelet dense bodies but are free of pulmonary dysfunction, and inflammatory bowel disease (Wei, 2006). The HPS5 mouse strain, ruby eye-2 (r*u2*), has been shown to contain melanosomes with abnormal morphology in the eye and skin. In particular, an abundance of spherical immature melanosomes are observed, while fewer stage II melanosomes with characteristic ellipitical shape are encountered. These observations suggest that a defect in HPS5 results in a block in melanosomes biogenesis at the step between stage I and II melanosomes.

Three patients with mutations in **HPS6** have been reported in the literature (Zhang et al., 2003). Clinical manifestation of HPS6 included OCA and platelet dysfunction but no pulmonary or gastrointestinal symptoms. HPS6 is represented in the mouse strain ruby eye (*ru*).

The *DTNBP1* gene encoding the dysbindin protein is mutated in **HPS7**. A single patient reported in 2003 experienced OCA, platelet dysfunction (easy bruisability and bleeding

tendency), and mild pulmonary dysfunction. In sandy (*sdy*) mice, choroidal melanocytes show decreased numbers of small, irregularly shaped melanosomes, while melanosomes biogenesis was found to be blocked at or before stage I in dorsal follicular melanocytes

HPS8 is caused by a mutation in *BLOC1S3* that leads to OCA and mild platelet dysfunction that manifests as easy bruising, epistaxis, and hemorrhaging after surgery. The corresponding mouse strain, reduced pigment (*rp*) exhibits melanocytes with predominantly immature melanosomes that result in decreased melanin levels due to abnormal tyrosinase localization (Wei, 2006).

Chediak-Higashi Syndrome

Chediak-Higashi Syndrome (CHS) is a rare autosomal recessive disorder characterized by the presence of giant inclusions in granule containing cells, including enlarged melanosomes in melanocytes (Boissy and Nordlund, 1997). Defects in these cell types result in immune deficiency, variable degrees of OCA, and platelet storage pool deficiency.

CHS - Clinical Presentation

The hallmark feature of CHS is the presence of giant intracellular granules. In melanocytes, this takes the form of abnormally large, hypopigmented melanosomes that are unable to be transferred to neighboring keratinocytes (Zhao et al., 1994). Giant aggregates of melanin can also be observed by transmission electron microscopy (Valenzuela and Morningstar, 1981). This results in a characteristic silvery metallic sheen of the hair, although actual hair color can range from blond to light brown. Skin color may vary from white to gray tones, although the degree of pigment dilution may be

mild and may only be discernable in comparison with siblings. Hypopigmentation also extends to the eyes, with reduced melanin content observed in the retina, iris, and choroid (Huizing et al., 2001a). Visual acuity is also decreased in CHS patients, with additional symptoms of nystagmus and photophobia.

Platelet dysfunction in CHS is similar to HPS symptoms and takes the form of easy bruisability, mucosal bleeding, and epistaxis (Huizing et al., 2001a). A debilitating, recurrent manifestation of CHS are frequent infections, particularly of the skin and respiratory organs (Huizing et al., 2001a). Although treatable with antibiotics, response to treatment is slow. Patients suffer from neutropenia and a closer examination of CHS cells reveals the presence of giant granules in neutrophils, lymphocytes, eosinophils, and platelets that appear to hinder leukocyte migration. Impaired NK function is also observed which contributes to immune deficiency and the development of the accelerated phase (Abo et al., 1982).

It is thought that the lack of NK cell function allows for the sudden onset of an accelerated CHS disease phase that resembles infectious mononucleosis and which can present shortly after birth or many years later (Padgett et al., 1967). Other studies attribute the accelerated phase to uncontrolled T-cell and macrophage activation (Kaplan et al., 2008). Symptoms of the accelerated phase include fever, anemia, neutropenia and in some cases thrombocytopenia, hepatosplenomegaly, lymphadenopathy, and jaundice (Huizing et al., 2001a). Lymphohistiocytic infiltration into major organs of the body results in organ failure and morbidity (Kaplan et al., 2008). The persistence of the accelerated phase can be fatal unless patients are treated with a bone marrow transplant (Spritz et al., 2003). Bone marrow transplantation has been show to reverse the leucocyte defect in the mouse model of CHS, *beige* (Kazmierowski et al.,

1976) and in a clinical trial seven of 10 children who received a bone marrow transplantation none experienced recurrence of the accelerated phase (Haddad et al., 1995). Bone marrow transplantation does not however improve the progressive neuropathy associated with CHS.

CHS patients experience progressive primary neurological impairment that can take the form of peripheral or cranial neuropathy, autonomic dysfunction, sensory deficits, loss of deep tendon reflexes, seizures, and spinocerebellar degeneration (Introne et al., 1999). Pathological examination has revealed the presence of lymphohistiocytic infiltrates throughout the nervous system as well as cytoplasmic inclusions in cell types including astrocytes, Schwann cells, satellite cells of the dorsal spinal ganglia of some patients (Sung et al., 1969).

CHS - Gene structure and cell biology

There is evidence of locus variability in animal models of CHS including Aleutian mink, cattle, cats, killer whales, and rats (Introne et al., 1999), however in humans, mutation of the *LYST* gene is the only documented cause of CHS to date. The molecular diagnosis of CHS is however rendered difficult by the large size of the LYST gene (11kb) and because mutations have been identified throughout the entire length of the gene. It is therefore possible that additional genes will be implicated in human CHS with the advance of sequencing techniques in the future.

It is known from animal studies that mutations in *LYST* result in giant inclusions in granule-containing cells, however the mechanism by which this occurs and the role of *LYST* in normal cells is still under investigation. A series of HEAT- and ARM-like domains, known to be involved in vesicle transport and membrane association

respectively, have been identified in the LYST amino terminus while the presence of additional domains further suggest that LYST may function in vesicle trafficking along the microtubule system (Huizing et al., 2001a). It is thought that the C-terminus of LYST may function at the trans golgi network to sort proteins destined for endosomes and lysosomes while the N-terminus binds microtubules, allowing for the travel of vesicles to the cell periphery (**Figure 1.8**). The formation of giant vesicles in the absence of functional LYST remains to be explored, however additional studies have identified interactions between LYST and SNARES which may suggest a role for LYST in membrane fission and / or fusion events (Westbroek et al., 2007).

In melanocytes, loss of LYST results in a perinuclear accumulation of the melanosomal proteins tyrosinase and Tyrp1, rather than the normal even distribution throughout the cytoplasm (Zhao et al., 1994). This is due to a failure in the fusing of tyrosinase containing microvesicles with premelanosomes. Similar missorting of cytolytic enzymes in T- and NK cells results in defective cytotoxic activity in these cells (Introne et al., 1999).

CHS - Mouse Model

The human and mouse LYST proteins are 82% identical and 88% similar. The *beige* (*be*) mouse strain which carries a mutation in the *LYST* gene exhibits hypopigmentation of the coat and eyes (Lutzner et al., 1967). Like in humans, the degree of hypopigmentation can vary, however giant melanosomes are reproducibly observed. Importantly for disease modeling, *beige* mice do not experience the accelerated phase, although this may perhaps be attributable to the shorter lifespan of mice.

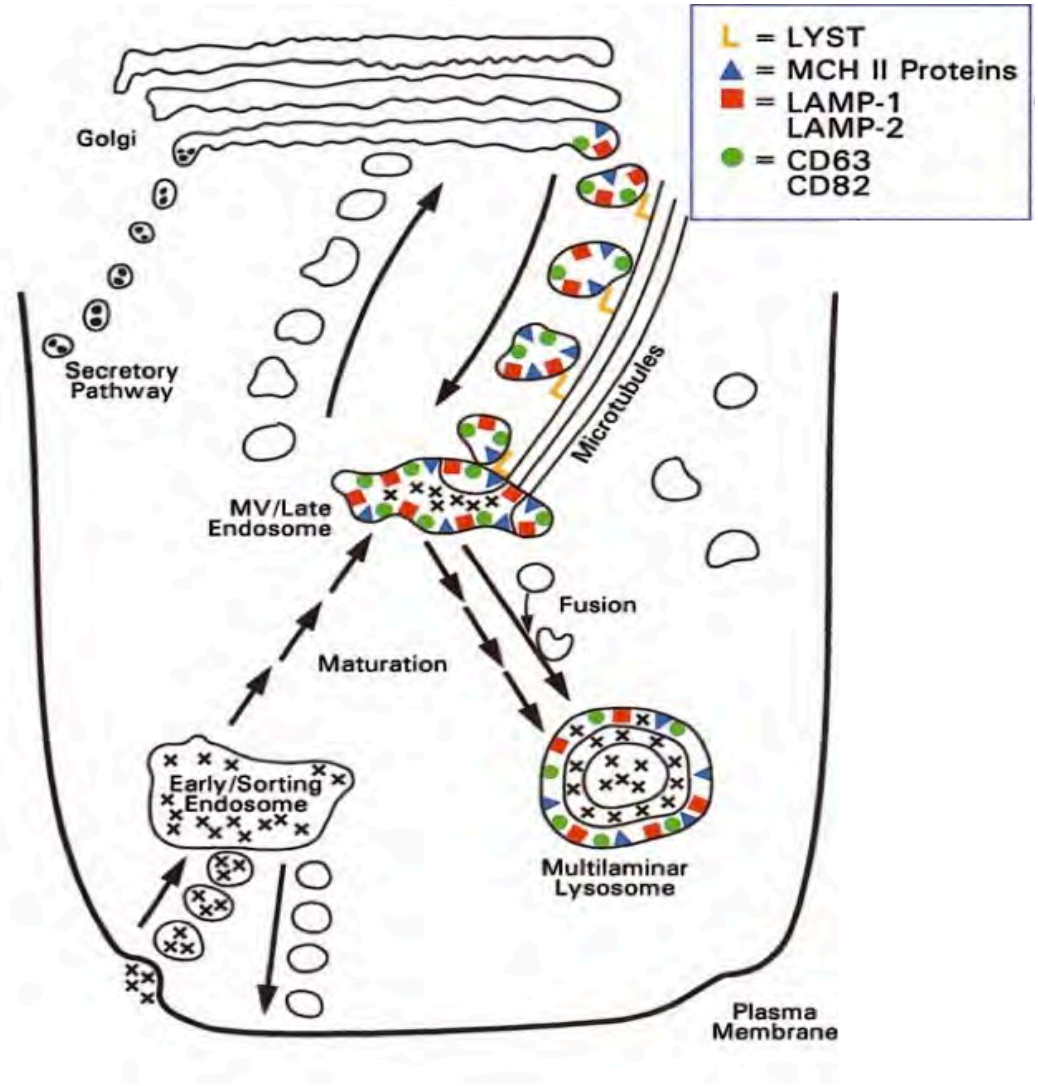

Figure 1.8. A simplified model for the role of LYST in vesicle trafficking. TGN-derived vesicles, including melanosomes, may attach to the microtubule network via LYST which then transports the vesicles to the cell periphery. In the absence of functional of LYST, as with Chediak-Higashi cells, immature vesicles accumulate in the perinuclear region and fuse to form giant granules. “Reprinted from Molecular Genetics and Metabolism, 68(2), Introne W, Boissy RE, Gahl WA., Clinical, molecular, and cell biological aspects of Chediak-Higashi syndrome, 283-303, Copyright 1999, with permission from Elsevier.”

Thesis Aims

The objective of this study was to use an ESC-based approach to establish a system for the stepwise induction of NC, melanoblast progenitors, and mature melanocytes. The approach was to fulfill the following three criteria:

1) Occur under **defined** conditions amenable for investigating the signaling requirements for neural crest and melanocyte specification and maturation.

2) Recapitulate the stepwise, **progressive** differentiation that occurs during development *in vivo* and allow us to isolate the different stages of neural crest and melanocyte maturation.

3) Be both **rapid** and **efficient** so as to be suitable for the generation of large numbers of pure melanocytes populations necessary for future high throughput screening studies.

In Chapter 3, we describe the adaptation of a protocol for the neural conversion of hESCs to rapidly and efficiently yield a population of *Sox10::GFP* expressing NC under defined, small molecule-based conditions. We demonstrate the expression of various neural crest associated markers within 11 days of differentiation and further explore the kinetics of neural crest specification. We further identify a unique competency window during which hESC-derived cells respond to NC-specifying WNT signals which drive NC induction within the context of our approach.

In Chapter 4, we identify a subpopulation of melanoblast progenitors within the NC population generated in Chapter 3. We establish that co-expression of *Sox10::GFP* and

c-kit are a suitable paradigm for the prospective identification and isolation of this population, the yield of which can be increased by exposure to BMP4 and EDN3. To our knowledge, this is the first report of the derivation of human melanoblasts from hESCs. We subsequently determine conditions for the maturation of these cells to a pigmented, functional state that closely resemble adult primary melanocytes.

In Chapter 5, we highlight the utility of our system for disease-modeling applications through a proof-of-principle demonstration in which we recapitulate known pigmentation defects in HPS- and CH-melanocytes derived from patient-specific iPSCs. The robustness of our differentiation protocol is demonstrated by the high degree of fidelity among melanocyte phenotypes derived from multiple iPSC clones.

Our results offer novel insights into human NC and melanocyte specification and present a defined and efficient protocol for generating human melanocytes from pluripotent stem cells that faithfully reproduce patient specific pigmentations defects.

CHAPTER TWO

Materials and Methods

Pluripotent Stem Cell Culture. Undifferentiated hESCs (H9/WA-09), and iPSCs were cultured on mitotically inactivated mouse embryonic fibroblasts (MEFs) in ES cell media containing 20% knockout serum replacement (KSR) as previously described (Kriks et al., 2011).

Neural Crest and Melanocyte Differentiation. Neural induction using the dual SMAD inhibition protocol was performed as previously described (Chambers et al., 2009; Chambers et al., 2011; Lee et al., 2010). Briefly, dissociated hESCs and iPSCs were plated on matrigel at a density of 18,000-25,000 cells/cm^2 in MEF-conditioned hES medium containing 10 ng/ml FGF2 and 10μM ROCK-inhibitor (Y-27632). Cells were allowed to reach 70-80% confluence over 3 days. Differentiation was initiated by switching to media that included knockout serum replacement media with 500nM LDN193189 (Stemgent) and 10μM SB431542 (Tocris). Beginning at day 4 the knockout serum replacement media was gradually replaced with increasing amounts of “N2” prepared media. For NC differentiation, the DSi protocol was adapted by treating with 3μM CHIR99021 (Stemgent) beginning day 2 and withdrawing LDN193189 and SB431542 at days 3 and 4 respectively. Melanocyte-biased NC (BE condition) cells were additionally treated with 25ng/ml BMP4 and 100nM EDN3 beginning at day 6 of differentiation. Cells were collected on day 11 for analysis or passaging.

Melanocyte Maturation and Maintenance. Day 11 dissociated BE-derived cells were replated on poly-ornithine, laminin, and fibronectin coated plates in NB/Mel media.

NB/Mel media was prepared by replacing the WNT3A-CM component in Mel-1 media (Fang et al., 2006) with Neurobasal ® medium (Invitrogen) containing 2% B27 supplement (Invitrogen), 3μM Chir, 25 ng/ml BMP4, and 500 μM dbcAMP. Cells were fed every other day and passaged weekly for maintenance and expansion.

Induced Pluripotent Stem Cell Derivation. Control (GM17569, GM00969), CH (GM02075 (Nagle et al., 1996)), HPS1 (GM14609) and HPS2 (GM17890 (Huizing et al., 2002)) fibroblasts were obtained from the Coriell Cell Repository. Fibroblasts were maintained and expanded in DMEM with 10% FBS. iPS cells were generated from fibroblasts as previously described (Papapetrou et al., 2011). Briefly, $1x10^5$ fibroblasts were plated per well of a gelatin-coated 6-well plate and transduced 24 h later with a single polycistronic vector co-expressing Oct4, Klf4, Sox2, and c-myc in the presence of 4 μg/ml polybrene. The media was changed 24 hours later and replaced daily from thereon. At day 5 or 6 cells were dissociated and replated on MEFs in hES media. Cells were fed daily with hES media. Following the appearance of hESC-like colonies after approximately 3-4 weeks, individual colonies were isolated and clonally expanded to establish iPS cell lines.

Microscopy, antibodies, and flow cytometry. Adherent cells were fixed with 4% paraformaldehyde for 15 minutes, washed with PBS and, in the case of intracellular markers, permeabilized using 0.3% Triton X in PBS before blocking with 1% BSA. Primary antibodies used for microscopy included GFP (Abcam), Sox10 (Santa Cruz), HMB45 (Dako), MITF (Abcam), Pax6 (Covance), Oct4 (Santa Cruz), and Nanog (R&D). For flow cytometry, cells were dissociated with accutase and blocked with 2% FBS in PBS before staining. Antibodies used for flow cytometry included HNK-1 (Sigma), p75 (Advanced cell targeting), and c-kit (eBioscience).

Quantitative RT-PCR. Total RNA was isolated using TRIzol reagent following manufacturer's protocol (Invitrogen). For heavily pigmented melanocytes, additional purification steps were taken to remove contaminating melanin by repeating the phenol-chloroform step and subsequently performing RNA clean up with RNeasy columns (Qiagen). cDNA was generated using QuantiTect Reverse Transcription kit (Qiagen). Primers for real-time quantitative PCR (qRT-PCR) were obtained from Applied Biosystems.

Gene expression profiling. Total RNA was isolated using TRIzol reagent following manufacturer's protocol (Invitrogen). All samples were processed by the MSKCC Genomics Core Facility and hybridized to the Illumina Human 12 Oligonucleotide array. Data analysis was conducted using Partek Genomics Suite software. Significant differences were defined as those with a fold change greater than 2 and FDR of less than 0.05.

Electron Microscopy. hESC- as well as control- and disease iPS-derived melanocytes were collected for electron microscopy. Samples were processed and images were collected by the Rockefeller University Electron Microscopy Resource Center. Image analysis and quantification was performed using Metamorph software (Molecular Devices). For quantification, cell outlines were determined manually and a threshold was set to discriminate between mitochondria and melanosomal vesicles. 10-15 micrographs were analyzed for each sample.

In ovo transplantation. Melanocyte precursors were derived from a hESC line constitutively expressing eGFP using the BE protocol. At day 11, cells were rendered to

single cells and sorted for c-kit expression. C-kit positive cells were grafted into the migration staging area at the fifth to last somite in chicken embryos that had developed 20-25 somites. After 16 or 72 hours, embryos were collected and sequentially incubated in 10, 20, and 30% sucrose before embedding in OCT. 20-30μm cryosections were prepared using a Leica CM3050 cryostat.

Pigmentation Quantification. Melanin content was quantified using previously described methods (Friedmann and Gilchrest, 1987; Wen-Jun et al., 2008). Briefly, $2.5x10^5$ melanocytes were collected and pelleted at 16,000xg for 30 seconds. Cells were washed twice with PBS and then dissolved in 250μl 1M NaOH for 40 minutes at 37°C. 100μl of cell lysate were transferred in duplicate to 96-well plates and the OD_{475} measured using a PerkinElmer EnSpire plate reader.

Organotypic Skin Reconstruct. Organotypic skin reconstructs were established as previously described (Meier et al., 2000). Briefly, an artificial dermal layer was established by seeding human dermal fibroblasts (Invitrogen) in collagen in transwell permeable supports (Corning). After several days, human epidermal keratinocytes and primary (control) or ES-derived melanocytes were introduced on top of the dermal layer and allowed to expand and stratify at the air-liquid interphase for an additional two weeks. Skin reconstructs were collected, fixed in 10% formalin and embedded in paraffin for sectioning and immunohistochemical processing.

Luciferase Assay. Cells were seeded in 24-well plates as described for NC differentiation. On day 1 of differentiation (one day prior to usual treatment with Chir) cells were transfected with 500ng/well of beta catenin reporter pTOPFlash or mutant control pFOPFlash (Veeman et al., 2003) and 5ng/well of Renilla reporter plasmid pRL-

TK in triplicate using Lipofectamine 2000 (Invitrogen) following manufacturer's protocol. Test compounds were added 24h after transfection. Cells were collected after a 24h incubation and analyzed using the dual luciferase reporter assay system (Promega) with a Promega Glomax 20/20 luminometer. Firefly absolute luminescence values were standardized to Renilla luciferase activity and subsequently normalized to pFOPFlash values.

Statistical Analysis. Throughout this study, averages across independent experiments were reported as means +/- SEM (standard error of the mean) unless otherwise indicated. For all two-way comparisons, unpaired t-tests were considered statistically significant if $p \leq 0.05$. Where indicated levels of significance were marked by asterisk as follows (*) $p \leq 0.05$; (**) $p \leq 0.01$; (***) $p \leq 0.001$.

CHAPTER THREE

Induction of Neural Crest from Human Pluripotent Stem Cells

Introduction

A defined protocol for the rapid and efficient neural conversion of hESCs has recently been developed by our group (Chambers et al., 2009). This approach is known as dual SMAD inhibition (DSi) inhibition as it relies on the inhibition of both arms of SMAD signaling by two small molecules; LDN-193189 (LDN) which inhibits BMP signaling and SB431542 (SB) which inhibits TGF-β, Activin, and Nodal signaling (**Figure 3.1**). Inhibition of both arms is required to trigger exit from the pluripotent state, prevent trophectoderm formation and block the formation of mesendoderm and non-neural ectoderm (Chambers et al., 2009). However NC specification requires intermediate levels of BMP signaling (Marchant et al., 1998) while activation of TGF-β signaling is thought to be required at a later timepoint to promote epithelial-to-mesenchymal transition (Xu et al., 2009). Studies in avian models have also established a strong requirement for Wnt signaling for early NC specification (García-Castro et al., 2002). Efficiency of NC induction was monitored with a *Sox10::GFP* hESC reporter line (Chambers et al., 2012a), which marks early multipotent NC stem cells and specific NC derivatives including melanocyte progenitors.

Results

Derivation of Neural Crest from Human ESCs

To reconcile the opposing requirements for BMP and TGF-β signaling in the DSi and NC induction, we hypothesized that withdrawal of BMP and TGF-β inhibitors at an intermediate time points may allow early inhibition of alternate lineages while facilitating

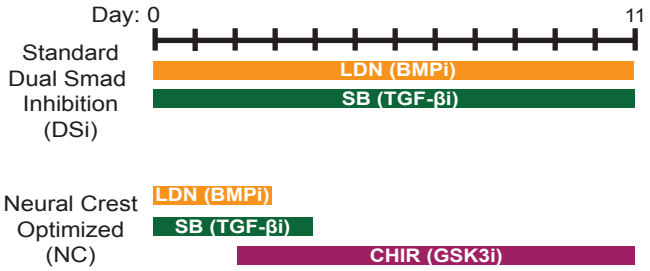

Figure 3.1. <u>Induction NC from hESCs using a modified dual SMAD inhibition protocol</u>. A dual SMAD inhibition (DSi) protocol (Chambers et al., 2009) can be modified to support highly efficient induction of a neural crest (NC) population by optimizing BMP, TGF-β, and Wnt signaling using three small molecule inhibitors LDN193189 (LDN), SB431542 (SB), Chir99021 (Chir) respectively.

NC specification at later stages by restoring endogenous BMP and TGF-β signaling (**Figure 3.1**). We also introduced a Wnt signal early in the differentiation to promote NC specification over CNS fate. While recombinant Wnt3a was found to efficiently promote induction of *Sox10::GFP* expressing NC (**Figure 3.2**), we found that Wnt signaling could also be activated more cost efficiently using the potent and cost-effective small molecule CHIR99021 (Chir), which functions as an agonist of Wnt signaling by selectively inhibiting glycogen synthase kinase 3β (GSK-3β) (Meijer et al., 2004; Ring et al., 2003),

We found that inhibition of BMP, TGF-β and Wnt signaling pathways, collectively referred to as the neural crest inductive "NC" condition (**Figure 3.1**), was sufficient to promote robust specification of *Sox10::GFP* expressing precursors (**Figures 3.3A,B**). Compared with the standard DSi protocol, the NC optimized condition increased the yield of *Sox10::GFP* positive cells greater than 20-fold (53% ± 14%; **Figure 3.3B**). Induction of *Sox10::GFP* occurred rapidly with GFP expression first detectable by flow cytometry at day 6 of differentiation and peaking by day 11 (**Figure 3.3C**). As previously suggested, the ratio between CNS and NC differentiation was found to be density dependent under DSi conditions (Chambers et al., 2009) while density-dependent differences in yield were less pronounced under NC conditions (**Figure 3.4**). Efficient induction of *Sox10::GFP* correlated with an increase in HNK-1 and p75 expression two markers previously found to define hESC-derived NC populations (Lee et al., 2007). *Sox10::GFP* did not however exclusively co-label with HNK-1 and p75 suggesting that these may not represent identical populations of NC (**Figure 3.5**). Specifically, the *Sox10::GFP* positive population contained p75 single positive cells, while the *Sox10::GFP* negative population also included p75/HNK1 double positive cells. NC conditions did not support the emergence of ZO-1 expressing neural rosettes or CNS-associated PAX6 expression (Elkabetz et al., 2008) (**Figure 3.3A**).

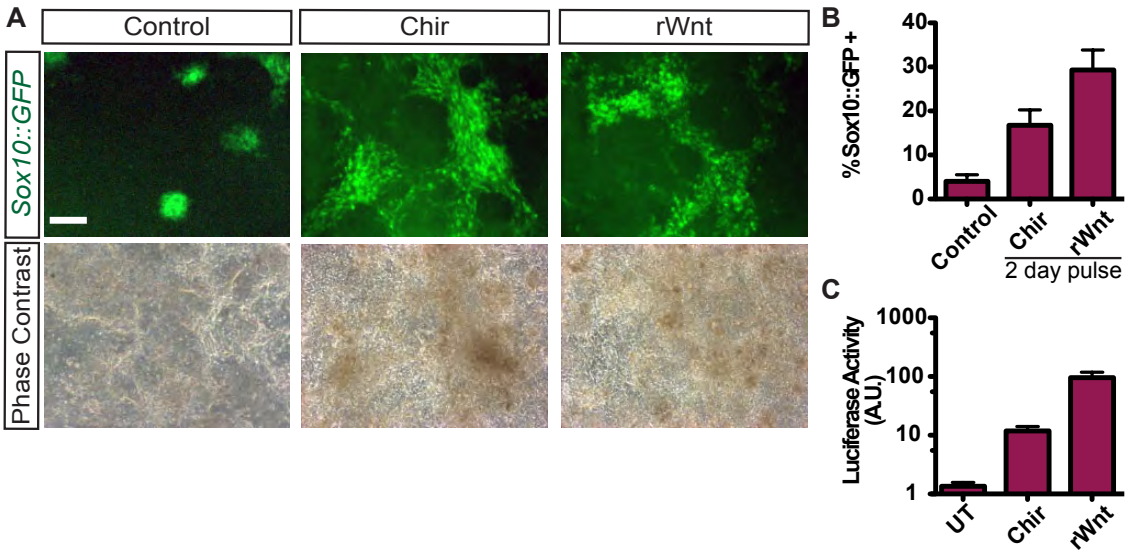

Figure 3.2. <u>Wnt activation drives induction of a *Sox10::GFP* expressing NC</u>. (**A-C**) *Sox10::GFP* hESCs were NC-differentiated in the presence or absence of a two-day pulse of 3μM of the GSK3-β inhibitor CHIR99021 (Chir) or 200ng/ml recombinant WNT3a (rWnt). For this assay Chir/Wnt treatment was limited to a two day pulse for cost efficiency. (**A**) Recombinant Wnt was able to support equal or greater induction of *Sox10::GFP* expressing populations when compared to Chir. Scale bars represent 100μm. (**B**) Flow cytometric quantification of *Sox10::GFP* induction. *Sox10::GFP* induction efficiency is represented as a percentage of total viable cells. (**C**) Wnt pathway activation in untreated (UT), Chir- or rWnt-treated conditions was assessed using a beta catenin luciferase reporter. Arbitrary units (A.U.). Error bars represent the s.e.m of three independent experiments.

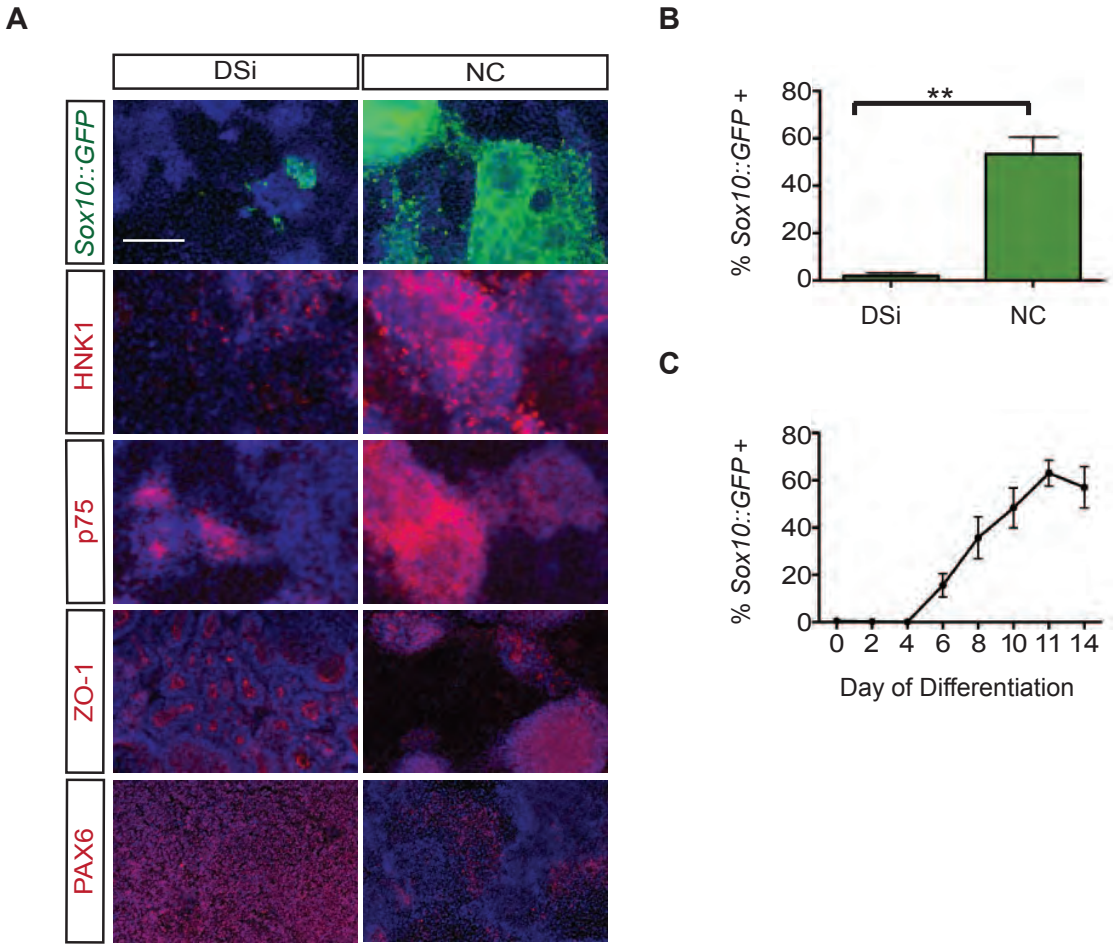

Figure 3.3. <u>Induction of NC from *Sox10::GFP* hESCs using a modified dual SMAD inhibition protocol</u>. (**A**) NC conditions support induction of a *Sox10::GFP* expressing population that co-expresses neural crest markers HNK-1 and p75 while down-regulating ZO-1 and PAX6 expressing CNS. Scale bars represent 200μm. (**B**) NC optimized conditions increase the yield of *Sox10::GFP* positive cells greater than 20-fold (53% ± 14%, n=4, p=0.002) over the DSi condition. (**C**) Using FACS analysis, *Sox10::GFP* was first detected at day 6 of NC differentiation and peaked by day 11. *Sox10::GFP* induction efficiency is represented as a percentage of total viable cells. ** p<0.01. Error bars represent the s.e.m of three independent experiments.

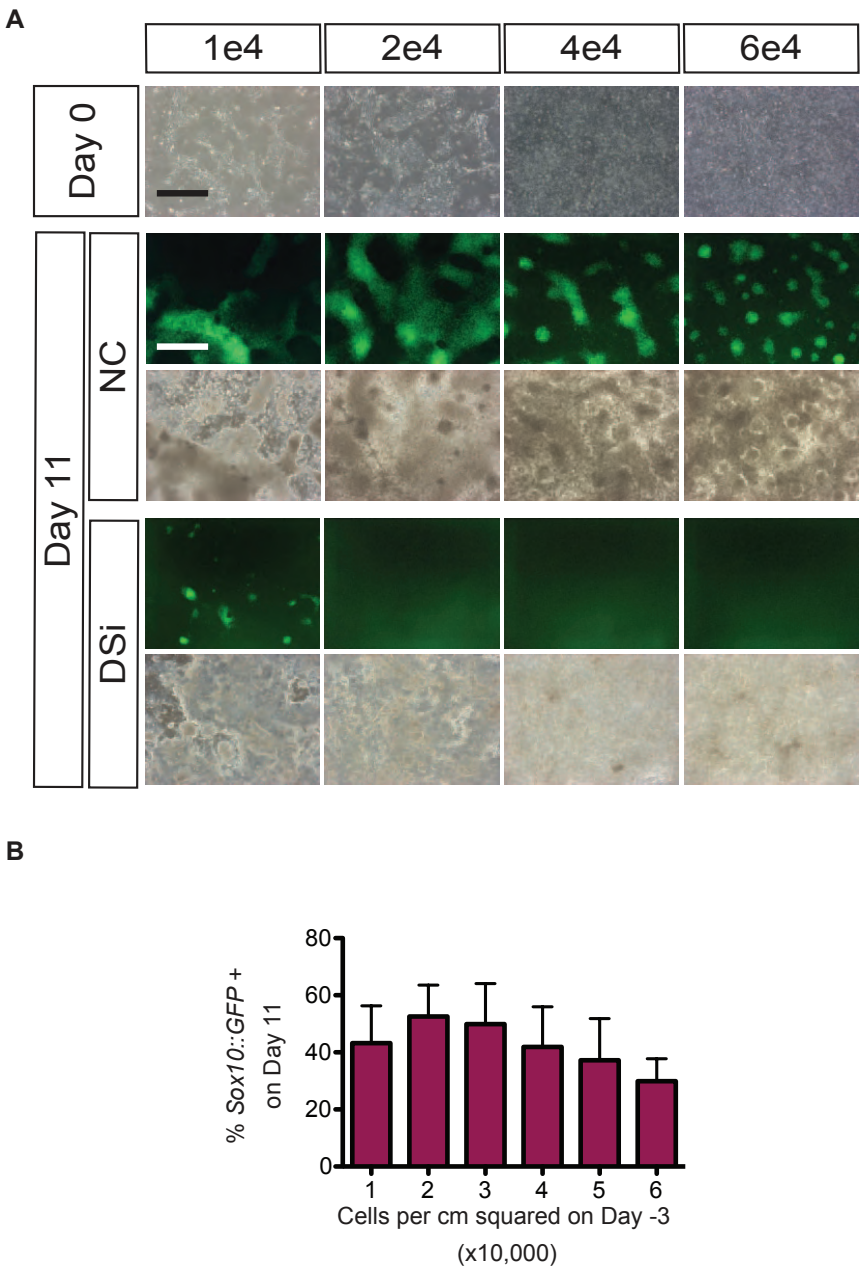

Figure 3.4. <u>Efficiency of *Sox10::GFP* expressing NC is partially density dependent</u>. (**A**) Cells were plated at a range of 1e4 – 6e4 cells/cm^2 on day -3 resulting in increasing confluence at day 0 for the start of differentiation (top row). The morphology and expression of *Sox10::GFP* at day 11 following NC and DSi induction is shown. Scale bars represent 500µm. (**B**) An initial plating density of 20,000 cells/cm2 results in an optimal confluence of 70-80% on day 0 of differentiation, which supports the maximal yield of *Sox10::GFP* expressing cells by day 11 as measured by FACS. Error bars represent the s.e.m of three independent experiments.

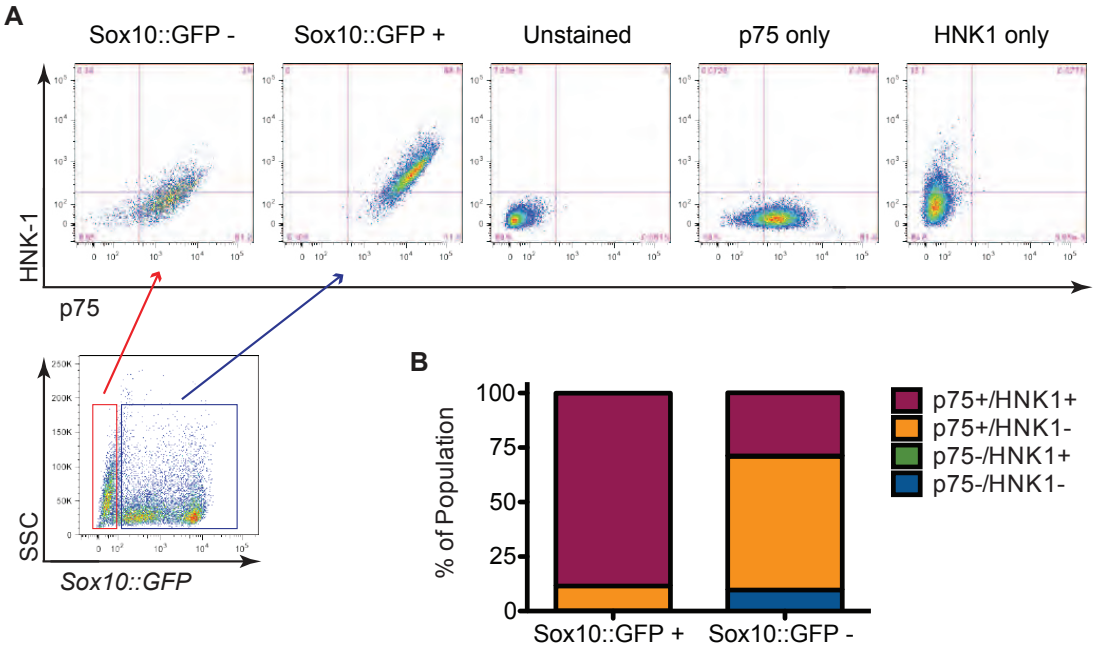

Figure 3.5. <u>The Sox10::GFP expressing population induced under NC conditions is not identical with p75+/HNK1+ cells</u>. (**A**) NC-derived day 11 cells were analyzed by FACS for *Sox10::GFP* and NC marker HNK-1 and p75 expression. Expression of NC markers HNK-1 and p75 were determined by flow cytometry in the *Sox10::GFP* positive and negative populations of day 11 NC-derived cells. (**B**) Quantification of data from (A) reveals the presence p75/HNK-1 double positive cells in the *Sox10::GFP* negative population confirming that the two sorting strategies do not identify the same population of cells.

hESC-Derived NC Express a HOX-negative NC Profile

Comparative gene expression analysis of day 11 DSi and NC cells further confirmed that NC differentiation conditions favored induction of NC associated markers including *SOX10, TFAP2A/B, SNAI2*, and *EDNRA/B* as well as genes associated with WNT (*WNT3A, LEF1*) and Notch signaling (*DLL3, HEY2*) (**Figure 3.6**) while DSi cells expressed high levels of genes associated with CNS (*PAX6*, *HES5*) and forebrain state (*OTX2, LHX2*). Fate specific markers were also induced under both NC and DSi conditions with *BRN3A*, an early marker of sensory neurogenesis, observed following NC differentiation while genes associated with pigmentation such as tyrosinase-related protein 1 (*TYRP1*) and dopachrome tautomerase (*DCT*) were observed under DSi conditions, presumably due to the presence of retinal pigment epithelium cells that can be expanded from DSi conditions (**Figure 3.7**), although DCT is also expressed in the mouse forebrain (Steel et al., 1992). Unlike previously reported NC populations derived from hESC using stromal co-culture conditions (Lee et al., 2007), NC-derived cells did not exhibit high levels of HOX gene expression suggesting that these cells correspond to the HOX-negative NC lineage previously shown to be particularly plastic (Creuzet et al., 2005; Le Douarin et al., 2004). A-P axial level including HOX gene expression could however be manipulated using caudalizing cues such as FGF2 or retinoic acid (RA) treatment (**Figure 3.8**).

Dissecting Signaling Contributions to NC Specification

To further investigate the individual contributions of the BMP, TGF-β, and GSK-3β inhibitors to NC specification, we performed timed withdrawal experiments during the 11-day differentiation or omitted factors entirely (**Figure 3.9**). While a brief treatment with LDN was required for *Sox10::GFP* induction, 2-3 days of treatment appeared to be

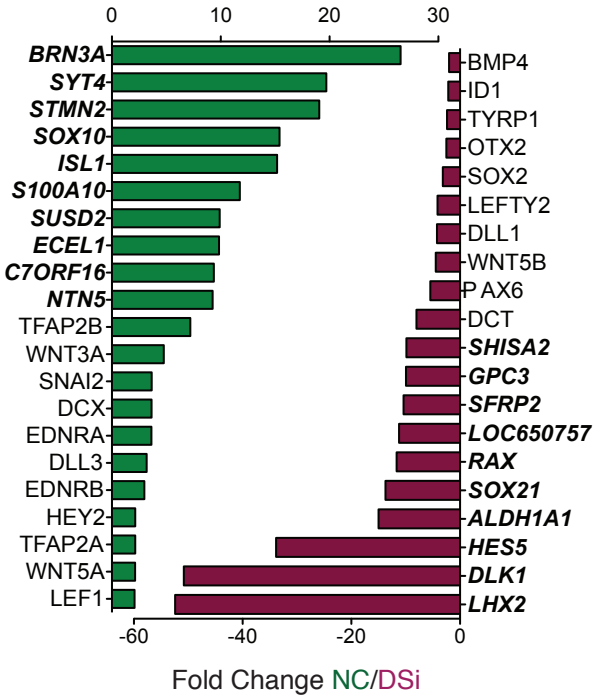

Figure 3.6. NC conditions support induction of a neural crest gene expression profile. Significantly up- (green) and downregulated (red) genes at day 11 in NC-induced cells compared to DSi cells. Bold genes represent top 10 most differentially regulated genes.

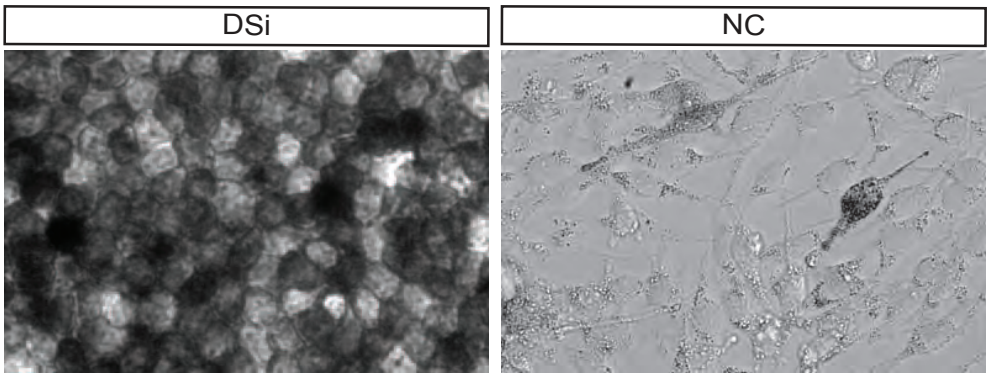

Figure 3.7. DSi- and NC-derived pigmented cells exhibit different morphologies. Induction of pigmented cells matured from either DSi- or NC-induced cells exhibit typical morphology of retinal pigment epithelium or melanocytes, respectively.

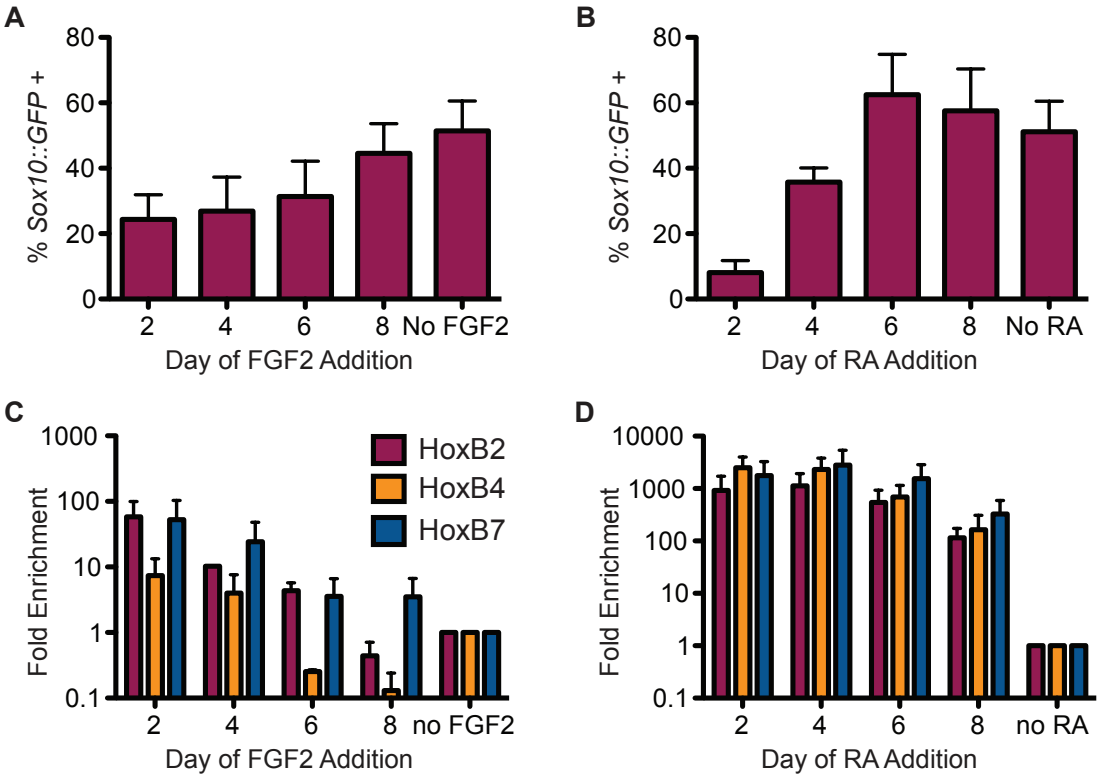

Figure 3.8. NC-derived cells can be caudalized following treatment with RA or FGF2. (**A**, **B**) Effect of FGF2 and RA on efficiency of *Sox10::GFP* induction was assessed. *Sox10::GFP* induction efficiency is represented as a percentage of total viable cells. (**C**, **D**) Expression of anterior Hox genes in NC-derived cells can be induced through treatment with FGF2 or RA. Error bars represent the s.e.m of at least three independent experiments.

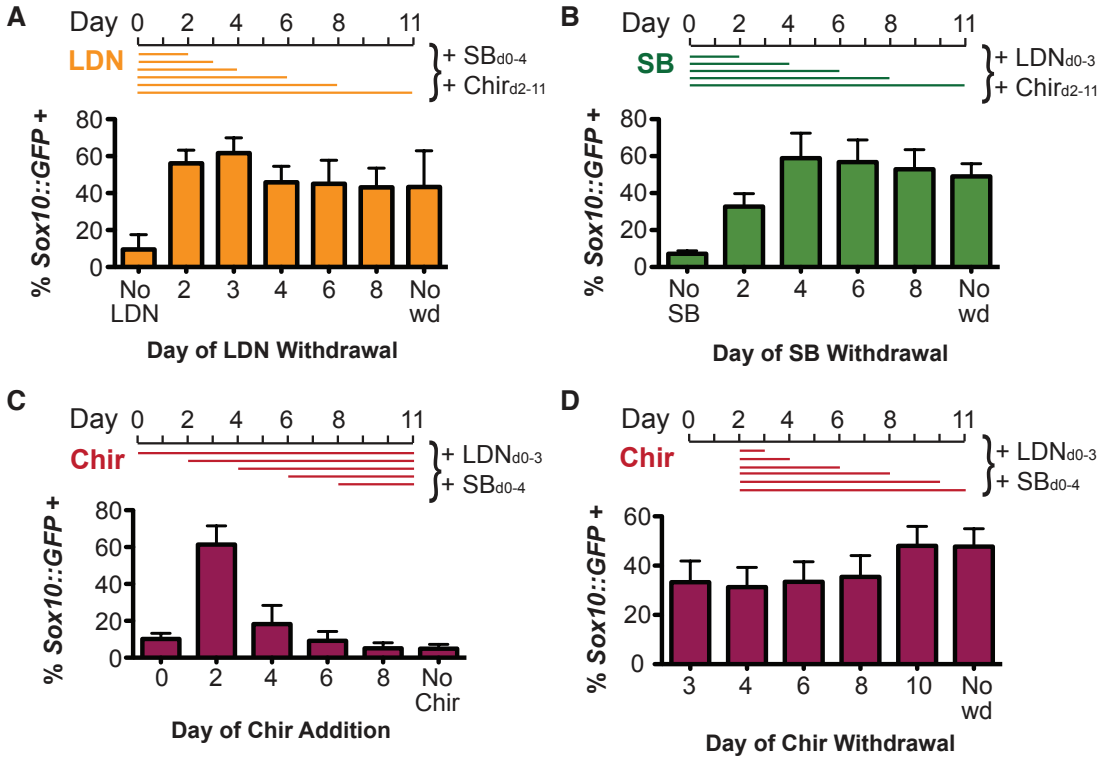

Figure 3.9. Neural crest induction is driven by a narrow window of Wnt activation. BMP inhibitor LDN193189 (LDN, **A**) and TGF-β inhibitor SB431542 (SB, **B**) are individually withdrawn at various timepoints within the context of the NC protocol and induction of *Sox10::GFP* assessed at day 11 by FACS. Treatment with GSK-3β inhibitor CHIR99021 (Chir) is initiated (**C**) or withdrawn (**D**) at various timepoints and induction of *Sox10::GFP* assessed at day 11 by FACS. *Sox10::GFP* induction efficiency is represented as a percentage of total viable cells. All error bars represent the s.e.m of at least three independent experiments.

sufficient for optimal NC specification (**Figure 3.9A**). These findings contrast with a recent report in which treatment with Noggin, another BMP inhibitor used in the original DSi protocol, was found to be dispensable for the induction of a p75+/HNK1+ NC population (Menendez et al., 2011). We observed similar requirements for TGF-β/Activin inhibition. Conditions in which the inhibitor SB was omitted entirely were not permissive for NC differentiation while withdrawal at any point after day 4 allowed for robust *Sox10::GFP* induction (**Figure 3.9B**). Continued treatment with either the BMP or TGF-β inhibitors for the entire 11 days of the differentiation did not negatively impact the *Sox10::GFP* yield, suggesting that de-repression of endogenous BMP or TGF-β signaling is not essential for triggering NC differentiation (**Figure 3.9A,B**).

NC Induction is driven by a narrow window of GSK-3β inhibition

When we investigated the requirements for Wnt activation using the small molecule Chir, we observed a narrow window during which Chir treatment is essential for *Sox10::GFP* induction. While Chir exposure starting at day 2 of the differentiation resulted in optimal *Sox10::GFP* induction, changing the onset of Chir treatment by as little as 1-2 days resulted in a near complete loss of *Sox10::GFP* expression (**Figure 3.9C**). When we investigated the minimal duration of Wnt activity required for *Sox10::GFP* induction, we found that a single day of Chir treatment was sufficient to achieve 70% of the maximal yield (**Figure 3.9D**). To test whether a short pulse of Chir treatment can induce a subsequent wave of endogenous Wnt signaling, we performed luciferase-based Wnt reporter assays. We observed that β catenin levels remained elevated three days after a single day pulse of Chir treatment, suggesting that endogenous Wnt signaling was indeed triggered by brief Chir exposure (**Figure 3.10**). However, blocking endogenous Wnt signaling after 1-2 days of Chir treatment using the axin stabilizing small molecule

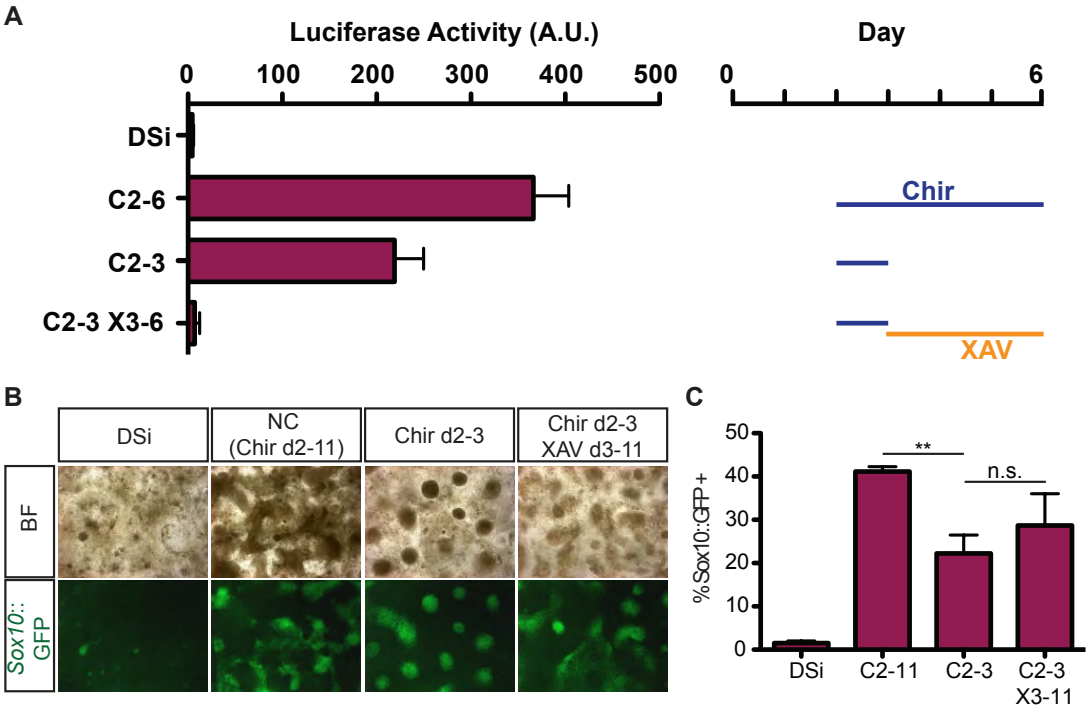

Figure 3.10. <u>A brief inductive pulse of Wnt at Day 2 is sufficient to specify NC induction</u>. (**A**) A luciferase reporter system was used to quantify Wnt pathway activation at day 6 in the absence of Chir treatment (DSi), in the presence of 3μM CHIR99021 (Chir) (C2-6), and endogenous Wnt signaling following a one-day inductive pulse of Chir (C2-3). The capacity of XAV-939 (XAV) to inhibit endogenous Wnt signaling was also quantified (C2-3 X3-6). Arbitrary units (A.U.). (**B**,**C**) Inhibition of endogenous Wnt signaling following a single day pulse of Chir treatment did not affect the efficiency of *Sox10::GFP* induction. (**B**) Brightfield (BF) and fluorescence images showing expression of *Sox10::GFP* expressing cells at day 11. (**C**) The efficiency of *Sox10::GFP* induction was quantified at day 11 by flow cytometry. Error bars represent the s.e.m. of four independent experiments. *Sox10::GFP* induction efficiency is represented as a percentage of total viable cells. ** $p \leq 0.01$, n.s. not significant.

XAV-939 (XAV) did not affect the efficiency of NC induction (**Figure 3.10**). Our data indicate that Wnt signaling is not required beyond a brief inductive pulse to specify NC fate.

Chir Induces Sequential Wnt Signaling, NC Specification, and Neurogenesis

We next performed global gene expression analysis to determine the transcripts regulated immediately after Chir exposure (**Figures 3.11**). Within 24 hours of Chir addition, the most upregulated gene was *SP5*, a transcription factor downstream of Wnt and beta-catenin signaling implicated in anterior-posterior patterning (Fujimura et al., 2007; Weidinger et al., 2005). Upregulation of *AXIN2* and *WNT1* at 24 hours and 6 days after Chir addition further confirmed that Chir treatment induces endogenous Wnt signaling. In contrast, *SIX3*, a negative regulator of Wnt signaling required for vertebrate forebrain development (Braun et al., 2003; Lagutin et al., 2003; Lavado et al., 2008) and *HESX1* and *SOX3*, two additional forebrain markers, were suppressed following Chir treatment (**Figure 3.11A**). By day 6 of the differentiation, the timepoint when *Sox10::GFP* expression was first observed, induction of various additional NC markers was observed including *EDNRA, SOX10, SNAI2, TFAP2A/B, FOXD3, SOX9, and PAX3* while various CNS and forebrain markers were suppressed (**Figure 3.11B**). By days 8 (**Figure 3.11C**) and 11 (**Figure 3.11D**) more mature, cell type specific markers were upregulated including *ASCL1, EDNRB*, and *OLIG2*. Our global transcriptome profiling data therefore establish a model in which treatment with the GSK-3β inhibitor Chir during the NC protocol first induces a surge of Wnt signaling which is followed by markers of NC specification, and a subsequent neurogenic wave.

Day 2 Represents a Wnt-Responsive NC Patterning Window

We next determined whether the surprisingly narrow window during which Wnt signaling

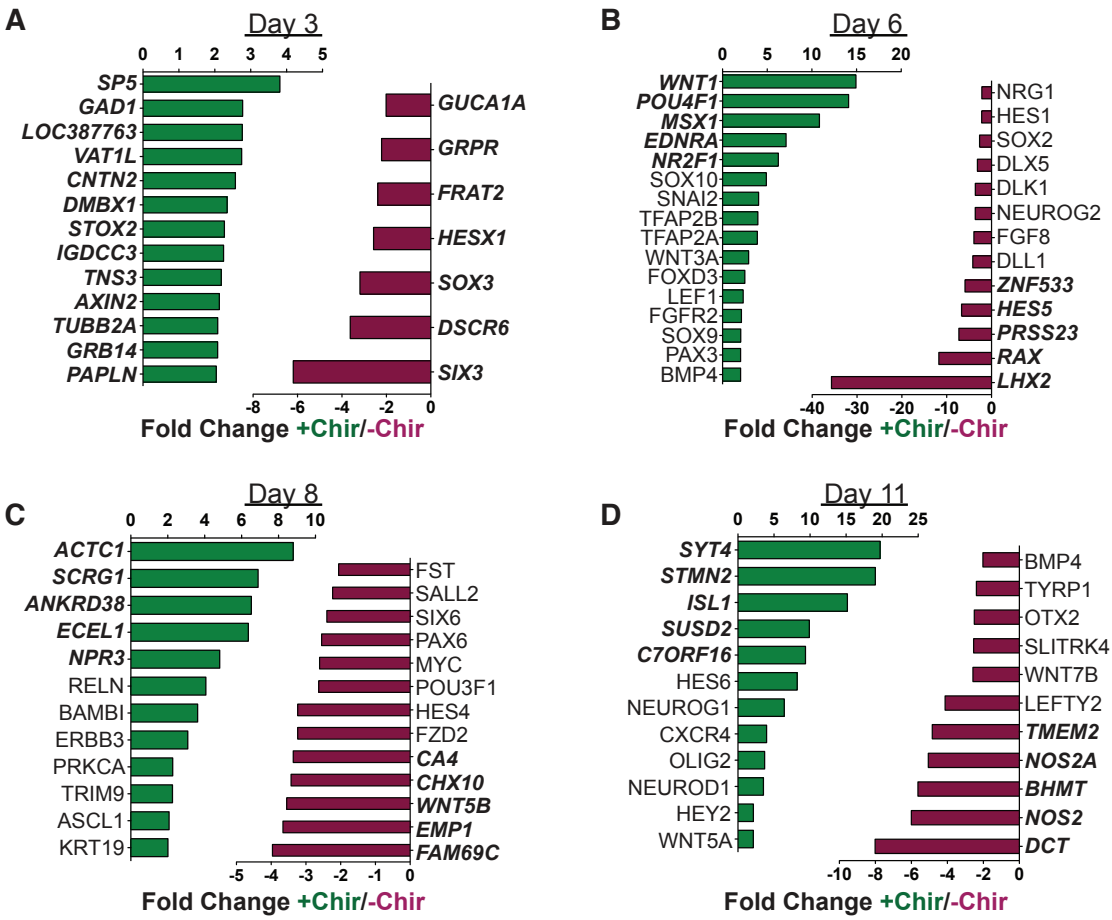

Figure 3.11. GSK-3β inhibition induces successive waves of Wnt activation, NC induction, and neutralization. The effects of CHIR99021 (Chir) treatment on gene expression at days 3 (**A**), 6 (**B**), 8 (**C**), and 11 (**D**) were determined by comparative microarray analysis of NC cells derived in the presence (green) or absence (red) of Chir. Bold genes represent top 5 most differentially regulated genes.

drives NC specification reflects a unique temporal competence of the cells that respond to NC-inductive Wnt signaling. Our gene expression analysis had identified genes induced with 24 hours and 4 days of Chir treatment (**Figures 3.12**). We asked whether these genes would also be induced when Chir treatment was delayed until day 4 of differentiation, a timepoint that does not efficiently support NC specification (**Figure 3.9C**). We found that many of the genes upregulated within 24 hours of Chir treatment, including those known to be direct targets of Wnt signaling, are not induced when cells are treated with Chir at day 4 (**Figure 3.12A**). In fact, upon delayed Chir treatment, many Chir responsive genes were expressed at levels comparable with DSi conditions. Intriguingly, levels of the negative Wnt regulator *SIX3*, which is usually downregulated upon Chir treatment, remained elevated with late Chir treatment. Induction of late Wnt responsive genes was similarly lost (**Figure 3.12B**). These data indicate that cells lose competency to NC-inductive Wnt signals and undergo a default anterior neuroectodermal program.

Discussion

We have described an approach for the rapid and highly efficient induction of NC from hESCs. To our knowledge this is the first report of a method for the isolation of hESC-derived NC under defined conditions, which has also allowed us to investigate the pathways critical in early NC specification. We further demonstrate that the A-P axial identity of the NC population is responsive to FGF2 and RA caudalizing cues.

The Role of BMP in Human NC Specification

The specification of NC during mouse and chick development is dependent on both WNT and intermediate levels of BMP signaling generated by neighboring non-neural ectoderm and mesodermal tissues

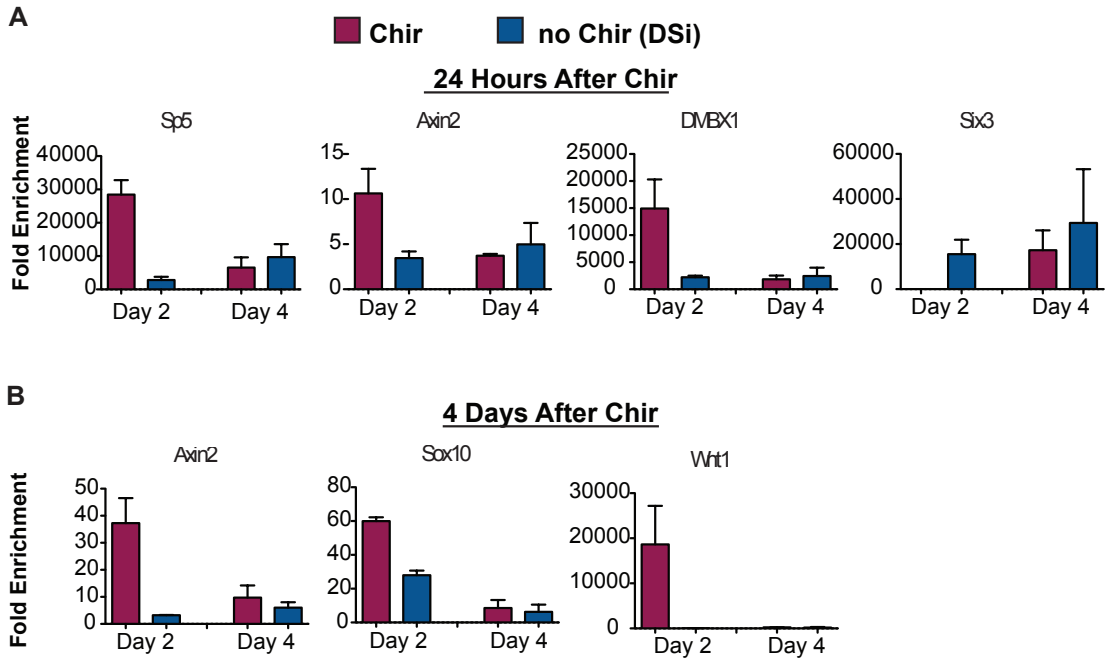

Figure 3.12. Cells are not competent to respond to NC-inductive Wnt signals after day 2. (**A**, **B**) Gene expression levels following treatment with Chir at Day 2 or Day 4 were determined by qRT-PCR either 24 hours or 4 days after Chir treatment. Cells grown in the absence of Chir (i.e. DSi conditions) were collected in parallel as a negative control. Genes were selected based on previous microarray data (**Figure 3.11)**. (**A**) Genes previously found to be upregulated within 24 hours of Chir treatment at Day 2 were not induced when Chir treatment was delayed until Day 4 (Sp5, Axin2, DMBX1). Conversely downregulation of the negative Wnt regulator Six3 did not occur when cells were treated with Chir at Day 4. (**B**) Wnt and NC-associated genes normally observed within 4 days of Chir treatment were also not induced when Chir treatment was delayed. Fold enrichment was normalized to gene expression levels at day 0.

(García-Castro et al., 2002; Kléber et al., 2005; LaBonne and Bronner-Fraser, 1998; Marchant et al., 1998; Patthey et al., 2008). The requirement for BMP signaling is however preceded in Xenopus models by an early need for BMP inhibition that promotes robust acquisition of neural plate identity that establishes the competence to respond to subsequent NC inductive cues (LaBonne and Bronner-Fraser, 1998; Steventon et al., 2009). While we were able to confirm a similar requirement for early BMP inhibition in the induction of human NC, we surprisingly did not find that continued BMP inhibition negatively impacted NC induction even though studies in chick and xenopus embryos have implicated BMP signaling during both NC induction and maintenance (Kléber et al., 2005; Marchant et al., 1998; Selleck et al., 1998). Our data are also distinct from previous observations in p75/HNK-1 expressing NC precursors derived from hESC via a rosette intermediate (Lee et al., 2007). Under those conditions there was a significant decrease in the percentage of putative NC precursors following treatment with the BMP inhibitor noggin and an increase following exposure to BMP4. These discrepancies may reflect inherent differences in rosette- versus non-rosette derived NC, with the former reflecting the stage of NC delamination whereas the accelerated NC derivation conditions presented here may represent an early NC induction stage prior to the presence of a distinct neuroepithelial intermediate. Alternatively, as *Sox10::GFP* expression and p75/HNK-1 coexpression appear to identify overlapping but distinct NC populations, it is possible that these two subtypes of NC may exhibit different requirements for BMP signaling. It should be noted that a recent immunohistochemical study of Carnegie Stage 12 to 18 human embryos found that HNK-1 only labeled a small subset of migrating NC cells, while p75 expression also broadly labeled non-NC populations (Betters et al., 2010). Future studies will be required to dissect the exact contribution of BMP pathway manipulations during hESC differentiation to NC and to define whether differential requirements reflect distinct developmental NC stages or

subtypes.

The Role of Wnt in Human NC Specification

The use of Chir in our protocol offers a simple and cost-effective strategy to activate Wnt signaling during NC induction. While we were able to demonstrate robust induction of *Sox10::GFP* upon exposure to high doses of WNT3a (**Figure 3.2**), the concentrations of WNT3a required were cost-prohibitive and not practical for routine NC induction. Chir treatment triggers rapid activation of Wnt signaling pathway molecules and robust induction of a *TCF::luciferase* reporter (**Figure 3.2**). The critical role for Wnt signaling in our NC induction conditions is consistent with findings in avian systems which have demonstrated that Wnt signaling is necessary and sufficient for NC induction (García-Castro et al., 2002). Similar requirements for Wnt signaling for the induction of a p75, HNK-1 co-expressing human NC population have also been reported (Lee et al., 2007; Menendez et al., 2011). Our study is however unique in addressing the temporal requirements for Wnt signaling during human NC specification. The very narrow window during which Wnt signaling promoted *Sox10::GFP* induction was unexpected and offers a powerful tool to mechanistically define competency factors acting together with Wnt in NC specification. One hypothesis is that loss of competency correlates with the time course of Dkk1 induction and anterior CNS fate specification observed during DSi (Fasano et al., 2010). This is supported by our own observations that the negative Wnt regulator *SIX3* continues to be expressed when Chir treatment is not initiated until day 4. It is tempting to speculate that knockdown of *SIX3* may restore NC-competence to cells at this late timepoint. Furthermore, it has recently been reported that sequential activation of Wnt signaling in the mouse embryo affects NC lineage specification, particularly along sensory neuronal and melanocyte lineages (Hari et al., 2012). It will be interesting to define whether *SOX10::GFP* NC cells induced following a Chir pulse

treatment are functionally distinct from those generated upon long-term Chir treatment, particularly in conditions when endogenous Wnt signaling was further suppressed by treatment with XAV.

CHAPTER FOUR

Induction of Melanocytes from Human Pluripotent Stem Cells

Introduction

The NC is a multipotent population, however previously generated hESC-derived NC populations did not support melanocyte differentiation (Lee et al., 2007). Differentiation along the melanocyte lineage has been found to be strongly dependent on Wnt signaling through regulation of the melanocyte master regulator MITF (Dunn et al., 2000; Takeda et al., 2000), while EDN3 and SCF promote proliferation and survival of melanoblast progenitors (Baynash et al., 1994; Yoshida et al., 1996).

Results

NC-Derived Cells Include a Melanoblast Subpopulation

To confirm the melanocyte competence of our NC-derived cells, we identified a subpopulation of presumptive melanoblasts at day 11 of differentiation based on co-expression of *Sox10::GFP* and microphthalmia-associated transcription factor (MITF) (**Figure 4.1**). MITF positive cells lacking *Sox10::GFP* expression were also observed, which may be due to downregulation of the BAC reporter, as we observed continued SOX10 protein expression by immunofluorescence (**Figure 4.7C**).

Prospective Identification and Isolation of Melanoblasts by SOX10 and KIT Expression

To prospectively identify and isolate melanoblasts from the heterogeneous population of NC cells, we selected KIT (c-kit) as a putative cell surface marker of early melanocyte progenitors. C-kit has previously been identified as uniquely marking the melanocyte-competent sub-fraction of NC cells (Luo et al., 2003a; Reid et al., 1995) and plays an

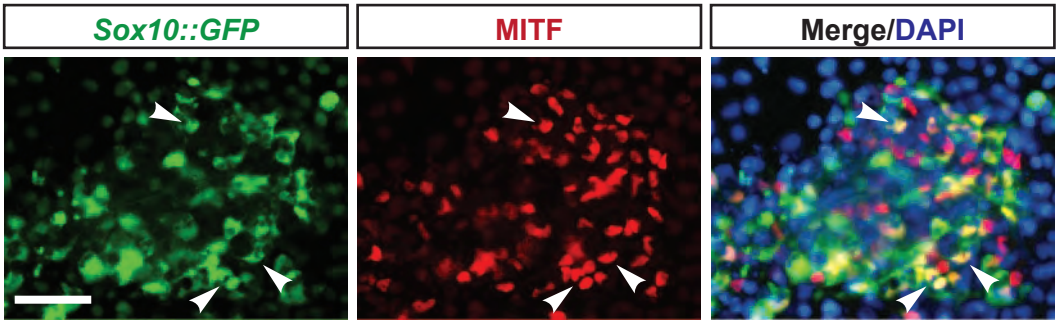

Figure 4.1. NC-derived cells include a Sox10/MITF coexpressing melanoblast subpopulation. Melanocyte progenitors can be identified in day 11 NC protocol-derived populations by coexpression of *Sox10::GFP* and the melanocyte transcription factor MITF (arrowheads). Scale bar represents 50μm.

important role in melanocyte migration (Kunisada et al., 1998b; Yoshida et al., 1996), proliferation (Kunisada et al., 1998b; Yoshida et al., 1996), and maturation (Kunisada et al., 1998b). Using FACS analysis we confirmed that 9% ± 2% of the population at day 11 of the differentiation co-expressed *Sox10::GFP* and c-kit, while 59% ± 3% only expressed *Sox10::GFP* (**Figure 4.2A**). Purified *Sox10::GFP*, c-kit co-expressing (GFP+/cKit+) cells expressed higher levels of the melanocyte markers *MITF-M* and *DCT* when compared to GFP+/cKit- cells (**Fig. 4.2B**), confirming the utility of c-kit and Sox10 co-expression as an appropriate strategy for melanoblast isolation.

BMP4 and EDN3 Enhance Melanoblast Yield

We performed a candidate screen for factors that increase the percentage of GFP+/cKit+ cells. Contrary to predictions based on literature in other model systems, SCF signaling at this timepoint did not enhance melanoblast induction, however we identified BMP and Endothelin 3 (EDN3) as two factors that did enhance melanoblast yield when introduced at day 6 of the differentiation (**Figure 4.3A**). The role of BMP signaling during melanocyte specification has been well established (Dunn et al., 2000; Nissan et al., 2011; Takeda et al., 2000; Thomas and Erickson, 2008), while endothelins have been implicated in the maintenance and proliferation of melanocyte precursors (Baynash et al., 1994; Dupin and Le Douarin, 2003; Lahav et al., 1996; Reid et al., 1996). Combined treatment with both BMP4 and EDN3 (hereafter referred to as the "BE" condition), significantly increased the percentage of GFP+/cKit+ cells to 37% ± 3% (**Figure 4.3B**). We observed robust expression of *SOX10, KIT, MITF-M*, and *DCT* within the GFP+/cKit+ population under both NC (**Figure 4.2B**) and BE conditions (**Figure 4.4A**). However, BE-derived melanoblasts expressed significantly higher levels of *MITF-M* and *DCT* than the same population derived with the NC protocol (**Figure 4.4B**), suggesting that treatment with BMP4 and EDN3 not only enhances melanoblast yield

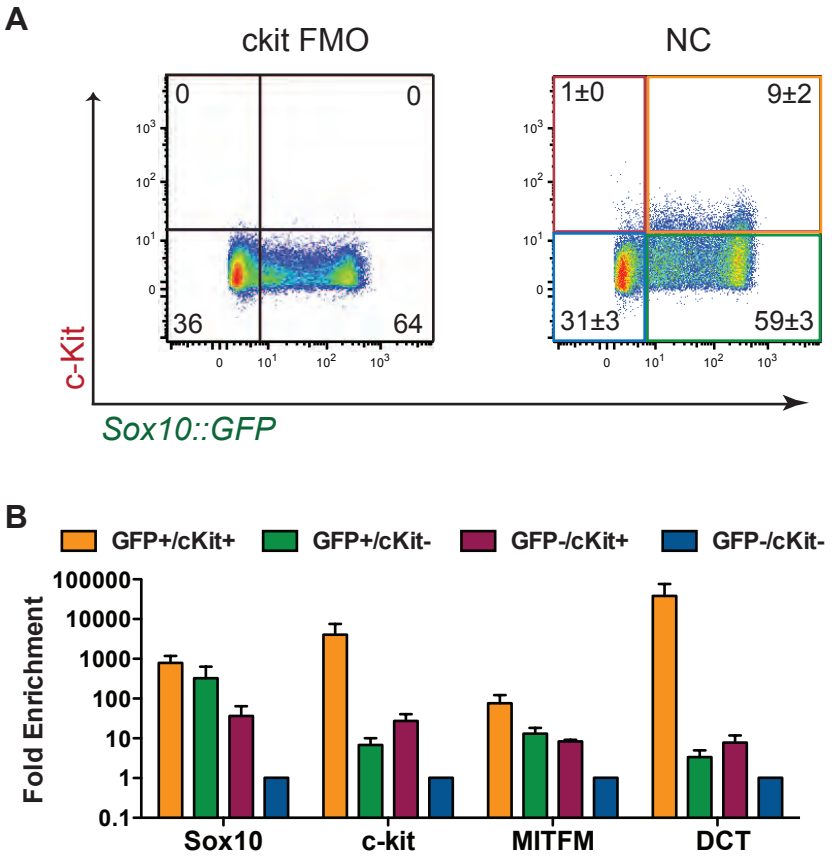

Figure 4.2. C-kit and Sox10 expression can be used to prospectively identify and isolate melanoblasts. (**A**) Flow cytometry reveals the presence of a *Sox10::GFP* and c-kit co-expressing population following NC induction. C-kit "fluorescence minus one" (FMO) was used a negative control for c-kit staining. (**B**) 4-way FACS sorting for *Sox10::GFP* and c-kit reveals an enrichment of the melanocyte markers MITFM and Dct in the SOX10/ckit double positive population by qRT-PCR. All error bars represent the s.e.m of at least three independent experiments

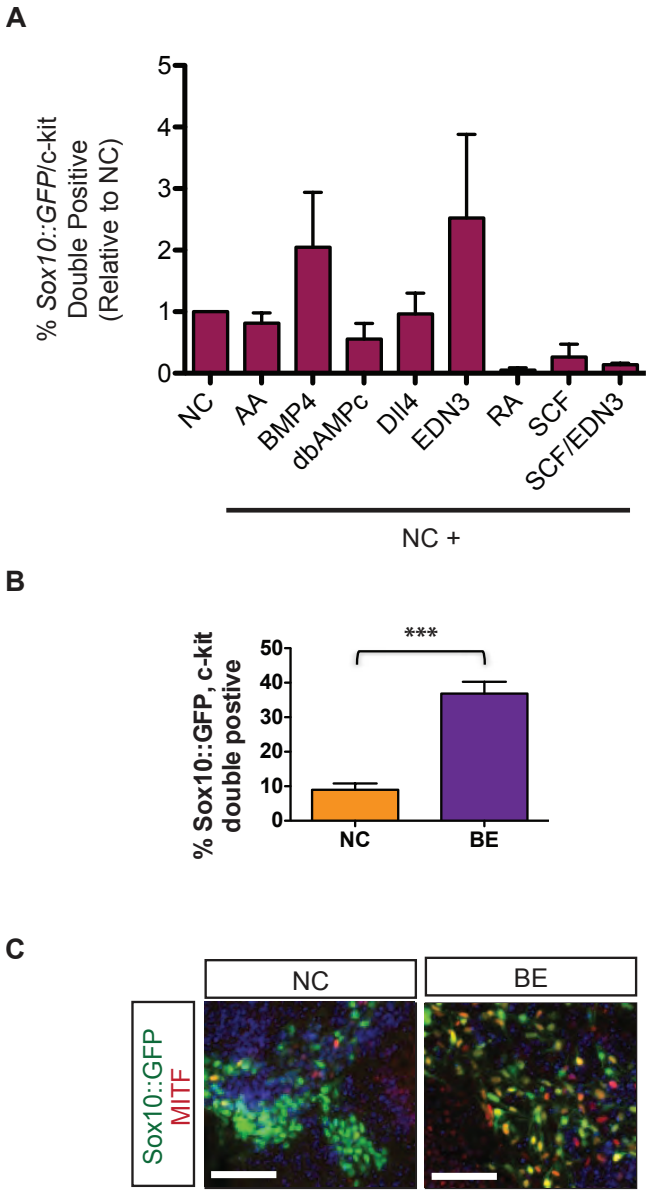

Figure 4.3. <u>Treatment with BMP4 and EDN3 promotes melanoblast specification</u>. (**A**) A targeted small screen was conducted to identify factors that enhance melanocyte progenitor yield. Ascorbic acid (AA), BMP4, dibutyryl cyclic AMP (dbcAMP), delta-like 4 (Dll4), EDN3, retinoic acid (RA), and stem cell factor (SCF) were added to the NC basal condition and assayed for their effects on *Sox10::GFP*, c-kit coexpressing melanocyte progenitor yield by flow cytometry. Error bars represent the s.e.m of three independent experiments. (**B**) Additional treatment with BMP4 and EDN3 (BE) beginning at day 6 significantly enhances the yield of *Sox10::GFP*, c-kit double positive melanocyte progenitors (n=4, p=0.0005). All error bars represent the s.e.m of at least three independent experiments. (**C**) BE-derived melanocyte progenitors exhibit spindle-like melanocyte morphology. Scale bars represent 50μm.

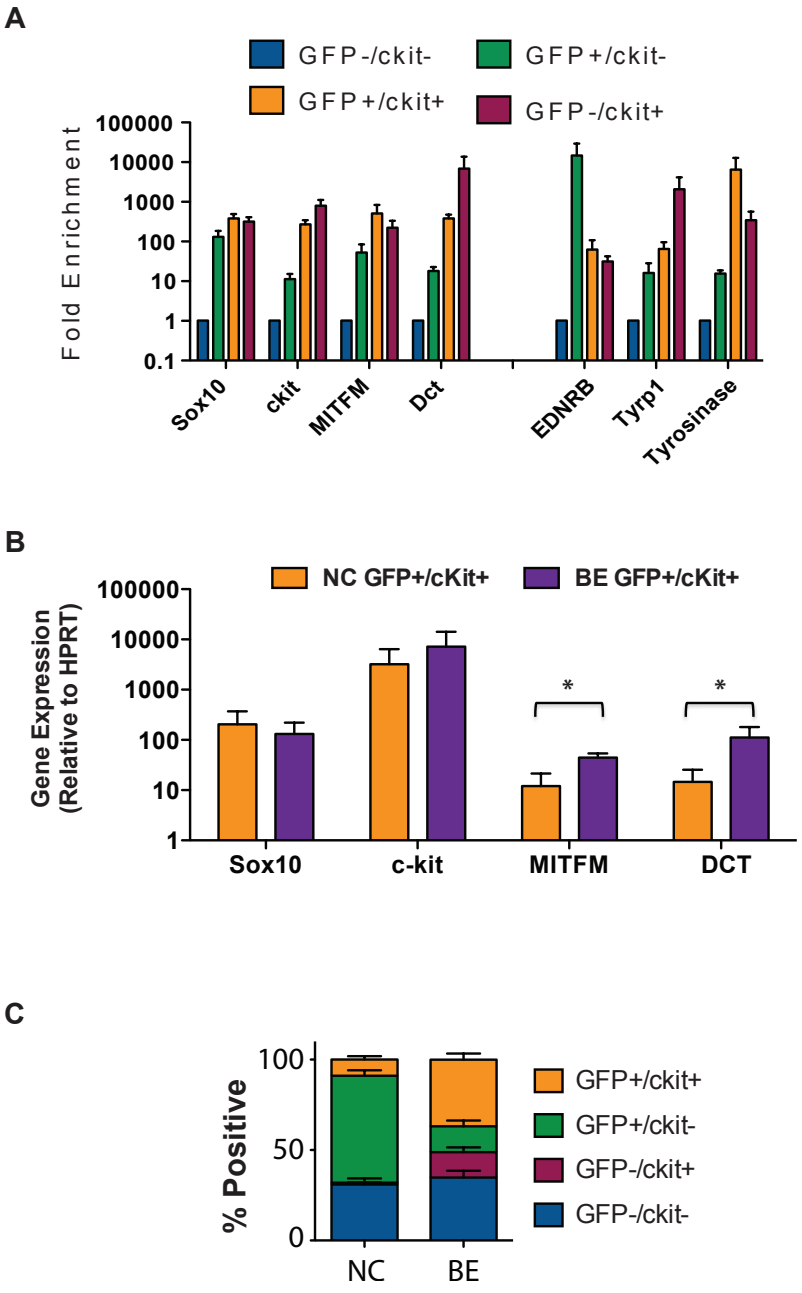

Figure 4.4 BE treatment enhances induction of a melanoblast marker expression. (**A**) Expression of early and late melanocyte markers in BE-derived melanocyte progenitors was confirmed by qRT-PCR. Error bars represent the s.e.m of three independent experiments. (**B**) BE-derived melanocyte progenitors express significantly higher levels of MITF and DCT than NC-derived cells by qRT-PCR (n=3, p=0.03(MITF), p=0.05(DCT)). (**C**) BE treatment increases the yield of *Sox10::GFP*, c-kit double positive melanocyte progenitors at the expense of *Sox10::GFP* single positive NC cells. All error bars represent the s.e.m of at least three independent experiments. * p≤0.05

but also further drives their maturation. A comparison of the relative proportions of *Sox10::GFP* and c-kit expressing populations following NC and BE treatment revealed that BE conditions increased the yield of double positive melanocyte progenitors, while the percentage of *Sox10::GFP* single positive NC was reduced (**Figure 4.4C**). The percentage of double negative (GFP-/cKit-) however remained unchanged. This change in population makeup could be due to a direct fate switch within the existing NC population. However, we cannot rule out that increased proliferation of the existing melanoblasts, or inhibition of non-melanocyte NC contribute to the BE-mediated increase in melanocyte precursors. Comparative global gene expression profiling of cell populations derived with the NC and BE protocols confirmed the enhanced expression of various melanocyte associated markers, including *TYRP1, MLANA, DCT, TYR*, and *SILV*, following treatment with BE (**Figures 4.5**). In contrast, NC-derived populations displayed a gene expression profile associated with sensory and nociceptor neuron fates (Chambers et al., 2012a). BE treatment also induced substantial upregulation of COL3A1 and CRYAA (**Figure 4.5A**). Our group has previously observed transient expression of COL3A1, and several crystallin transcripts in neural rosette stage cells (Elkabetz et al., 2008). However, future studies are required to address whether COL3A1 and CRYAA are expressed in NC stage melanocyte precursors or represent contamination with another cell type induced under BE conditions, as those gene expression analyses were performed on unpurified BE bulk populations. BE-derived *Sox10::GFP* cells that co-expressed MITF exhibited an elongated, spindle-like morphology compatible with the appearance of melanocyte progenitors (**Figure 4.3C**).

Maturation and Characterization of Melanocytes

Melanoblast progenitors were isolated on day 11 based on *Sox10::GFP* and c-kit expression and replated in maturation media (**Figure 4.6A**). We next established defined

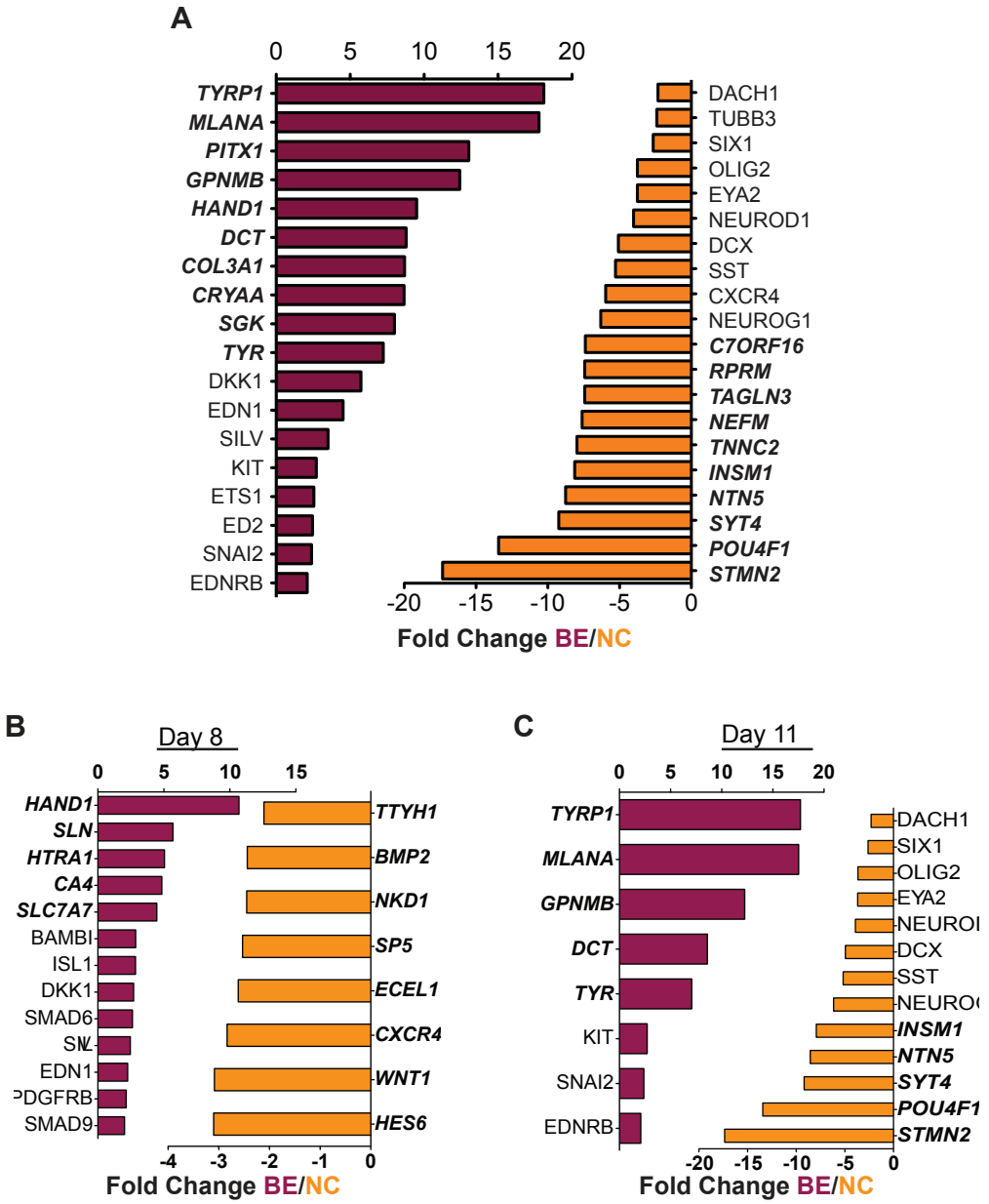

Figure 4.5. BE treatment enhances the induction of a melanocyte-associated transcriptional profile. (**A**) Comparative gene expression analysis identified significantly up- (red) and downregulated (orange) genes at day 11 in BE-induced cells compared to NC cells. Bold genes represent top 10 most differentially regulated genes. (**B**, **C**) Global gene expression changes first detected at days 8 and 11 of BMP4 and END3 treated cells were identified when compared to NC-derived cells. (**B**) Day 8 gene expression was characterized by upregulation of early melanocyte lineage-associated markers premelanosome protein (PMEL, i.e. SILV) and endothelin 1 (EDN1) and a concurrent decrease in Wnt signaling suggested by upregulated Wnt inhibitor dickkopf homolog 1 (DKK1) and decreased levels of Wnt1. (**C**) The majority of melanocyte-associated markers were not upregulated until day 11. Bold genes represent top 5 most differentially regulated genes.

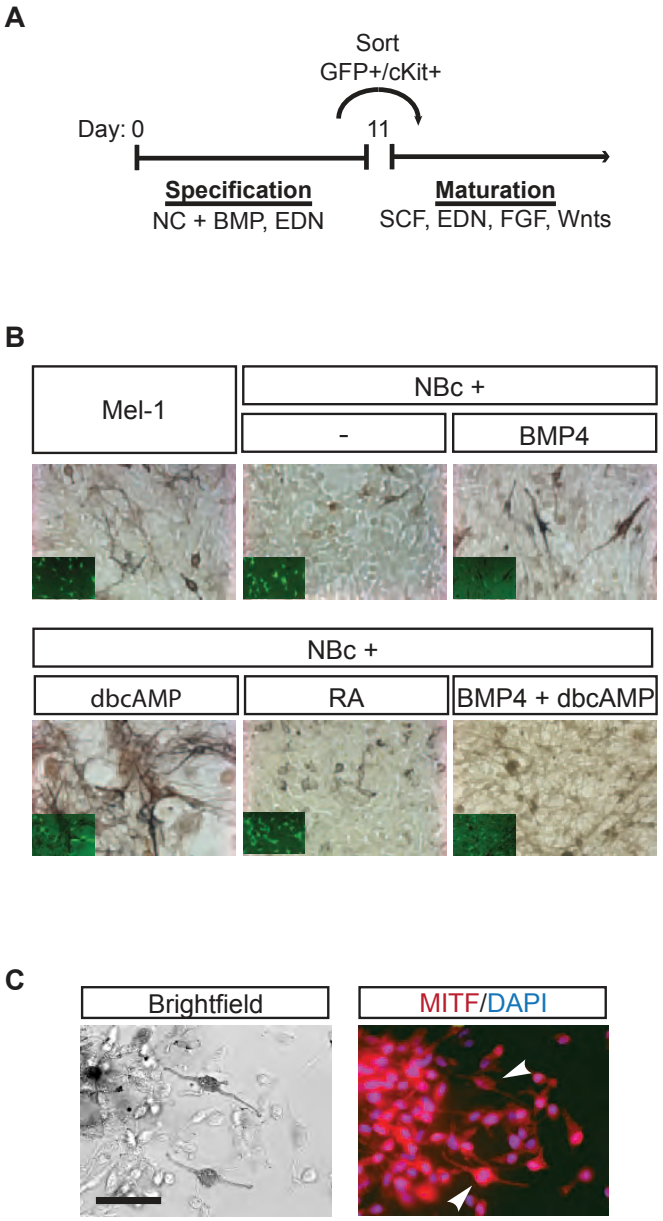

Figure 4.6 hESC-derived melanoblasts can be matured to a pigmented state under defined conditions. (**A**) BE-derived melanocyte progenitors can be matured to a pigmented state following culture in media containing SCF, EDN3, FGF2, BMP, cAMP and Wnt signaling factors. (**B**) Complete neurobasal media (NBc) containing B27, Chir, SCF, END3 and FGF2 was supplemented with BMP4, dibutyryl cyclic AMP (dbcAMP), or retinoic acid (RA) and compared with Mel-1 (Fang et al., 2006) media containing Wnt3a-conditioned media for its ability to support maturation of hES-derived melanocytes to a pigmented, spindle-like morphology. Insets show *Sox10::GFP* expression of corresponding image. (**C**) Pigmented cells expressing MITF can be observed as early as one week after passaging. Scale bar represents 20μm.

culture conditions for melanocyte maturation. A previous melanocyte differentiation medium was based on the use of conditioned media from a WNT3A producing murine cell line (Fang et al., 2006). While we found the same media to be sufficient for maturation of BE-derived melanoblasts to a pigmented, terminally differentiated state (**Figure 4.6B**), we developed defined maturation conditions using a medium containing SCF, EDN3, FGF2, Chir, cyclic AMP, BMP4, and B27 (**Figure 4.6B**). Under these conditions, pigmented cells were first observed by brightfield microscopy six days after sorting and co-expressed the melanocyte marker MITF (**Figure 4.6C**). By day 20 of differentiation, most clusters were pigmented (**Figure 4.7A**) and cell pellets became darkly colored by passage five (**Figure 4.7B**). Extended culture supported the propagation of an essentially pure population of melanocytes expressing typical melanocyte transcription factors such as MITF and SOX10 and melanosomal markers including tyrosinase-related protein 1 (TYRP1) and premelanosome protein (PMEL) (**Figure 4.7C,D**). A comparison of gene expression profiles of mature melanocytes and day 11 melanoblast progenitors revealed that maturation had supported the induction of several late stage melanocyte markers including oculocutaneous albinism II (OCA2), tyrosinase (TYR), and melan-A (MLANA), while NC markers such as TFAP2C, EDNRA and EDN1 had been downregulated (**Figure 4.8**).

Functional Characterization of hESC-Derived Melanocytes

Electron microscopy of human ES-derived melanocytes (ES-melanocytes) revealed the presence of numerous pigmented melanosomes, representing all four stages of melanosome maturation (**Figure 4.9A**). In primary skin, melanocytes reside adjacent to the basement membrane at the interface of the epidermal and dermal layers. In an organotypic skin reconstruct assay in which melanocytes and keratinocytes were seeded onto a preformed layer of fibroblasts and collagen, ES-melanocytes phenocopied the

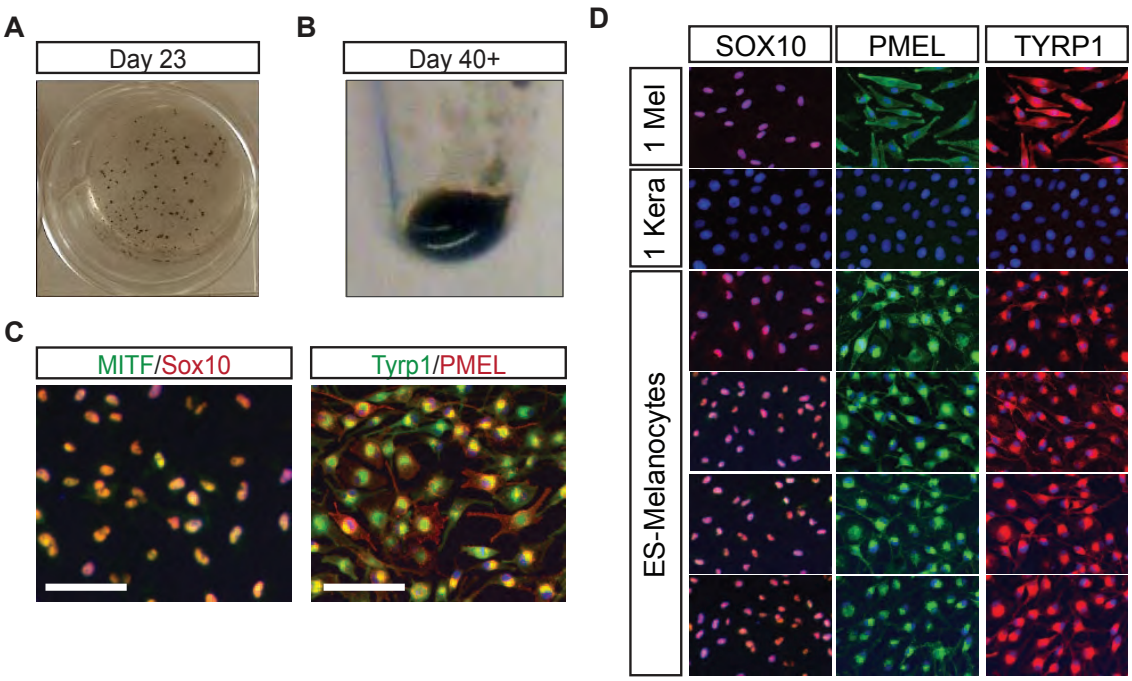

Figure 4.7. <u>hESC-derived melanocytes are pigmented and express mature markers.</u> (**A**, **B**) Cells become progressively more pigmented with macroscopic pigmented clusters discernable in tissue culture wells within 3 weeks (**A**) and cell pellets of $1x10^6$ cells taking on a darkly pigmented phenotype (**B**). (**C**) Extended culture supports the propagation of nearly pure populations of mature melanocytes expressing transcription factors SOX10 and MITF and melanosomal markers TYRP1 and PMEL. Scale bar represents 50μm. (**D**) The induction of ES-melanocytes using the BE protocol is highly reproducibly as assessed by immunofluorescence staining for SOX10, PMEL, and TYRP1 in four independently derived lines. Primary melanocytes (1 Mel) and keratinocytes (1 Kera) are shown as respective positive and negative controls. DAPI nuclear staining is depicted in the blue channel.

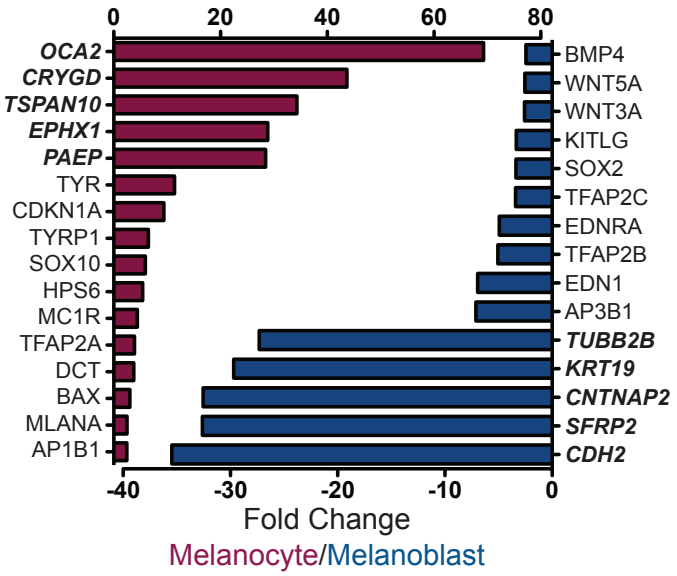

Figure 4.8. <u>Defined maturation conditions promote induction of late melanocyte markers</u>. Mature melanocytes exhibit elevated levels of mature marker expression (red) and downregulation of neural crest and stem cell-associated markers (blue) compared to melanocyte progenitors in gene expression analyses. Bold genes represent top 5 most differentially regulated genes.

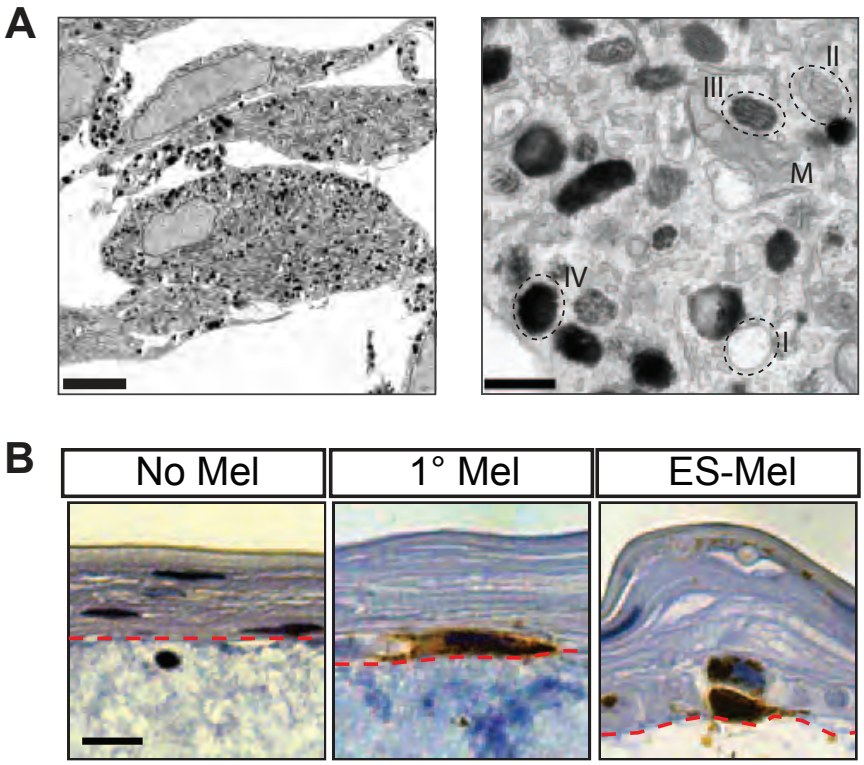

Figure 4.9. <u>hESC-derived melanocytes form melanosomes and home to the basement membrane</u>. (**A**) Numerous pigmented melanosomes, representing all four stages of melanosome maturation (I-IV), are visible in the cytoplasm of ES-derived melanocytes by electron microscopy. Scale bar represents 5μm (left) and 500nm (right). (**B**) Primary and ES-derived melanocytes were seeded onto artificial skin reconstructs which were generated by establishing a mixture of melanocytes and keratinocytes on top of a pre-formed "dermal" layer of collagen and fibroblasts. Tyrosinase positive (IHC brown) ES-derived melanocytes home to the basement membrane as predicted. Scale bar represents 2μm. No melanocyte negative control – left, primary melanocytes – middle, ES-melanocytes – right. Dotted line shows the interface between the dermal and epidermal layers.

localization of primary control melanocytes and correctly homed to the basement membrane (**Figure 4.9B**). To further assess the *in vivo* migration properties of ES-melanocytes, a constitutively GFP-expressing hESC line was differentiated under BE conditions and resulting melanoblasts were injected into the migration staging area (Erickson and Goins, 1995) at the trunk of 13-15 HH stage chick embryos (**Figure 4.10A**). While most NC derivatives are known to migrate along a ventromedial migration pathway between the neural tube and adjacent somites we predicted that our ES-melanocytes would also follow a dorsolateral pathway along the ectoderm, a migration behavior that is unique to the melanocyte lineage (Bronner-Fraser, 1986; Erickson and Goins, 1995; Reedy et al., 1998; Thomas and Erickson, 2008; Wakamatsu et al., 1998). ES-melanocytes were highly migratory post-injection and dispersed widely along the A-P axis. 16 hours after transplantation BE-derived melanoblasts were seen migrating along the dorsolateral pathway beneath the ectoderm (**Figure 4.10B,C**), while after 72 hours GFP-positive melanocytes had exclusively invaded the epidermis, demonstrating the selective migration and survival of ES-melanocytes *in vivo* (**Figure 4.10D**). Migration along the dorsolateral pathway and invasion of the dermal layer were not observed in non-melanocyte competent ES-derived NC populations (data not shown; see also (Lee et al., 2007)).

hESC-Derived Melanocytes Closely Resemble Primary Adult Melanocytes

Gene expression profiles of ES-melanocytes were more similar to adult than neonatal primary melanocytes (**Figure 4.11**), although ES-melanocytes differed from both populations in their lack of HOX gene expression. It is possible that patterning conditions for BE-derived melanocytes specify a more anterior population of melanocytes as compared to primary cells isolated from posterior regions such as breast, abdominal, and foreskin tissues. Caudal melanocytes expressing HOXB2 and HOXB4 could

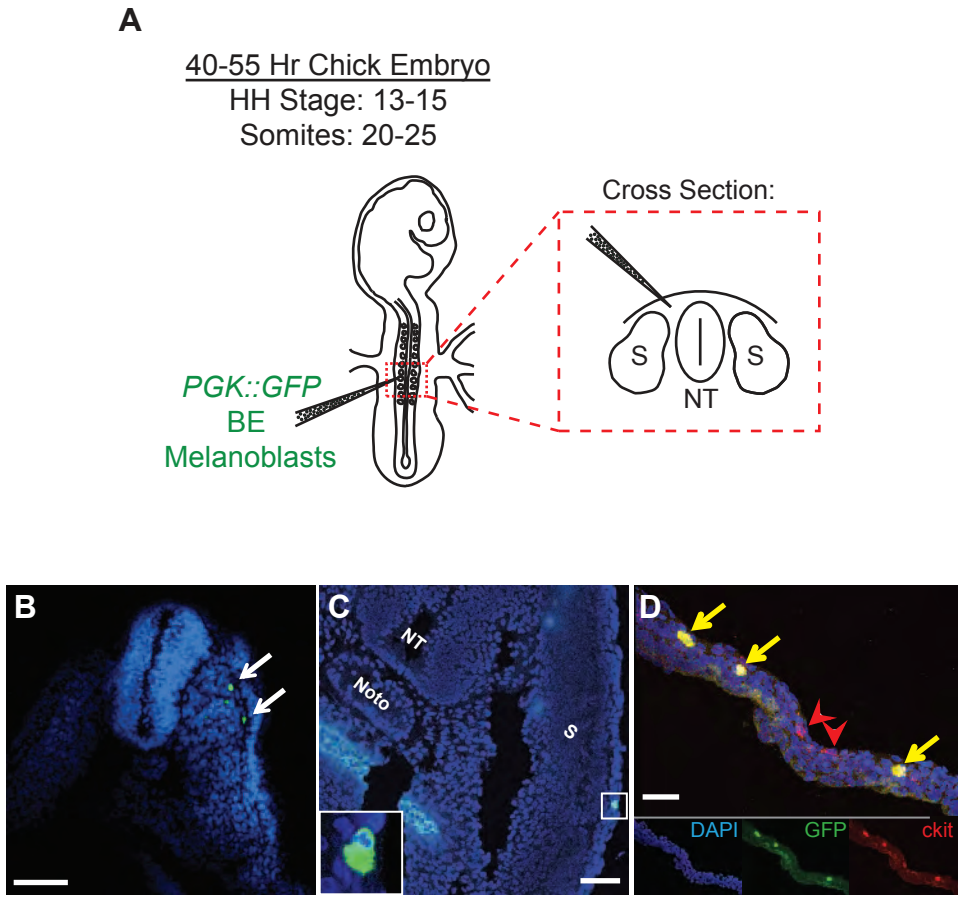

Figure 4.10. hESC-derived melanocytes phenocopy dorsolateral migration in vivo. (**A**) Migration capacity is assayed by *in ovo* transplantation of BE-derived melanocytes constitutively expressing GFP in to the migration staging area between the somites and dorsal neural tube. (**B, C**) 16 hours post transplant cells are observed migrating along the dorsolateral pathway. Scale bars represent 100μm (B) and 50μm (C). Neural tube (NT), notochord (Noto), and somite (S). (**D**) By 72 hours, GFP- and KIT-expressing ES-derived cells invade the chick epidermis (yellow arrows) adjacent to endogenous c-kit expressing melanocytes (red arrowheads) Scale bar represents 25μm.

A

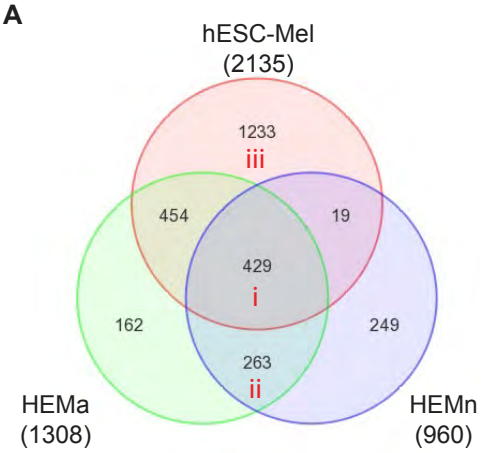

B

i	ii	iii
Top 5 GO Terms		
Pigmentation During Development	Response to Virus	Establishment of Protein Localization
Pigmentation	Coenzyme Metabolic Process	Protein Transport
Melanin Biosynthetic Process	Cofactor Metabolic Process	Protein Localization
Melanocyte Differentiation	Response to Organic Substance	Vesicle-Mediated Transport
Pigment Cell Differentiation	Response to Reactive Oxygen Species	Intracellular Transport

Selected Genes						Top 10 Genes		
Gene	P-value	Fold-Change	Gene	P-value	Fold-Change	Gene	P-value	Fold-Change
TYRP1	7.62E-15	88.62	HOXB7	2.11E-15	7.35	CRYGD	3.55E-13	31.89
OCA2	5.78E-17	79.41	HOXC4	3.46E-15	4.01	PAEP	5.01E-11	30.17
TYR	7.69E-12	73.13	HOXC8	9.66E-15	3.70	SLC38A8	2.51E-09	16.10
SOX10	4.67E-16	69.55	HOXC6	6.93E-13	3.43	NCCRP1	1.22E-08	15.24
MLANA	7.06E-17	50.31	HOXB2	2.15E-08	2.41	DLL3	1.61E-07	14.68
DCT	9.01E-09	38.35				LOC388588	2.25E-07	13.28
SILV	1.68E-13	36.22				CLIP3	6.35E-07	12.42
TFAP2A	2.66E-10	17.56				MAPK4	1.34E-10	11.33
						PTGDS	1.04E-05	11.15
						SH3TC1	2.88E-08	10.09

Figure 4.11. Gene expression profiles of hESC-derived melanocytes closely resemble primary melanocytes. (**A**) Comparative gene expression profiles of hESC-derived melanocytes (hESC-Mel), primary adult and neonatal human epidermal melanocytes (HEMa and HEMn). Gene lists were defined as genes upregulated greater than two-fold with and FDR<0.05 compared to hESCs. Similarity between hESC-Mel and HEMa is highly significant based on hypergeometric distribution ($p=6.7x10^{-9}$). (**B**) Top five gene ontology (GO) terms and selected genes from indicated regions of Venn diagram (A).

however be established from precursors treated with RA during the early stages of differentiation (**Figure 4.12**). ES-derived melanocytes also uniquely upregulated genes associated with protein localization and transport (**Figure 4.11B**) perhaps reflecting the increased melanin production observed when compared to primary melanocytes.

SOX10 and KIT Single Positive Populations are also Melanocyte Competent

Temporal analysis of *Sox10::GFP* and c-kit expression during NC induction showed that *Sox10::GFP* expressing cells could be detected by day 6 of differentiation while *Sox10::GFP*, c-kit co-expressing cells did not emerge before day 10 (**Figure 4.13**). To test the competency of Sox10 positive cells to give rise to c-kit+ melanoblasts, we isolated *Sox10::GFP* and c-kit single positive cells (GFP+/cKit- and GFP-/cKit+, respectively) as well as double positive and double negative cells, by flow cytometry and replated each in maturation media. Cells were again assayed for *Sox10::GFP* and c-kit expression after 5 and 12 days. As predicted, GFP+/cKit- cells gave rise to GFP+/cKit+ and GFP-/cKit+ progeny, while GFP- cells lacked this plasticity (**Figure 4.14A**). More importantly, GFP and cKit single positive populations eventually differentiated into MITF expressing pigmented cells (**Figure 4.14B**), although GFP+/cKit- cells did so with delayed kinetics. Meanwhile the GFP-/cKit- population never gave rise to pigmented cells and could not be propagated in our maturation media. These data illustrate that, even without sorting for SOX10 or c-kit, BE-treated cells can efficiently generate melanocytes using our defined maturation conditions greatly facilitating studies in hESC lacking a SOX10 reporter or in disease specific iPSCs.

Discussion

Our study has also established a readily scalable, defined protocol that generates pure populations of mature melanocyte with great efficiency. Our cells recapitulate all

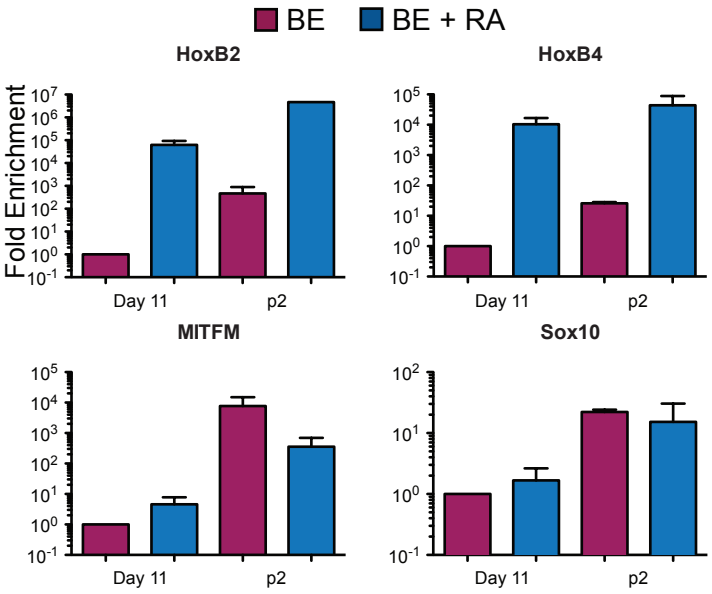

Figure 4.12. <u>hESC-derived melanocytes can be caudalized by early RA treatment</u>. Melanocytes derived in the presence of retinoic acid from day 6 to day 11 express higher levels of HoxB2 and HoxB4 than melanocytes derived under regular BE conditions, while still maintaining expression of melanocyte markers MITFM and Sox10.

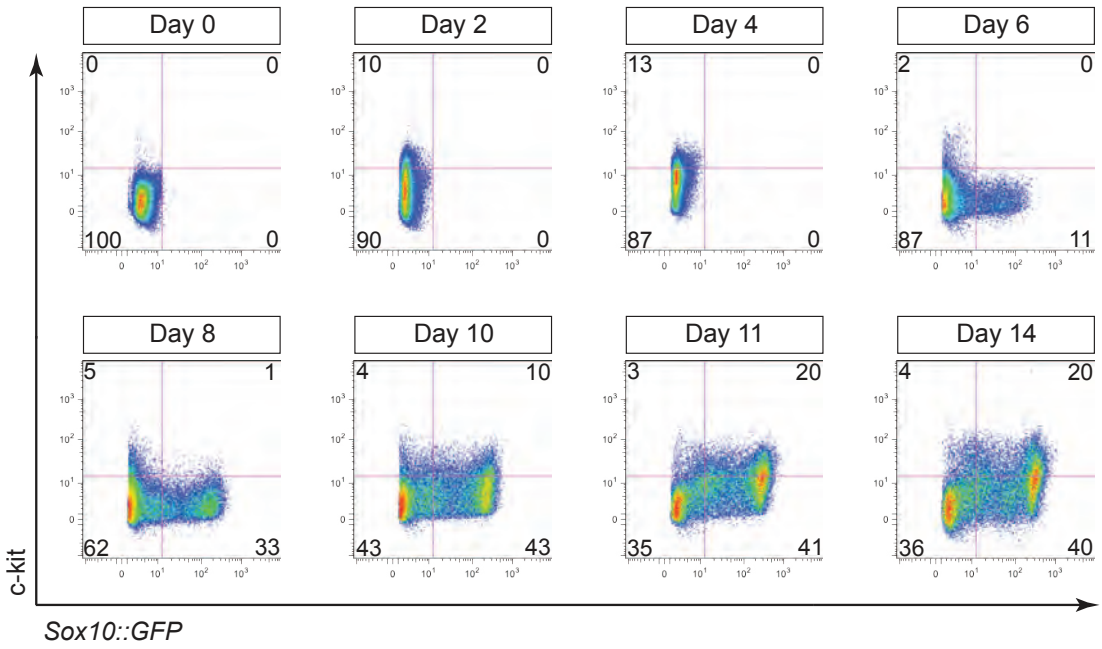

Figure 4.13. <u>SOX10 and KIT are sequentially induced during melanoblast specification</u>. FACS analysis reveals the sequential induction of *Sox10::GFP* and c-kit in melanocyte progenitors under NC differentiation conditions.

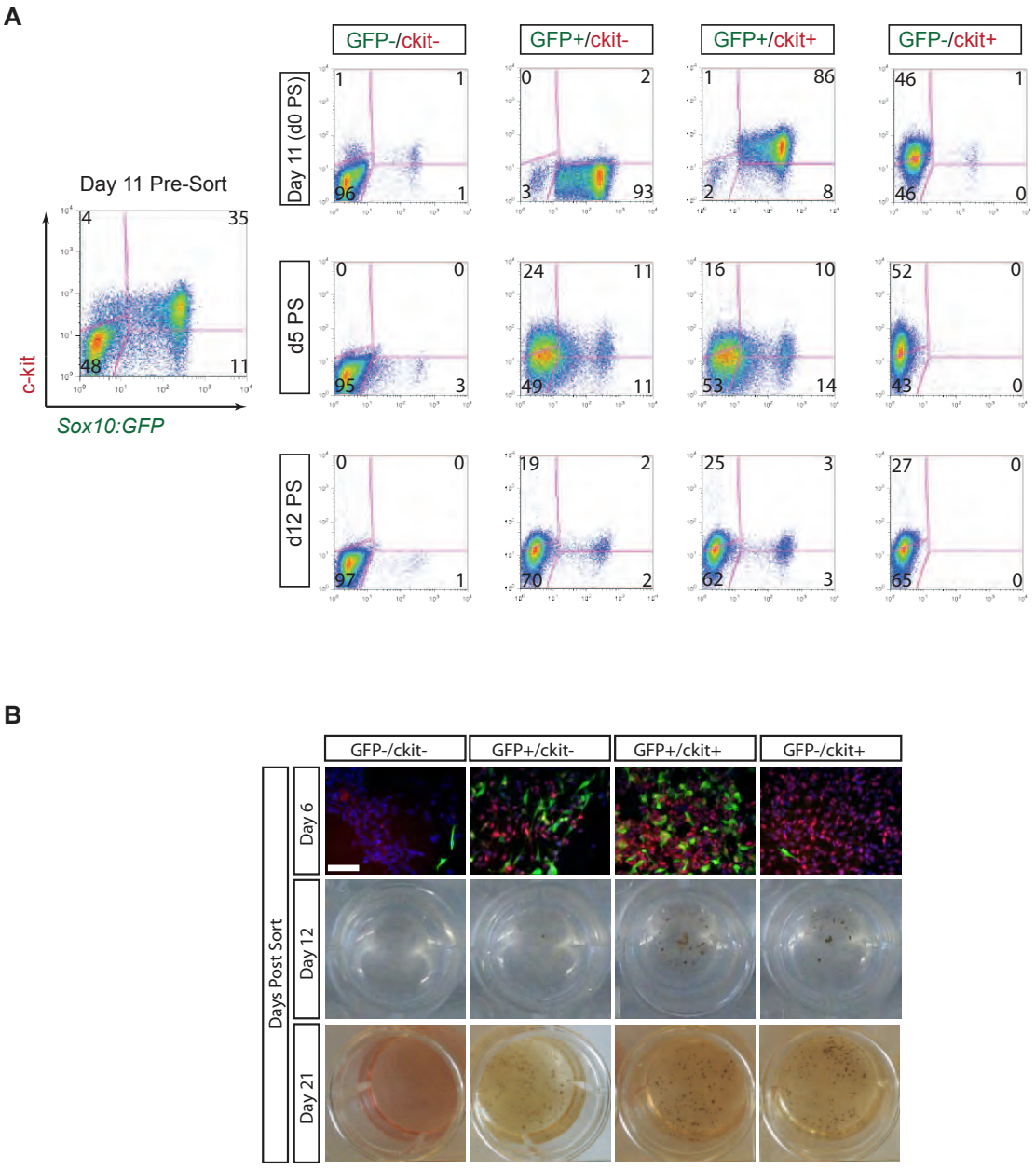

Figure 4.14. <u>SOX10 and KIT single positive populations are also melanocyte competent</u>. (**A**) Day 11 BE-derived cells were FACS isolated based on *Sox10::GFP* and c-kit expression and maintained in melanocyte maturation media. Expression of *Sox10::GFP* and c-kit were reassessed immediately post-sort (PS) or 5 or 12 days PS. (**B**) *Sox10::GFP* and c-kit populations were assayed for *Sox10::GFP* (green) and MITF (red) expression by immunofluorescence. Scale bar represents 100μm. Gross levels of pigmentation were determined at 12 days and 21 days post sort.

structural features of wild-type melanocytes, making them suitable for a wide range of applications and future studies. Furthermore, to our knowledge this is the first protocol that allows for the stage-specific isolation of melanocyte progenitors and mature melanocytes. This will be of particular interest in studies investigating melanocyte development and malignant transformation. We also demonstrate that the axial levels of NC and melanocyte precursor populations can be readily patterned using caudalizing FGF and RA cues. The ability to derive Hox-positive versus Hox-negative human NC cells is particularly intriguing as it will enable studies on the unique plasticity reported for Hox-negative NC in the avian system (Le Douarin et al., 2004).

A recent study has also identified Schwann cells as an additional source of melanocytes (Adameyko et al., 2009) while EDN3 has been shown to induce the reversion of melanocytes to a bipotent progenitor (Dupin et al., 2000). It will be interesting to further explore this close association between glial and melanocyte fates although the reported expression of Schwann cell associated markers in murine melanoblasts (Colombo et al., 2011) highlights the need for a thorough and careful analysis to differentiate between the origin of melanocytes from a bipotent glial-melanocyte progenitor and the derivation of melanocytes from Schwann cell precursors.

CHAPTER FIVE

The Use of hPSC-Derived Melanocytes for Disease Modeling

Introduction

The field of *in vitro* disease modeling has undergone a drastic paradigm shift since the discovery of iPSCs in 2006 (Park et al., 2008c; Takahashi et al., 2007; Takahashi and Yamanaka, 2006). It is now possible to generate patient-specific iPSCs that can be expanded and differentiated to virtually any cell type. In fact, one could argue that our ability to establish disease modeling systems for any given disorder is now only limited by our ability to derive the affected cell type from iPSCs and establish assays that faithfully and accurately reflect the disease phenotype.

While there have been many reports of iPS-based disease modeling studies in recent years, including an iPSC based model for the NC-affected disease Familial Dysautonomia from our own group (Lee et al., 2009; Lee et al., 2012), the detection of disease-specific phenotypes in this system has been more difficult and to our knowledge, no attempt has been made at modeling melanocyte-associated diseases using iPSC technology.

We therefore sought to dovetail the melanocyte differentiation protocol described in this work with an application in iPS-based disease modeling. We identified two melanocyte-associated disorders, Hermansky-Pudlak Syndrome (HP) which in broad terms appears to be a disorder of melanosome formation and Chediak-Higashi Syndrome (CH) which reflects a defect in melanosome trafficking (**Figure 5.1**). We sought to determine whether pluripotent stem cell-derived melanocytes could be used to model these genetic pigmentation defects, both of which manifest with hypopigmentation.

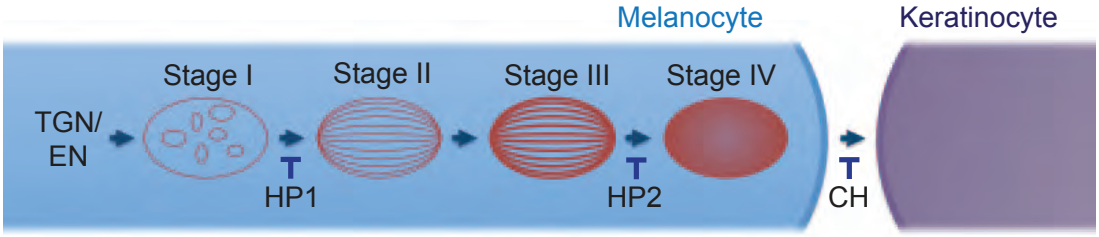

Figure 5.1. Modeling defects in melanosome biogenesis and transfer with iPS-derived melanocytes. Hermansky-Pudlak Syndrome (HP) and Chediak Higashi (CH) Syndrome are disorders with defects in melanosome biogenesis and trafficking amenable for iPS-based disease modeling. Trans-Golgi Network (TGN) and Endosomal Network (EN).

Results

Derivation of HP- and CH-Specific iPSCs

Patient and control fibroblasts were obtained from the Coriell Cell Repository (http://ccr.coriell.org) and the mutational status of each was confirmed. Fibroblasts from a patient with HP subtype 1 (HP1) were found to carry a mutation in HP1 while an HP2 patient was found to be compound heterozygous for mutations in AP3B1 (**Figure 5.2**). Mutations in the LYST gene of the CH patient were also confirmed (**Figure 5.2**). Three independent iPS lines were established from each patient and control fibroblast donor using a single polycistronic lentiviral vector expressing Oct4, Klf4, Sox2, and c-Myc (Papapetrou et al., 2011) (**Table 5.1**). The resulting iPSCs exhibited hESC-like morphology and expressed the pluripotent transcription factors Oct4 and Nanog as well as cell surface markers Tra-1-60, SSEA3, and SSEA4 **(Figure 5.3)**.

HP- and CH-iPSC Derived Melanocytes Exhibit Disease-Specific Pigmentation Defects

Mature melanocytes expressing PMEL, SOX10, TYRP1, and MITF were derived at comparable efficiencies from each of the patient and control iPSC clones using the BE differentiation protocol (**Figure 5.4**) further illustrating the robustness of our differentiation protocol. All HP2 iPS-derived melanocytes exhibited a near complete loss of pigmentation both at the macroscopic level and when quantified after cell lysis, while HP1 melanocytes exhibited a more subtle phenotype detectable only after quantification (**Figures 5.5**). CH melanocytes exhibited pigmentation levels lower than those observed with an African American control (Control 1) but comparable to a Caucasian control (Control 2) (**Figures 5.5**), compatible with the hypothesis that CH affects melanosome transfer rather than production. Differences in pigmentation could also be assayed by

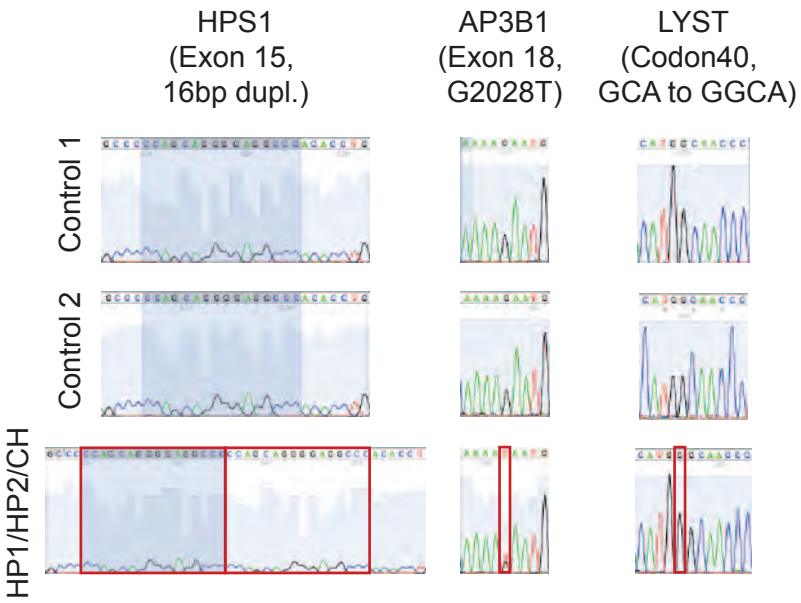

Figure 5.2. <u>Mutational status of control- and patient-derived fibroblasts</u>. (**A**) Control and disease (HP1, HP2, and CH) derived fibroblasts were sequenced to confirm the presence of disease-specific mutations.

Cell Line	Coriell ID	Description	Mutation	Sex	Age	Race	iPS Lines
C1	GM17569	Xeroderma pigmentosum (unaffected)	n/a	Male	29Yr	African American	3
C2	GM00969	apparently healthy non-fetal tissue	n/a	Female	2Yr	Caucasian	2
HP2	GM17890	Hermansky-Pudlak Syndrome 2; HPS2	AP3B1	Male	4 Yr	Other (Cajun, Houma Indian, African American)	4
CH	GM02075	Chediak-Higashi Syndrome; CHS	LYST	Female	1Yr	Caucasian	3
HP1	GM14609	Hermansky-Pudlak Syndrome; HPS	HPS	Female	26Yr	Caucasian	3

Table 5.1. Summary of control and patient-specific fibroblasts characteristics. Control- and patient- derived fibroblasts were obtained from the Coriell Cell Repository. Donor information was provided by Coriell.

.

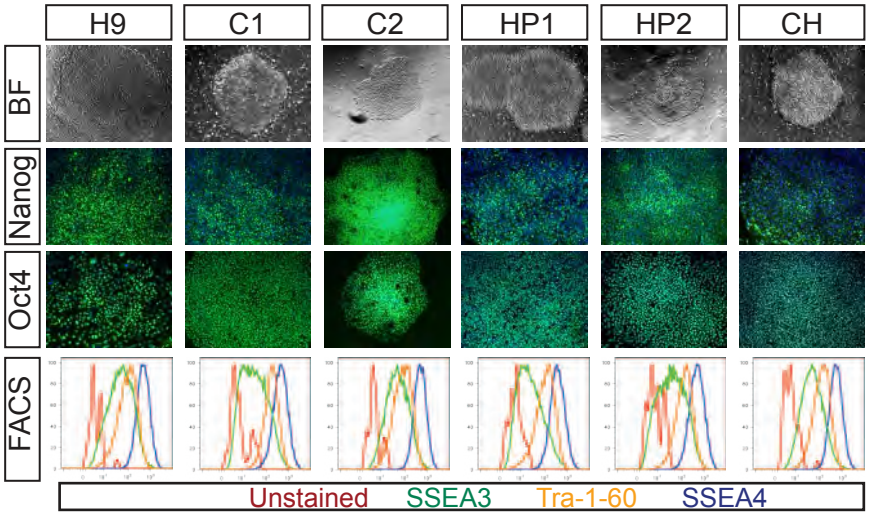

Figure 5.3. Characterization of control and disease-specific iPSCs. (**B**) Control- and disease-derived iPSCs exhibit typical ES morphology and express the pluripotency-associated transcription factors Nanog and Oct4. Expression of ES cell surface markers SSEA3 (green), SSEA4 (blue), and Tra-1-60 (orange) was determined by FACS and compared with unstained cells (red). Shown are representative images for each donor.

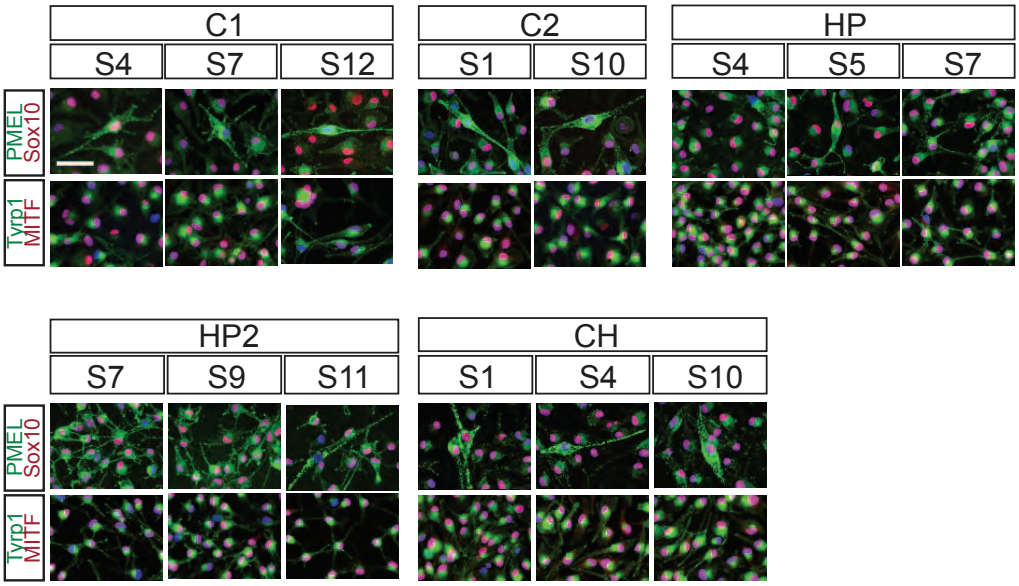

Figure 5.4. Expression of transcription tactors and melanosomal proteins in melanocytes established from control and patient-specific iPSCs. Expression of transcription factors (SOX10 and MITF) and melanosomal markers (TYRP1 and PMEL) are consistent across all melanocytes derived from multiple control and disease-specific iPS clones. Scale bar represents 50μm.

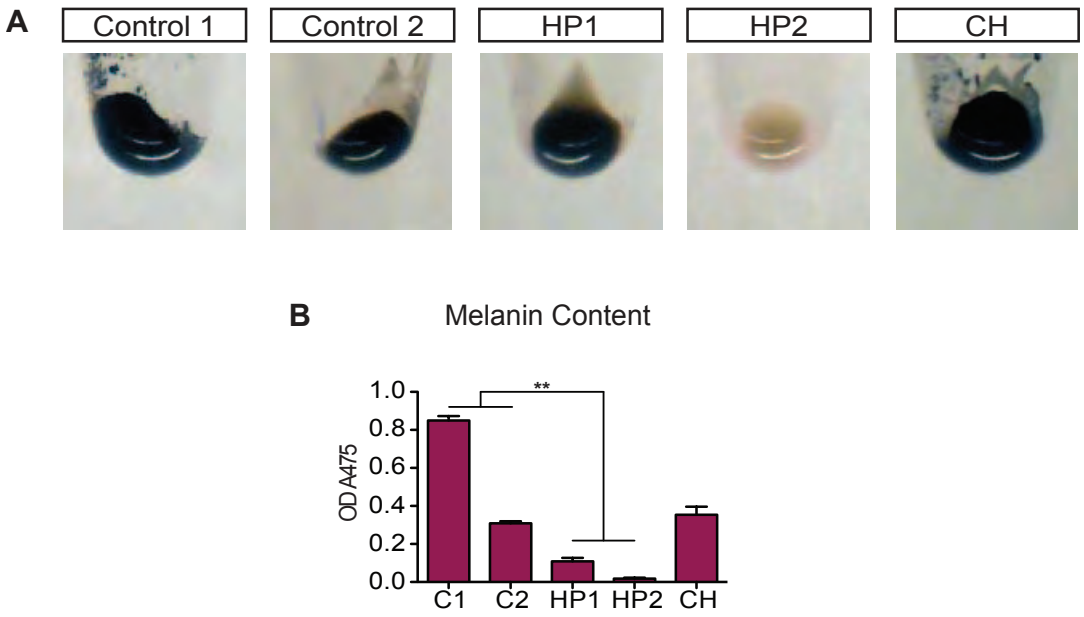

Figure 5.5. Hypopigmentation in HP iPS-derived melanocytes. (**A**) 1e6 melanocytes were pelleted to examine gross levels of pigmentation. Cell pellets of HP2-derived melanocytes exhibit a near lack of pigmentation while HP1-derived melanocytes exhibit a more subtle defect. (**B**) Melanin content was determined from the absorbance of cell lysates at 475nm. This assay readily reflects differences in pigmentation levels between melanocytes derived from African-American (C1) and Caucasian (C2) control iPSCs.

FACS analysis, with higher levels of pigmentation correlating to higher side scatter (SSC) values (**Figure 5.6**). All disease-related phenotypes were consistent among melanocytes derived from each of three independently derived iPS clones, indicating that disease behavior reflects genome-specific differences rather than iPS clonal variability.

Ultrastructural Characterization of Melanocytes Derived from HP- and CH-iPSCs

The nature of the individual pigmentation defects could be further analyzed at the EM level, with HP1 and HP2-derived melanocytes exhibiting a notable reduction in mature melanosomes (**Figure 5.7A**) as quantified using computer-assisted image analysis (**Figure 5.7B-E)**. There was a significant decrease in the ratio of melanosome to total cell area when compared to both C1 and C2 controls (**Figure 5.7E**). At higher magnification numerous dark punctae that may correspond to free melanin in the cytoplasm were also discernible in HP2 cells (**Figure 5.7A**). In contrast, CH melanocytes exhibited the most striking phenotype with significant increases in both melanosome number and size (**Figures 5.7**). Increased melanosome number and size could be further corroborated by immunofluorescence staining for the early melanosomal marker PMEL (**Figure 6B**). High magnification EM analysis revealed that CH-derived melanocytes exhibit mature but strikingly enlarged melanosomes not seen in the melanocytes derived from any of the other disease or control lines (**Figure 5.4**). Global gene expression analyses in which control- and disease-derived melanocytes were compared revealed few differences at the transcript level (**Figure 5.8**). This likely reflects the biological nature of the diseases in which downstream processes are disrupted with little opportunity for transcriptional feedback. These data also again highlight the robust nature of our differentiation protocol in which clones derived independently from control- and disease lines clustered together with high degrees of similarity.

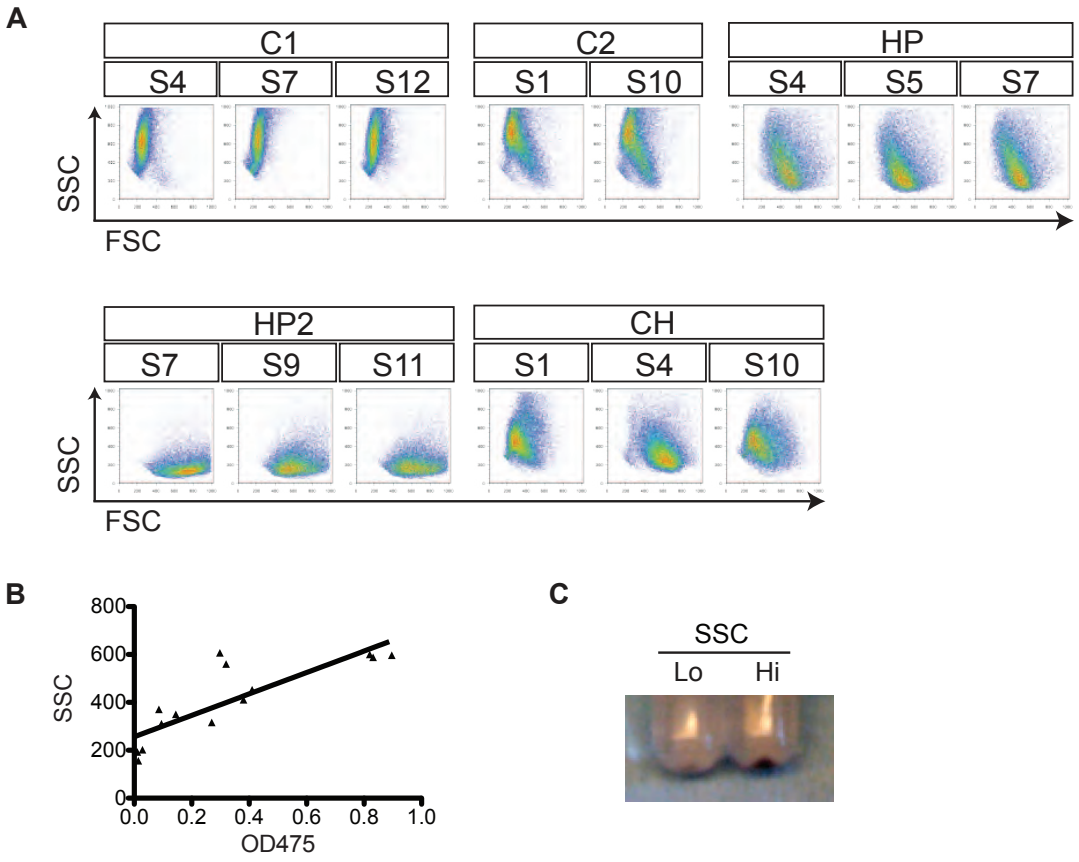

Figure 5.6. FACS side scatter correlates with pigmentation. (**A**) Side scatter (SSC) phenotype by flow cytometric analysis are consistent across all melanocytes derived from multiple iPS clones. (**B**) Pigmentation levels of control- and disease-derived melanocytes were measured by OD475 and correlated with SSC by flow cytometry (r^2= 0.7). (**C**) hESC-derived NC containing melanocytes and other neural crest derivatives were sorted into SSC low and high populations and 1x10^6 cells were pelleted to assess gross levels of pigmentation.

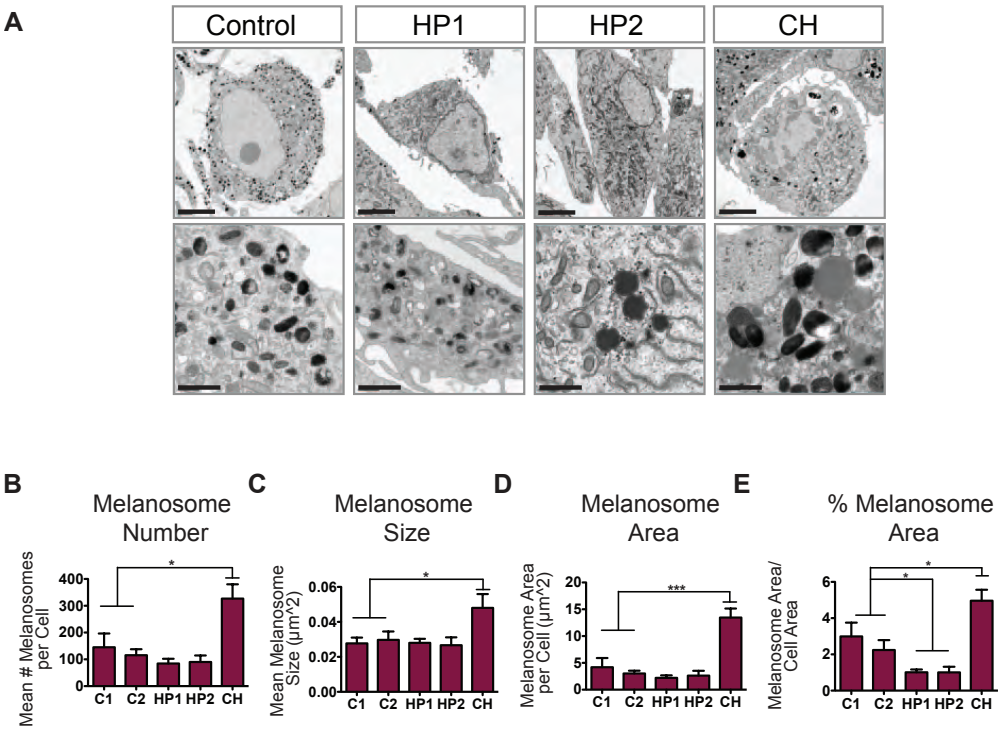

Figure 5.7. <u>Ultrastructural disease-specific phenotypes in iPS-derived melanocytes</u>. (**A**) HP1- and HP2-associated pigmentation defects can be observed in electron micrographs while CH-derived melanocytes exhibit disease-typical enlarged melanosomes. Scale bars represent 5µm (top row) and 1µm (bottom row). (**B-E**) Stereological quantification of melanosome phenotype observed in electron micrographs. Error bars represent the s.e.m. from melanocytes derived from three independent iPS lines for each disease (2 lines were derived from donor C2).

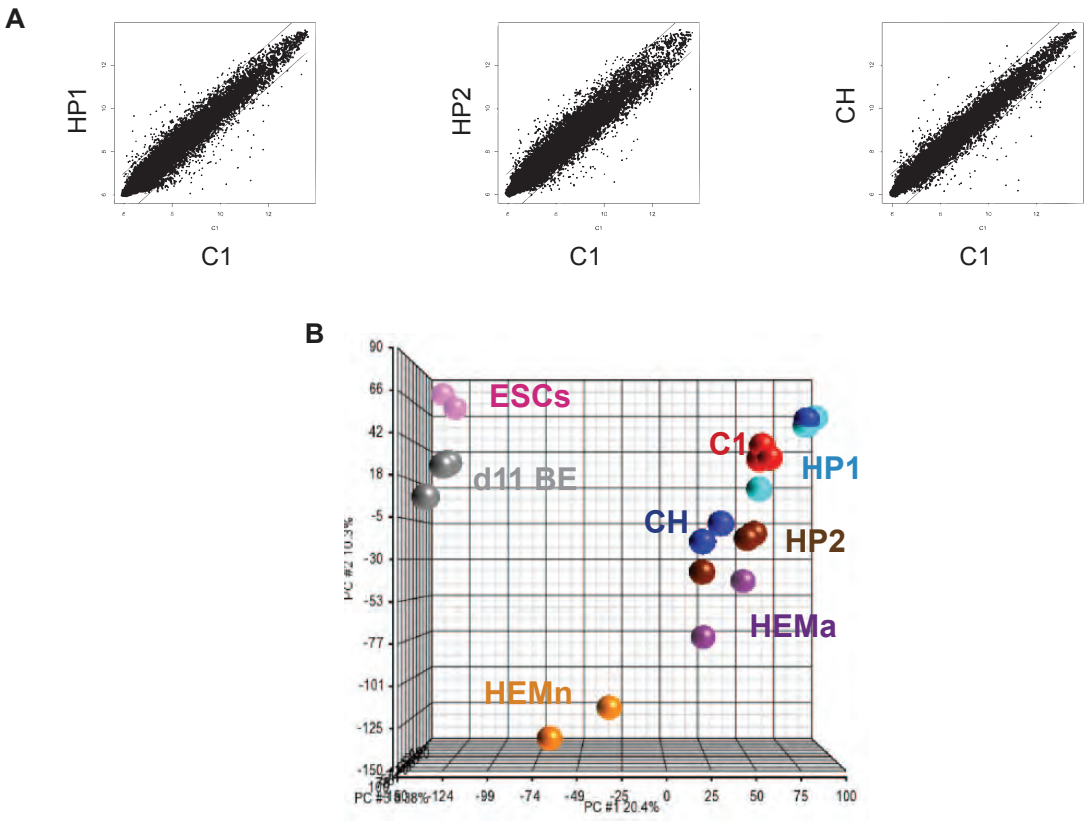

Figure 5.8. <u>Comparative gene expression analysis of control- and disease-derived melanocytes</u>. (**A**) Global gene expression patterns were compared between control (C1) and disease-derived melanocytes (HP1, HP2, and CH). Lines indicate 2-fold changes between the two samples. C1 control-derived melanocytes are highly similar to HP- (r^2=0.97), HP2- (r^2=0.96), and CH-derived melanocytes (r^2=0.97). (**B**) Principle component analysis (PCA) of global gene expression patterns of hESCs, melanocyte progenitors (d11 BE), control- (C1), and disease-derived (HP1, HP2, CH) melanocytes, and neonatal (HEMn) and adult human epidermal melanocytes (HEMa).

Disease- and Control-Derived Melanocytes Do Not Differ in their Migratory or Proliferative Capacity

It has been described that the HPS1 mouse model *pale ear* (*ep*) exhibts hypopigmented ears, tails, and paws due to increased numbers of dermal melanocytes at these sites in spite of having a coat color that is similar to their parental strain (Wei, 2006). It is not known whether this might reflect a disease-associated defect in melanocyte migration, survival, or proliferation in these locations. To investigate the migratory properties of HP-melanocytes, timelapse microscopy was performed over 18 hours and migratory behavior quantified (**Figure 5.9**). However no significant differences were observed between genotypes. Similarly, disease- and control-derived iPS melanocytes did not exhibit differences in proliferation as assessed by Ki67 staining (**Figure 5.10**). These experiments were conducted in mature melanocytes and we cannot rule out whether defects in migration or proliferation would have manifested themselves at the progenitor stage in day 11 BE-derived melanoblasts.

Discussion

The derivation of pluripotent stem cells from human fibroblasts (Park et al., 2008c; Takahashi et al., 2007; Yu et al., 2007) has been successfully applied for modeling human disease (Dimos et al., 2008; Ebert et al., 2009; Park et al., 2008a), including disorders of the neural crest such as familial dysautonomia, (Lee et al., 2009). In the current study we present the first example of modeling melanocyte-specific disorders, deriving patient-specific iPSCs from two distinct genetic syndromes. In each case we were able to successfully generate patient specific melanocytes and to define pigmentation defects characteristic of each disorder *in vitro*. Previous iPS-based disease modeling studies have suffered greatly from variability observed between iPS lines. Therefore the unusual degree of fidelity observed between melanocyte clones derived

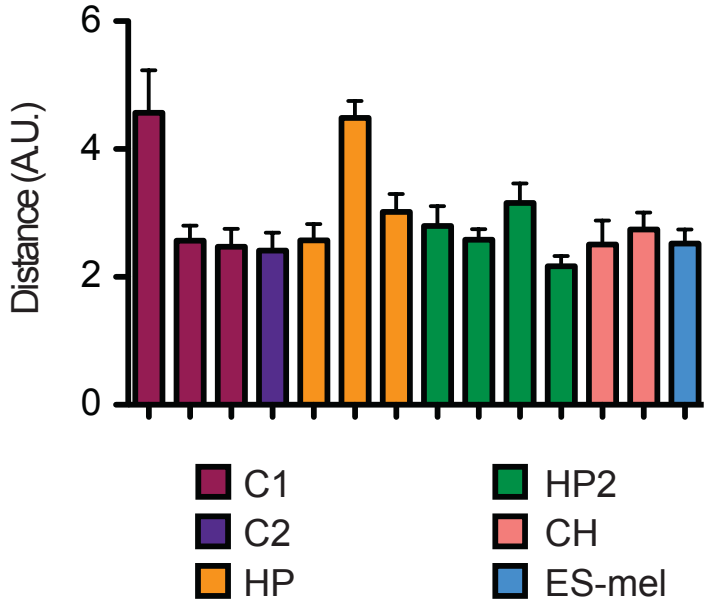

Figure 5.9. No differences in migratory behavior are observed between disease- and control-specific iPS-melanocytes. Timelapse microscopy was performed every 5 minutes over 18hrs and migration behavior analyzed using Metamorph software. The average distance migrated (Arbitrary Units – A.U.) was determined for multiple clones for melanocytes derived from Control- (C1 and C2) and disease-specific (HP, HP2, CH) iPSCs as well as an ES-derived melanocyte clone were analyzed. Each data set represents the average of 11 to 27 cells analyzed. Error bars represent standard error of the mean.

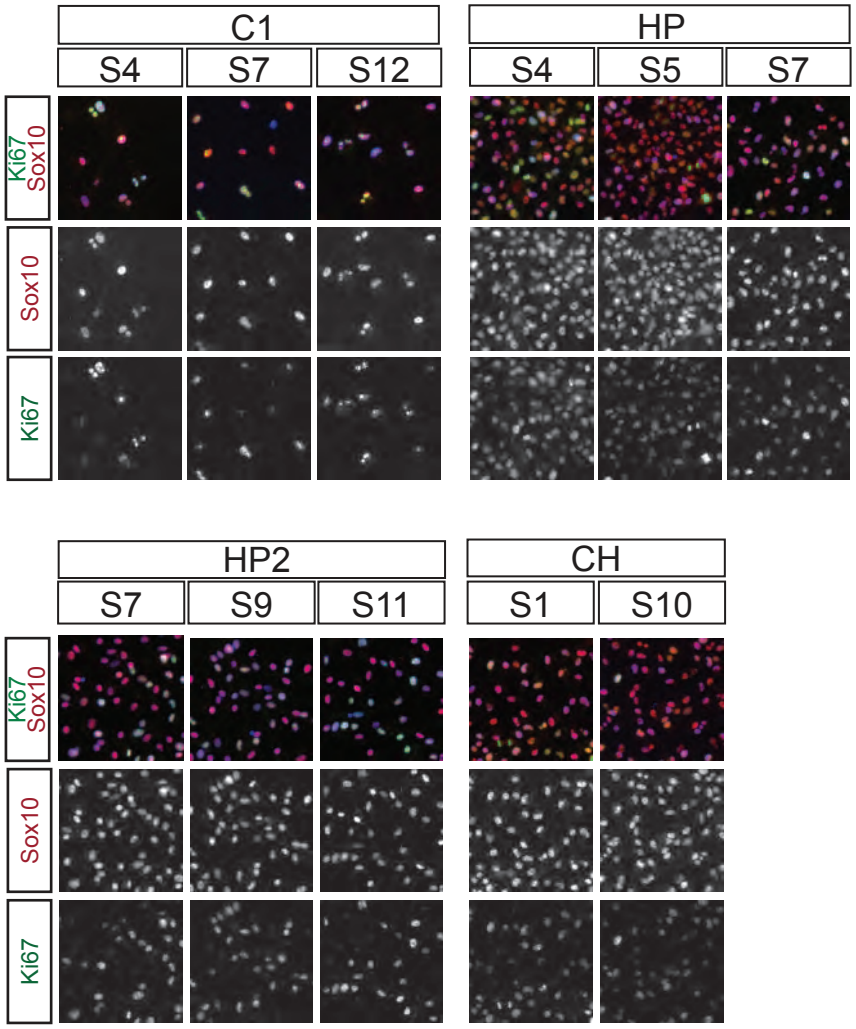

Figure 5.10. <u>No differences in proliferative behavior are observed between disease- and control-specific iPS-melanocytes.</u> Melanocytes derived from control (C1) and disease-specific (HP, HP2, CH) iPSCs were stained for SOX10 (green) and Ki67 (red).

from multiple iPS lines illustrates the highly robust nature of our melanocyte induction protocol. This establishes the framework for high throughput screening studies to further explore disease biology or to identify novel candidate drugs affecting melanocytes specification or levels of pigmentation. A particularly attractive strategy for the future might be the use of disease-specific melanocytes in the identification of drugs that reverse easily screened pigmentation defects associated with HP1 as a surrogate assay for compounds that may also correct lysosomal function in other disease relevant cell types such as pulmonary pneumocytes.

CHAPTER SIX

Discussion and Future Directions

In the body of work described herein we have determined the conditions that allow for the progression from human pluripotent stem cell to NC, the subsequent specification of this NC population along the melanocyte lineage and the maturation to a functional melanocyte stage. This differentiation occurs rapidly and with high efficiency so that scalable, pure populations of cells can be isolated at each step. We have characterized each stage in terms of marker expression and function and in the process have defined pathways critically involved in each step of the differentiation. Finally by combining this approach with patient-specific iPSCs we have shown that our system is highly amenable for disease modeling and future therapeutic studies (**Figure 6.1**). We believe the platform established here will allow for a broad range of applications and future investigations. Below we discuss a sampling of potential future directions for each stage of the project.

Future Studies of Neural Crest

In our studies we have identified defined conditions for the derivation of NC from hPSCs. Previously described approaches had required the formation of EBs or stromal coculture (Lee et al., 2007; Zhou and Snead, 2008), which had obscured the signaling inputs governing NC development, particularly for the very earliest steps of NC specification. Our system therefore offers a unique opportunity to investigate previously inaccessible events and requirements governing early human NC lineage induction. Of particular interest is the question of whether NC arises from a previously specified neural plate or

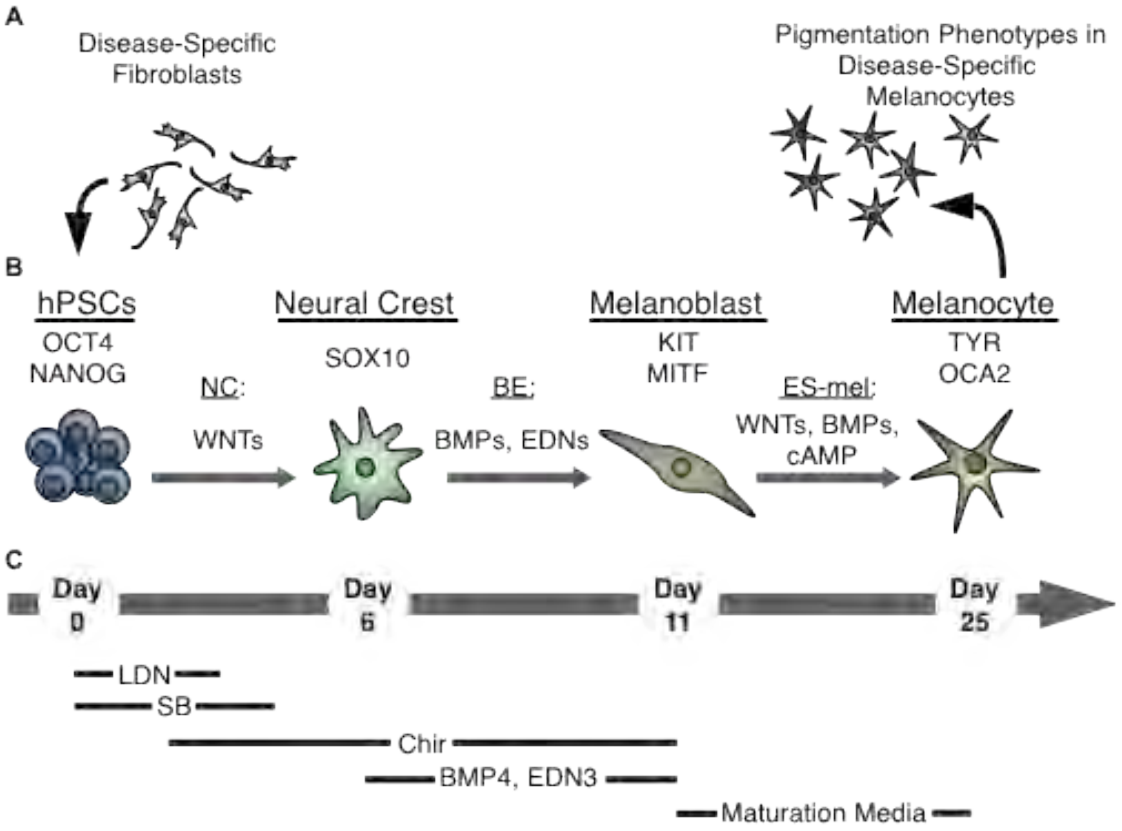

Figure 6.1. Disease-specific melanocytes that faithfully recapitulate pigmentation defects can be derived from human pluripotent stem cells using a stepwise differentiation paradigm. A) Disease specific fibroblasts from HP- and CH- donors were reprogrammed to establish hPSCs. (**B**) Exposure of Oct4 and Nanog expressing hPSCs to the WNT-activating NC protocol resulted in the emergence of a Sox10-positive NC population by day 6. Subsequent additional treatment with BMP4 and EDN3 (BE) skewed the specification along the melanocytic lineage to allow for the establishment of a melanoblast progenitor population expressing KIT and MITF at day 11. Further maturation under ES-melanocyte (ES-mel) conditions in the presence of WNTs, BMP4, and cAMP supported the induction of late melanocyte markers tyrosinase (TYR) and oculocutaneous albinism II (OCA2). Mature melanocytes were used to model the disease-specific pigmentation defects of HP and CH. (C) Growth conditions supporting each stage of differentiation are summarized below.

whether the induction of NC and neural plate occur as independent events. The approach for the induction of NC established here is based upon a protocol for the induction of neural plate derived CNS tissues (Chambers et al., 2009). As such, this system is highly amenable for investigations that compare the signaling requirements for specification of these two lineages and the early relationship between these populations. Sox2, a transcription factor expressed in the early neural plate has been found to inhibit induction of neural crest although it is again upregulated at later stages of NC development (Cimadamore et al., 2011; Luo et al., 2003b; Papanayotou et al., 2008; Wakamatsu et al., 2004). An experiment in which Sox2 is knocked down early during differentiation to prevent induction of a neural plate population would therefore allow us to address whether a Sox10-expressing NC population can be specified independently of neural plate.

Our group has now established multiple approaches for the derivation of NC from hESCs. The work here was preceded by a stromal co-culture protocol in which NC were derived from a rosette precursor (Lee et al., 2007). It was shown that the neural tube-like rosette structures were surrounded by a p75/HNK1 co-expressing population that was multipotent. While the NC derived with our novel protocol have now been shown to also support differentiation into nociceptors (Chambers et al., 2012b) and Schwann cells (unpublished data) in addition to the melanocyte lineage described here, the full potential of this population has not been explored. It will be of great interest to explore whether the multiple NC populations established by our group represent different stages of NC with different *in vivo* counterparts and whether they display variable differentiation potential.

Our work has identified a unique temporal window at day 2 of our differentiation during which cells are competent to respond to Wnt patterning cues that drive NC specification. While we have identified a subset of Wnt responsive genes, some of which have been reported as direct targets of Wnt signaling in the literature, we have not established the full repertoire of day 2 Wnt target genes. ChIP-Seq analysis of β-catenin binding sites could allow for novel insights into the mechanism and transcriptional networks involved in early human NC specification.

Additional work by our group has established that the brief early patterning window observed during NC specification, also applies to the induction of floor plate (Fasano et al., 2010) and placode fates (unpublished data). It is intriguing to speculate that this may reflect a highly permissive epigenetic state that exists at or around day two during which gene targets are briefly accessible to patterning factors. Whether this recapitulates an *in vivo* developmental stage or whether it represents an event during the switch from pluripotent ESC to a developmentally more restricted differentiation cascade will also require further investigation.

Future Studies of Melanocytes

In addition to the evident application of hESC-derived melanocytes for studying basic melanocyte biology or in screens for cosmetic factors regulating pigmentation, several previously inaccessible questions are now open to investigation with our system.

While we were able to propagate hESC-derived melanocytes for upwards of 25 passages we did not investigate whether this extended in vitro culture could be attributed to a subpopulation of adult melanocyte stem cells present in our culture system. One report of single cell transcriptional profiling of melanocyte stem cells from the mouse hair

bulge has suggested that melanocyte stem cells express Dct and Pax3 while notably lacking expression not only of mature melanocyte markers such as Tyrosinase, Silver, Mc1r but also embryonic melanoblast markers such as Ednrb, Kit, Sox10, and Mitf (Osawa et al., 2005). It will be of great interest to identify whether a subpopulation of melanocyte stem cells expressing this marker signature can be identified in our culture conditions.

Recent studies have reported that a subpopulation of epidermal melanocytes can arise from nerve fiber-associated Schwann cell precursors (Adameyko et al., 2009). In addition, the close lineage association between melanocytes and Schwann cells both in terms of their common bipotent progenitor and their ability to dedifferentiate to this state upon EDN3 exposure is intriguing (Dupin et al., 2000). Our group has recently made considerable progress in defining conditions for the derivation of Schwann cells from ESCs. This system along with our own melanocyte differentiation protocol will allow for detailed investigations into the transcriptional network regulating the fate switch between melanocyte and Schwann cells. It will be interesting to see whether hESC-derived melanocytes and Schwann cell can undergo fate switching upon EDN3 exposure as has been reported *in vivo*.

The ability to isolate melanoblasts and mature melanocytes using our system provides a unique opportunity to investigate the effects of developmental stage of the cell of origin in malignant melanoma. It has been established in other oncogenic systems, for example with hematopoietic malignancies, that the transformation of less differentiated progenitor cells results in a more aggressive and invasive phenotype than transformation of a more differentiated cell. The transformation of melanoblasts and mature melanocytes with clinically relevant oncogenes and tumor suppressors will allow us to

test whether the same phenomenon applies to malignant melanoma. Comparison of gene signatures from transformed melanoblasts and melanocytes with patient melanoma samples will further allow us to test whether either can be correlated with clinical outcome. Finally, a complementary investigation into the sequential and combinatorial transformation of melanocytes with clinically relevant oncogenes and tumor suppressors may yield novel insights into the transformation requirements of human melanocytes.

Future Directions in Disease Modeling

The establishment of disease-specific melanocytes will be greatly useful not only for high throughput drug screening studies for HP and CH, but also for the establishment of further melanocyte-associated disease models, for example a CDKN2A mutant model of familial melanoma.

As a disease modeling platform, iPSC-based technology is uniquely suited for the identification and validation of high throughput screening drug targets across multiple cells types. Both HPS and CHS are multi-system disorders in which defects are seen in multiple LRO-containing cell types. As such, pigmentation defects are not of primary concern to patients who experience morbidity due to other manifestations including restrictive lung disease and immune dysfunction. However, the establishment of patient-specific iPSCs, which can be differentiated to a readily scalable and pure population of melanocytes that recapitulate the pigmentation defects associated with these disorders, can be used as a highly tractable surrogate system for identifying compounds that may not only ameliorate the pigmentation defect but other symptoms as well. Potential hit compounds identified through melanin production assays could therefore be subsequently validated in other patient specific iPSC-derived cell types. HPS patients,

for example develop pulmonary fibrosis as the disease progresses. It would therefore be possible to test the effects of hit compounds identified using iPSC-derived melanocytes in iPSC-derived type II pneumocytes.

The system of CHS, HPS1, and HPS2 iPSC-derived melanocytes we have established here effectively creates a model system with defects at different stages of melanocyte biogenesis and processing. As such, it would be highly amenable for further investigation into the process of melanosome formation, particularly regarding the cellular machinery involved at different stages of cargo trafficking. Since our system allows us to generate large quantities of pure melanocytes, we are uniquely situated to investigate the structural components and cargo load of disease-specific melanocytes by performing mass spectrometry analysis of isolated melanosomes.

In summary, our study has offered novel insights into the precise signaling requirements for early neural crest induction, melanocyte lineage specification, and melanocyte maturation. These can now be harnessed to establish unlimited numbers of melanocytes suitable for a broad range of applications including new model system for the study of melanocyte pathologies and malignant melanoma origination.

BIBLIOGRAPHY

Abo, T., Roder, J.C., Abo, W., Cooper, M.D., and Balch, C.M. (1982). Natural killer (HNK-1+) cells in Chediak-Higashi patients are present in normal numbers but are abnormal in function and morphology. J Clin Invest *70*, 193-197.

Adameyko, I., Lallemend, F., Aquino, J.B., Pereira, J.A., Topilko, P., Müller, T., Fritz, N., Beljajeva, A., Mochii, M., Liste, I.*, et al.* (2009). Schwann cell precursors from nerve innervation are a cellular origin of melanocytes in skin. Cell *139*, 366-379.

Alvarez Martinez, C.E., Binato, R., Gonzalez, S., Pereira, M., Robert, B., and Abdelhay, E. (2002). Characterization of a Smad motif similar to Drosophila mad in the mouse Msx 1 promoter. Biochem Biophys Res Commun *291*, 655-662.

Amiel, J., Attié, T., Jan, D., Pelet, A., Edery, P., Bidaud, C., Lacombe, D., Tam, P., Simeoni, J., Flori, E.*, et al.* (1996). Heterozygous endothelin receptor B (EDNRB) mutations in isolated Hirschsprung disease. Hum Mol Genet *5*, 355-357.

Ando, H., Niki, Y., Ito, M., Akiyama, K., Matsui, M.S., Yarosh, D.B., and Ichihashi, M. (2012). Melanosomes are transferred from melanocytes to keratinocytes through the processes of packaging, release, uptake, and dispersion. J Invest Dermatol *132*, 1222-1229.

Ando, H., Niki, Y., Yoshida, M., Ito, M., Akiyama, K., Kim, J.-H., Yoon, T.-J., Matsui, M.S., Yarosh, D.B., and Ichihashi, M. (2011). Involvement of pigment globules containing multiple melanosomes in the transfer of melanosomes from melanocytes to keratinocytes. Cell Logist *1*, 12-20.

Aoki, H., Motohashi, T., Yoshimura, N., Yamazaki, H., Yamane, T., Panthier, J.J., and Kunisada, T. (2005). Cooperative and indispensable roles of endothelin 3 and KIT signalings in melanocyte development. Dev Dyn *233*, 407-417.

Aoki, Y., Saint-Germain, N., Gyda, M., Magner-Fink, E., Lee, Y.-H., Credidio, C., and Saint-Jeannet, J.-P. (2003). Sox10 regulates the development of neural crest-derived melanocytes in Xenopus. Dev Biol *259*, 19-33.

Aruga, J., Minowa, O., Yaginuma, H., Kuno, J., Nagai, T., Noda, T., and Mikoshiba, K. (1998). Mouse Zic1 is involved in cerebellar development. J Neurosci *18*, 284-293.

Assady, S., Maor, G., Amit, M., Itskovitz-Eldor, J., Skorecki, K.L., and Tzukerman, M. (2001). Insulin production by human embryonic stem cells. Diabetes *50*, 1691-1697.

Aybar, M.J., Nieto, M.A., and Mayor, R. (2003). Snail precedes slug in the genetic cascade required for the specification and migration of the Xenopus neural crest. Development *130*, 483-494.

Bajpai, R., Chen, D.A., Rada-Iglesias, A., Zhang, J., Xiong, Y., Helms, J., Chang, C.-P., Zhao, Y., Swigut, T., and Wysocka, J. (2010). CHD7 cooperates with PBAF to control multipotent neural crest formation. Nature.

Baker, C.V., Bronner-Fraser, M., Le Douarin, N.M., and Teillet, M.A. (1997). Early- and late-migrating cranial neural crest cell populations have equivalent developmental potential in vivo. Development *124*, 3077-3087.

Baker, J.C., Beddington, R.S., and Harland, R.M. (1999). Wnt signaling in Xenopus embryos inhibits bmp4 expression and activates neural development. Genes Dev *13*, 3149-3159.

Bang, A.G., Papalopulu, N., Goulding, M.D., and Kintner, C. (1999). Expression of Pax-3 in the lateral neural plate is dependent on a Wnt-mediated signal from posterior nonaxial mesoderm. Developmental biology *212*, 366-380.

Barberi, T., Bradbury, M., Dincer, Z., Panagiotakos, G., Socci, N.D., and Studer, L. (2007). Derivation of engraftable skeletal myoblasts from human embryonic stem cells. Nat Med *13*, 642-648.

Baroffio, A., Dupin, E., and Le Douarin, N.M. (1988). Clone-forming ability and differentiation potential of migratory neural crest cells. Proceedings of the National Academy of Sciences of the United States of America *85*, 5325-5329.

Baroffio, A., Dupin, E., and Le Douarin, N.M. (1991). Common precursors for neural and mesectodermal derivatives in the cephalic neural crest. Development *112*, 301-305.

Barrallo-Gimeno, A., Holzschuh, J., Driever, W., and Knapik, E.W. (2004). Neural crest survival and differentiation in zebrafish depends on mont blanc/tfap2a gene function. Development *131*, 1463-1477.

Barth, K.A., Kishimoto, Y., Rohr, K.B., Seydler, C., Schulte-Merker, S., and Wilson, S.W. (1999). Bmp activity establishes a gradient of positional information throughout the entire neural plate. Development *126*, 4977-4987.

Baxter, L.L., Hou, L., Loftus, S.K., and Pavan, W.J. (2004). Spotlight on spotted mice: a review of white spotting mouse mutants and associated human pigmentation disorders. Pigment Cell Res *17*, 215-224.

Baynash, A.G., Hosoda, K., Giaid, A., Richardson, J.A., Emoto, N., Hammer, R.E., and Yanagisawa, M. (1994). Interaction of endothelin-3 with endothelin-B receptor is essential for development of epidermal melanocytes and enteric neurons. Cell *79*, 1277-1285.

Bellmeyer, A., Krase, J., Lindgren, J., and LaBonne, C. (2003). The protooncogene c-myc is an essential regulator of neural crest formation in xenopus. Developmental Cell *4*, 827-839.

Berson, J.F., Harper, D.C., Tenza, D., Raposo, G., and Marks, M.S. (2001). Pmel17 initiates premelanosome morphogenesis within multivesicular bodies. Mol Biol Cell *12*, 3451-3464.

Betancur, P., Bronner-Fraser, M., and Sauka-Spengler, T. (2010). Assembling neural crest regulatory circuits into a gene regulatory network. Annu Rev Cell Dev Biol *26*, 581-603.

Betters, E., Liu, Y., Kjaeldgaard, A., Sundström, E., and García-Castro, M.I. (2010). Analysis of early human neural crest development. Developmental biology *344*, 578-592.

Bilic, J., and Izpisua Belmonte, J.C. (2012). Concise review: Induced pluripotent stem cells versus embryonic stem cells: close enough or yet too far apart? Stem Cells *30*, 33-41.

Boissy, R.E. (2003). Melanosome transfer to and translocation in the keratinocyte. Exp Dermatol *12 Suppl 2*, 5-12.

Boissy, R.E., and Nordlund, J.J. (1997). Molecular basis of congenital hypopigmentary disorders in humans: a review. Pigment Cell Res *10*, 12-24.

Boissy, R.E., Richmond, B., Huizing, M., Helip-Wooley, A., Zhao, Y., Koshoffer, A., and Gahl, W.A. (2005). Melanocyte-specific proteins are aberrantly trafficked in melanocytes of Hermansky-Pudlak syndrome-type 3. Am J Pathol *166*, 231-240.

Boissy, R.E., Zhao, Y., and Gahl, W.A. (1998). Altered protein localization in melanocytes from Hermansky-Pudlak syndrome: support for the role of the HPS gene product in intracellular trafficking. Lab Invest *78*, 1037-1048.

Bonano, M., Tríbulo, C., De Calisto, J., Marchant, L., Sánchez, S.S., Mayor, R., and Aybar, M.J. (2008). A new role for the Endothelin-1/Endothelin-A receptor signaling during early neural crest specification. Developmental biology *323*, 114-129.

Bondurand, N., Kobetz, A., Pingault, V., Lemort, N., Encha-Razavi, F., Couly, G., Goerich, D.E., Wegner, M., Abitbol, M., and Goossens, M. (1998). Expression of the SOX10 gene during human development. FEBS Lett *432*, 168-172.

Bondurand, N., Pingault, V., Goerich, D.E., Lemort, N., Sock, E., Le Caignec, C., Wegner, M., and Goossens, M. (2000). Interaction among SOX10, PAX3 and MITF, three genes altered in Waardenburg syndrome. Hum Mol Genet *9*, 1907-1917.

Borycki, A.G., Li, J., Jin, F., Emerson, C.P., and Epstein, J.A. (1999). Pax3 functions in cell survival and in pax7 regulation. Development *126*, 1665-1674.

Braun, M.M., Etheridge, A., Bernard, A., Robertson, C.P., and Roelink, H. (2003). Wnt signaling is required at distinct stages of development for the induction of the posterior forebrain. Development *130*, 5579-5587.

Brewer, S., Feng, W., Huang, J., Sullivan, S., and Williams, T. (2004). Wnt1-Cre-mediated deletion of AP-2alpha causes multiple neural crest-related defects. Developmental biology *267*, 135-152.

Brewster, R., Lee, J., and Ruiz i Altaba, A. (1998). Gli/Zic factors pattern the neural plate by defining domains of cell differentiation. Nature *393*, 579-583.

Briggs, R., and King, T.J. (1952). Transplantation of Living Nuclei From Blastula Cells into Enucleated Frogs' Eggs. Proc Natl Acad Sci USA *38*, 455-463.

Brilliant, M.H. (2001). The mouse p (pink-eyed dilution) and human P genes, oculocutaneous albinism type 2 (OCA2), and melanosomal pH. Pigment Cell Res *14*, 86-93.

Britsch, S., Goerich, D.E., Riethmacher, D., Peirano, R.I., Rossner, M., Nave, K.A., Birchmeier, C., and Wegner, M. (2001). The transcription factor Sox10 is a key regulator of peripheral glial development. Genes Dev *15*, 66-78.

Bronner-Fraser, M. (1986). Analysis of the early stages of trunk neural crest migration in avian embryos using monoclonal antibody HNK-1. Developmental biology *115*, 44-55.

Bronner-Fraser, M., and Fraser, S. (1989). Developmental potential of avian trunk neural crest cells in situ. Neuron *3*, 755-766.

Bronner-Fraser, M., and Fraser, S.E. (1988). Cell lineage analysis reveals multipotency of some avian neural crest cells. Nature *335*, 161-164.

Brons, I.G.M., Smithers, L.E., Trotter, M.W.B., Rugg-Gunn, P., Sun, B., Chuva de Sousa Lopes, S.M., Howlett, S.K., Clarkson, A., Ahrlund-Richter, L., Pedersen, R.A.*, et al.* (2007). Derivation of pluripotent epiblast stem cells from mammalian embryos. Nature *448*, 191-195.

Byers, H.R., Maheshwary, S., Amodeo, D.M., and Dykstra, S.G. (2003). Role of cytoplasmic dynein in perinuclear aggregation of phagocytosed melanosomes and supranuclear melanin cap formation in human keratinocytes. J Invest Dermatol *121*, 813-820.

Camp, E., and Lardelli, M. (2001). Tyrosinase gene expression in zebrafish embryos. Dev Genes Evol *211*, 150-153.

Carvajal-Vergara, X., Sevilla, A., D'Souza, S.L., Ang, Y.-S., Schaniel, C., Lee, D.-F., Yang, L., Kaplan, A.D., Adler, E.D., Rozov, R.*, et al.* (2010). Patient-specific induced pluripotent stem-cell-derived models of LEOPARD syndrome. Nature *465*, 808-812.

Chadwick, K., Wang, L., Li, L., Menendez, P., Murdoch, B., Rouleau, A., and Bhatia, M. (2003). Cytokines and BMP-4 promote hematopoietic differentiation of human embryonic stem cells. Blood *102*, 906-915.

Chambers, S.M., Fasano, C.A., Papapetrou, E.P., Tomishima, M., Sadelain, M., and Studer, L. (2009). Highly efficient neural conversion of human ES and iPS cells by dual inhibition of SMAD signaling. Nat Biotechnol *27*, 275-280.

Chambers, S.M., Mica, Y., Studer, L., and Tomishima, M.J. (2011). Converting human pluripotent stem cells to neural tissue and neurons to model neurodegeneration. Methods Mol Biol *793*, 87-97.

Chambers, S.M., Qi, Y., Mica, Y., Lee, G., Zhang, X.-J., Niu, L., Bilsland, J., Cao, L., Stevens, E., Whiting, P.*, et al.* (2012a). Combined small molecule inhibition accelerates developmental timing and converts human pluripotent stem cells into nociceptors. Nat Biotechnol *(in press)*.

Chambers, S.M., Qi, Y., Mica, Y., Lee, G., Zhang, X.-J., Niu, L., Bilsland, J., Cao, L., Stevens, E., Whiting, P.*, et al.* (2012b). Combined small-molecule inhibition accelerates developmental timing and converts human pluripotent stem cells into nociceptors. Nat Biotechnol *30*, 715-720.

Cheng, Y., Cheung, M., Abu-Elmagd, M.M., Orme, A., and Scotting, P.J. (2000). Chick sox10, a transcription factor expressed in both early neural crest cells and central nervous system. Brain Res Dev Brain Res *121*, 233-241.

Cherry, A.B.C., and Daley, G.Q. (2012). Reprogramming cellular identity for regenerative medicine. Cell *148*, 1110-1122.

Cheung, M., Chaboissier, M.-C., Mynett, A., Hirst, E., Schedl, A., and Briscoe, J. (2005). The transcriptional control of trunk neural crest induction, survival, and delamination. Developmental Cell *8*, 179-192.

Cimadamore, F., Fishwick, K., Giusto, E., Gnedeva, K., Cattarossi, G., Miller, A., Pluchino, S., Brill, L.M., Bronner-Fraser, M., and Terskikh, A.V. (2011). Human ESC-derived neural crest model reveals a key role for SOX2 in sensory neurogenesis. Cell Stem Cell *8*, 538-551.

Clark, R.H., Stinchcombe, J.C., Day, A., Blott, E., Booth, S., Bossi, G., Hamblin, T., Davies, E.G., and Griffiths, G.M. (2003). Adaptor protein 3-dependent microtubule-mediated movement of lytic granules to the immunological synapse. Nat Immunol *4*, 1111-1120.

Clewes, O., Narytnyk, A., Gillinder, K.R., Loughney, A.D., Murdoch, A.P., and Sieber-Blum, M. (2011). Human Epidermal Neural Crest Stem Cells (hEPI-NCSC)-Characterization and Directed Differentiation into Osteocytes and Melanocytes. Stem cell reviews.

Cohen, A.M., and Konigsberg, I.R. (1975). A clonal approach to the problem of neural crest determination. Developmental biology *46*, 262-280.

Colombo, S., Champeval, D., Rambow, F., and Larue, L. (2011). Transcriptomic Analysis of Mouse Embryonic Skin Cells Reveals Previously Unreported Genes Expressed in Melanoblasts. J Invest Dermatol.

Cornell, R.A., and Eisen, J.S. (2005). Notch in the pathway: the roles of Notch signaling in neural crest development. Semin Cell Dev Biol *16*, 663-672.

Costin, G.-E., and Hearing, V.J. (2007). Human skin pigmentation: melanocytes modulate skin color in response to stress. FASEB J *21*, 976-994.

Creuzet, S., Couly, G., and Le Douarin, N.M. (2005). Patterning the neural crest derivatives during development of the vertebrate head: insights from avian studies. J Anat *207*, 447-459.

Crook, J.M., and Kobayashi, N.R. (2008). Human stem cells for modeling neurological disorders: accelerating the drug discovery pipeline. J Cell Biochem *105*, 1361-1366.

Cui, R., Widlund, H.R., Feige, E., Lin, J.Y., Wilensky, D.L., Igras, V.E., D'Orazio, J., Fung, C.Y., Schanbacher, C.F., Granter, S.R.*, et al.* (2007). Central role of p53 in the suntan response and pathologic hyperpigmentation. Cell *128*, 853-864.

Curchoe, C.L., Maurer, J., McKeown, S.J., Cattarossi, G., Cimadamore, F., Nilbratt, M., Snyder, E.Y., Bronner-Fraser, M., and Terskikh, A.V. (2010). Early Acquisition of Neural Crest Competence During hESCs Neuralization. PloS one *5*, e13890.

Davidson, D. (1995). The function and evolution of Msx genes: pointers and paradoxes. Trends Genet *11*, 405-411.

Davis, R.L., Weintraub, H., and Lassar, A.B. (1987). Expression of a single transfected cDNA converts fibroblasts to myoblasts. Cell *51*, 987-1000.

Deardorff, M.A., Tan, C., Saint-Jeannet, J.P., and Klein, P.S. (2001). A role for frizzled 3 in neural crest development. Development *128*, 3655-3663.

Delaune, E., Lemaire, P., and Kodjabachian, L. (2005). Neural induction in Xenopus requires early FGF signalling in addition to BMP inhibition. Development *132*, 299-310.

Dell'Angelica, E.C., Shotelersuk, V., Aguilar, R.C., Gahl, W.A., and Bonifacino, J.S. (1999). Altered trafficking of lysosomal proteins in Hermansky-Pudlak syndrome due to mutations in the beta 3A subunit of the AP-3 adaptor. Mol Cell *3*, 11-21.

Dessinioti, C., Stratigos, A.J., Rigopoulos, D., and Katsambas, A.D. (2009). A review of genetic disorders of hypopigmentation: lessons learned from the biology of melanocytes. Exp Dermatol *18*, 741-749.

Di Pietro, S.M., and Dell'Angelica, E.C. (2005). The cell biology of Hermansky-Pudlak syndrome: recent advances. Traffic *6*, 525-533.

Dick, A., Hild, M., Bauer, H., Imai, Y., Maifeld, H., Schier, A.F., Talbot, W.S., Bouwmeester, T., and Hammerschmidt, M. (2000). Essential role of Bmp7 (snailhouse) and its prodomain in dorsoventral patterning of the zebrafish embryo. Development *127*, 343-354.

Dimos, J., Rodolfa, K., Niakan, K., Weisenthal, L., Mitsumoto, H., Chung, W., Croft, G., Saphier, G., Leibel, R., Goland, R.*, et al.* (2008). Induced Pluripotent Stem Cells Generated from Patients with ALS Can Be Differentiated into Motor Neurons. Science.

Doi, A., Park, I.-H., Wen, B., Murakami, P., Aryee, M.J., Irizarry, R., Herb, B., Ladd-Acosta, C., Rho, J., Loewer, S.*, et al.* (2009). Differential methylation of tissue- and cancer-specific CpG island shores distinguishes human induced pluripotent stem cells, embryonic stem cells and fibroblasts. Nature Genetics *41*, 1350-1353.

Dorsky, R.I., Moon, R.T., and Raible, D.W. (1998). Control of neural crest cell fate by the Wnt signalling pathway. Nature *396*, 370-373.

Dorsky, R.I., Raible, D.W., and Moon, R.T. (2000). Direct regulation of nacre, a zebrafish MITF homolog required for pigment cell formation, by the Wnt pathway. Genes Dev *14*, 158-162.

Dottori, M., Gross, M.K., Labosky, P., and Goulding, M. (2001). The winged-helix transcription factor Foxd3 suppresses interneuron differentiation and promotes neural crest cell fate. Development *128*, 4127-4138.

Dunn, K.J., Williams, B.O., Li, Y., and Pavan, W.J. (2000). Neural crest-directed gene transfer demonstrates Wnt1 role in melanocyte expansion and differentiation during mouse development. Proc Natl Acad Sci USA *97*, 10050-10055.

Dupin, E., Glavieux, C., Vaigot, P., and Le Douarin, N.M. (2000). Endothelin 3 induces the reversion of melanocytes to glia through a neural crest-derived glial-melanocytic progenitor. Proc Natl Acad Sci USA *97*, 7882-7887.

Dupin, E., and Le Douarin, N.M. (2003). Development of melanocyte precursors from the vertebrate neural crest. Oncogene *22*, 3016-3023.

Dutton, K.A., Pauliny, A., Lopes, S.S., Elworthy, S., Carney, T.J., Rauch, J., Geisler, R., Haffter, P., and Kelsh, R.N. (2001). Zebrafish colourless encodes sox10 and specifies non-ectomesenchymal neural crest fates. Development *128*, 4113-4125.

Eakin, G.S., and Hadjantonakis, A.-K. (2006). Production of chimeras by aggregation of embryonic stem cells with diploid or tetraploid mouse embryos. Nat Protoc *1*, 1145-1153.

Ebert, A.D., Yu, J., Rose, F.F., Mattis, V.B., Lorson, C.L., Thomson, J.A., and Svendsen, C.N. (2009). Induced pluripotent stem cells from a spinal muscular atrophy patient. Nature *457*, 277-280.

Eiges, R., Urbach, A., Malcov, M., Frumkin, T., Schwartz, T., Amit, A., Yaron, Y., Eden, A., Yanuka, O., Benvenisty, N.*, et al.* (2007). Developmental study of fragile X syndrome using human embryonic stem cells derived from preimplantation genetically diagnosed embryos. Cell stem cell *1*, 568-577.

Elkabetz, Y., Panagiotakos, G., Al Shamy, G., Socci, N.D., Tabar, V., and Studer, L. (2008). Human ES cell-derived neural rosettes reveal a functionally distinct early neural stem cell stage. Genes Dev *22*, 152-165.

Elworthy, S., Lister, J.A., Carney, T.J., Raible, D.W., and Kelsh, R.N. (2003). Transcriptional regulation of mitfa accounts for the sox10 requirement in zebrafish melanophore development. Development *130*, 2809-2818.

Erickson, C.A., Duong, T.D., and Tosney, K.W. (1992). Descriptive and experimental analysis of the dispersion of neural crest cells along the dorsolateral path and their entry into ectoderm in the chick embryo. Developmental biology *151*, 251-272.

Erickson, C.A., and Goins, T.L. (1995). Avian neural crest cells can migrate in the dorsolateral path only if they are specified as melanocytes. Development *121*, 915-924.

Evans, M.J., and Kaufman, M.H. (1981). Establishment in culture of pluripotential cells from mouse embryos. Nature *292*, 154-156.

Fainsod, A., Steinbeisser, H., and De Robertis, E.M. (1994). On the function of BMP-4 in patterning the marginal zone of the Xenopus embryo. EMBO J *13*, 5015-5025.

Fang, D., Leishear, K., Nguyen, T.K., Finko, R., Cai, K., Fukunaga, M., Li, L., Brafford, P.A., Kulp, A.N., Xu, X.*, et al.* (2006). Defining the conditions for the generation of melanocytes from human embryonic stem cells. Stem Cells *24*, 1668-1677.

Fasano, C.A., Chambers, S.M., Lee, G., Tomishima, M.J., and Studer, L. (2010). Efficient derivation of functional floor plate tissue from human embryonic stem cells. Cell Stem Cell *6*, 336-347.

Feng, G.H., Bailin, T., Oh, J., and Spritz, R.A. (1997). Mouse pale ear (ep) is homologous to human Hermansky-Pudlak syndrome and contains a rare 'AT-AC' intron. Hum Mol Genet *6*, 793-797.

Friedmann, P.S., and Gilchrest, B.A. (1987). Ultraviolet radiation directly induces pigment production by cultured human melanocytes. J Cell Physiol *133*, 88-94.

Fujimura, N., Vacik, T., Machon, O., Vlcek, C., Scalabrin, S., Speth, M., Diep, D., Krauss, S., and Kozmik, Z. (2007). Wnt-mediated down-regulation of Sp1 target genes by a transcriptional repressor Sp5. The Journal of biological chemistry *282*, 1225-1237.

Fürthauer, M., Thisse, B., and Thisse, C. (1999). Three different noggin genes antagonize the activity of bone morphogenetic proteins in the zebrafish embryo. Developmental biology *214*, 181-196.

Ganat, Y.M., Calder, E.L., Kriks, S., Nelander, J., Tu, E.Y., Jia, F., Battista, D., Harrison, N., Parmar, M., Tomishima, M.J.*, et al.* (2012). Identification of embryonic stem cell-derived midbrain dopaminergic neurons for engraftment. J Clin Invest *122*, 2928-2939.

García-Castro, M.I., Marcelle, C., and Bronner-Fraser, M. (2002). Ectodermal Wnt function as a neural crest inducer. Science *297*, 848-851.

Gardner, J.M., Wildenberg, S.C., Keiper, N.M., Novak, E.K., Rusiniak, M.E., Swank, R.T., Puri, N., Finger, J.N., Hagiwara, N., Lehman, A.L.*, et al.* (1997). The mouse pale ear (ep) mutation is the homologue of human Hermansky-Pudlak syndrome. Proceedings of the National Academy of Sciences of the United States of America *94*, 9238-9243.

Gaspard, N., and Vanderhaeghen, P. (2010). Mechanisms of neural specification from embryonic stem cells. Curr Opin Neurobiol *20*, 37-43.

Gerecht-Nir, S., Ziskind, A., Cohen, S., and Itskovitz-Eldor, J. (2003). Human embryonic stem cells as an in vitro model for human vascular development and the induction of vascular differentiation. Lab Invest *83*, 1811-1820.

Gitelman, I. (1997). Twist protein in mouse embryogenesis. Developmental biology *189*, 205-214.

Glavic, A., Silva, F., Aybar, M.J., Bastidas, F., and Mayor, R. (2004). Interplay between Notch signaling and the homeoprotein Xiro1 is required for neural crest induction in Xenopus embryos. Development *131*, 347-359.

González, F., Boué, S., and Izpisúa Belmonte, J.C. (2011). Methods for making induced pluripotent stem cells: reprogramming à la carte. Nat Rev Genet *12*, 231-242.

Green, H., Easley, K., and Iuchi, S. (2003). Marker succession during the development of keratinocytes from cultured human embryonic stem cells. Proc Natl Acad Sci USA *100*, 15625-15630.

Gurdon, J.B. (1962). The developmental capacity of nuclei taken from intestinal epithelium cells of feeding tadpoles. J Embryol Exp Morphol *10*, 622-640.

Hacein-Bey-Abina, S., Von Kalle, C., Schmidt, M., McCormack, M.P., Wulffraat, N., Leboulch, P., Lim, A., Osborne, C.S., Pawliuk, R., Morillon, E.*, et al.* (2003). LMO2-associated clonal T cell proliferation in two patients after gene therapy for SCID-X1. Science *302*, 415-419.

Haddad, E., Le Deist, F., Blanche, S., Benkerrou, M., Rohrlich, P., Vilmer, E., Griscelli, C., and Fischer, A. (1995). Treatment of Chediak-Higashi syndrome by allogenic bone marrow transplantation: report of 10 cases. Blood *85*, 3328-3333.

Hall, B.K. (2000). The neural crest as a fourth germ layer and vertebrates as quadroblastic not triploblastic. Evol Dev *2*, 3-5.

Hanna, J., Wernig, M., Markoulaki, S., Sun, C.-W., Meissner, A., Cassady, J.P., Beard, C., Brambrink, T., Wu, L.-C., Townes, T.M.*, et al.* (2007). Treatment of sickle cell anemia mouse model with iPS cells generated from autologous skin. Science *318*, 1920-1923.

Hara, M., Yaar, M., Byers, H.R., Goukassian, D., Fine, R.E., Gonsalves, J., and Gilchrest, B.A. (2000). Kinesin participates in melanosomal movement along melanocyte dendrites. J Invest Dermatol *114*, 438-443.

Hari, L., Miescher, I., Shakhova, O., Suter, U., Chin, L., Taketo, M., Richardson, W.D., Kessaris, N., and Sommer, L. (2012). Temporal control of neural crest lineage generation by Wnt/β-catenin signaling. Development.

Hearing, V.J. (1999). Biochemical control of melanogenesis and melanosomal organization. J Investig Dermatol Symp Proc *4*, 24-28.

Hemmati-Brivanlou, A., and Thomsen, G.H. (1995). Ventral mesodermal patterning in Xenopus embryos: expression patterns and activities of BMP-2 and BMP-4. Dev Genet *17*, 78-89.

Hockemeyer, D., Soldner, F., Beard, C., Gao, Q., Mitalipova, M., DeKelver, R.C., Katibah, G.E., Amora, R., Boydston, E.A., Zeitler, B.*, et al.* (2009). Efficient targeting of expressed and silent genes in human ESCs and iPSCs using zinc-finger nucleases. Nature biotechnology *27*, 851-857.

Hockemeyer, D., Wang, H., Kiani, S., Lai, C.S., Gao, Q., Cassady, J.P., Cost, G.J., Zhang, L., Santiago, Y., Miller, J.C.*, et al.* (2011). Genetic engineering of human pluripotent cells using TALE nucleases. Nature biotechnology *29*, 731-734.

Hong, C.-S., and Saint-Jeannet, J.-P. (2005). Sox proteins and neural crest development. Semin Cell Dev Biol *16*, 694-703.

Hong, C.-S., and Saint-Jeannet, J.-P. (2007). The activity of Pax3 and Zic1 regulates three distinct cell fates at the neural plate border. Mol Biol Cell *18*, 2192-2202.

Honoré, S.M., Aybar, M.J., and Mayor, R. (2003). Sox10 is required for the early development of the prospective neural crest in Xenopus embryos. Developmental biology *260*, 79-96.

Hornyak, T.J. (2006). The developmental biology of melanocytes and its application to understanding human congenital disorders of pigmentation. Adv Dermatol *22*, 201-218.

Hornyak, T.J., Hayes, D.J., Chiu, L.Y., and Ziff, E.B. (2001). Transcription factors in melanocyte development: distinct roles for Pax-3 and Mitf. Mech Dev *101*, 47-59.

Hou, L., Arnheiter, H., and Pavan, W.J. (2006). Interspecies difference in the regulation of melanocyte development by SOX10 and MITF. Proceedings of the National Academy of Sciences of the United States of America *103*, 9081-9085.

Huizing, M., Anikster, Y., and Gahl, W.A. (2001a). Hermansky-Pudlak syndrome and Chediak-Higashi syndrome: disorders of vesicle formation and trafficking. Thromb Haemost *86*, 233-245.

Huizing, M., Sarangarajan, R., Strovel, E., Zhao, Y., Gahl, W.A., and Boissy, R.E. (2001b). AP-3 mediates tyrosinase but not TRP-1 trafficking in human melanocytes. Mol Biol Cell *12*, 2075-2085.

Huizing, M., Scher, C.D., Strovel, E., Fitzpatrick, D.L., Hartnell, L.M., Anikster, Y., and Gahl, W.A. (2002). Nonsense mutations in ADTB3A cause complete deficiency of the beta3A subunit of adaptor complex-3 and severe Hermansky-Pudlak syndrome type 2. Pediatr Res *51*, 150-158.

Idelson, M., Alper, R., Obolensky, A., Ben-Shushan, E., Hemo, I., Yachimovich-Cohen, N., Khaner, H., Smith, Y., Wiser, O., Gropp, M.*, et al.* (2009). Directed differentiation of human embryonic stem cells into functional retinal pigment epithelium cells. Cell stem cell *5*, 396-408.

Inoue, T., Hatayama, M., Tohmonda, T., Itohara, S., Aruga, J., and Mikoshiba, K. (2004). Mouse Zic5 deficiency results in neural tube defects and hypoplasia of cephalic neural crest derivatives. Developmental biology *270*, 146-162.

Introne, W., Boissy, R.E., and Gahl, W.A. (1999). Clinical, molecular, and cell biological aspects of Chediak-Higashi syndrome. Mol Genet Metab *68*, 283-303.

Ito, K., Morita, T., and Sieber-Blum, M. (1993). In vitro clonal analysis of mouse neural crest development. Dev Biol *157*, 517-525.

Itskovitz-Eldor, J., Schuldiner, M., Karsenti, D., Eden, A., Yanuka, O., Amit, M., Soreq, H., and Benvenisty, N. (2000). Differentiation of human embryonic stem cells into embryoid bodies compromising the three embryonic germ layers. Mol Med *6*, 88-95.

Jackson, I.J. (1994). Molecular and developmental genetics of mouse coat color. Annu Rev Genet *28*, 189-217.

Jiang, X., Gwye, Y., McKeown, S.J., Bronner-Fraser, M., Lutzko, C., and Lawlor, E.R. (2009). Isolation and characterization of neural crest stem cells derived from in vitro-differentiated human embryonic stem cells. Stem cells and development *18*, 1059-1070.

Jiao, Z., Mollaaghababa, R., Pavan, W.J., Antonellis, A., Green, E.D., and Hornyak, T.J. (2004). Direct interaction of Sox10 with the promoter of murine Dopachrome Tautomerase (Dct) and synergistic activation of Dct expression with Mitf. Pigment Cell Res *17*, 352-362.

Jin, E.J., Erickson, C.A., Takada, S., and Burrus, L.W. (2001). Wnt and BMP signaling govern lineage segregation of melanocytes in the avian embryo. Dev Biol *233*, 22-37.

Jones, N.C., and Trainor, P.A. (2005). Role of morphogens in neural crest cell determination. J Neurobiol *64*, 388-404.

Kaplan, J., De Domenico, I., and Ward, D.M. (2008). Chediak-Higashi syndrome. Curr Opin Hematol *15*, 22-29.

Kapur, R.P. (1999). Early death of neural crest cells is responsible for total enteric aganglionosis in Sox10(Dom)/Sox10(Dom) mouse embryos. Pediatr Dev Pathol *2*, 559-569.

Kaufman, D.S., Hanson, E.T., Lewis, R.L., Auerbach, R., and Thomson, J.A. (2001). Hematopoietic colony-forming cells derived from human embryonic stem cells. Proceedings of the National Academy of Sciences of the United States of America *98*, 10716-10721.

Kazmierowski, J.A., Elin, R.J., Reynolds, H.Y., Durbin, W.A., and Wolff, S.M. (1976). Chediak-Higashi syndrome: reversal of increased susceptibility to infection by bone marrow transplantation. Blood *47*, 555-559.

Kee, Y., and Bronner-Fraser, M. (2005). To proliferate or to die: role of Id3 in cell cycle progression and survival of neural crest progenitors. Genes Dev *19*, 744-755.

Kehat, I., Kenyagin-Karsenti, D., Snir, M., Segev, H., Amit, M., Gepstein, A., Livne, E., Binah, O., Itskovitz-Eldor, J., and Gepstein, L. (2001). Human embryonic stem cells can differentiate into myocytes with structural and functional properties of cardiomyocytes. J Clin Invest *108*, 407-414.

Kelsh, R.N., Harris, M.L., Colanesi, S., and Erickson, C.A. (2009). Stripes and belly-spots -- a review of pigment cell morphogenesis in vertebrates. Semin Cell Dev Biol *20*, 90-104.

Kitamura, K., Takiguchi-Hayashi, K., Sezaki, M., and Yamamoto (1992). Avian neural crest cells express a melanogenic trait migration from the neural tube: observations with the antibody, “MEBL-1”. Development *114*, 367-378.

Kléber, M., Lee, H.-Y., Wurdak, H., Buchstaller, J., Riccomagno, M.M., Ittner, L.M., Suter, U., Epstein, D.J., and Sommer, L. (2005). Neural crest stem cell maintenance by combinatorial Wnt and BMP signaling. The Journal of Cell Biology *169*, 309-320.

Klimanskaya, I., Chung, Y., Becker, S., Lu, S.-J., and Lanza, R. (2006). Human embryonic stem cell lines derived from single blastomeres. Nature *444*, 481-485.

Knight, R.D., Javidan, Y., Nelson, S., Zhang, T., and Schilling, T. (2004). Skeletal and pigment cell defects in the lockjaw mutant reveal multiple roles for zebrafish tfap2a in neural crest development. Dev Dyn *229*, 87-98.

Knight, R.D., Nair, S., Nelson, S.S., Afshar, A., Javidan, Y., Geisler, R., Rauch, G.-J., and Schilling, T.F. (2003). lockjaw encodes a zebrafish tfap2a required for early neural crest development. Development *130*, 5755-5768.

Kos, R., Reedy, M.V., Johnson, R.L., and Erickson, C.A. (2001). The winged-helix transcription factor FoxD3 is important for establishing the neural crest lineage and repressing melanogenesis in avian embryos. Development *128*, 1467-1479.

Kriks, S., Shim, J.-W., Piao, J., Ganat, Y.M., Wakeman, D.R., Xie, Z., Carrillo-Reid, L., Auyeung, G., Antonacci, C., Buch, A.*, et al.* (2011). Dopamine neurons derived from human ES cells efficiently engraft in animal models of Parkinson's disease. Nature *480*, 547-551.

Kuhlbrodt, K., Herbarth, B., Sock, E., Hermans-Borgmeyer, I., and Wegner, M. (1998). Sox10, a novel transcriptional modulator in glial cells. J Neurosci *18*, 237-250.

Kulessa, H., Frampton, J., and Graf, T. (1995). GATA-1 reprograms avian myelomonocytic cell lines into eosinophils, thromboblasts, and erythroblasts. Genes Dev *9*, 1250-1262.

Kunisada, T., Lu, S.Z., Yoshida, H., Nishikawa, S., Nishikawa, S., Mizoguchi, M., Hayashi, S., Tyrrell, L., Williams, D.A., Wang, X.*, et al.* (1998a). Murine cutaneous mastocytosis and epidermal melanocytosis induced by keratinocyte expression of transgenic stem cell factor. J Exp Med *187*, 1565-1573.

Kunisada, T., Yoshida, H., Yamazaki, H., Miyamoto, A., Hemmi, H., Nishimura, E., Shultz, L.D., Nishikawa, S., and Hayashi, S. (1998b). Transgene expression of steel factor in the basal layer of epidermis promotes survival, proliferation, differentiation and migration of melanocyte precursors. Development *125*, 2915-2923.

Kuo, J.S., Patel, M., Gamse, J., Merzdorf, C., Liu, X., Apekin, V., and Sive, H. (1998). Opl: a zinc finger protein that regulates neural determination and patterning in Xenopus. Development *125*, 2867-2882.

LaBonne, C., and Bronner-Fraser, M. (1998). Neural crest induction in Xenopus: evidence for a two-signal model. Development *125*, 2403-2414.

LaBonne, C., and Bronner-Fraser, M. (2000). Snail-related transcriptional repressors are required in Xenopus for both the induction of the neural crest and its subsequent migration. Developmental biology *221*, 195-205.

Lagutin, O.V., Zhu, C.C., Kobayashi, D., Topczewski, J., Shimamura, K., Puelles, L., Russell, H.R.C., McKinnon, P.J., Solnica-Krezel, L., and Oliver, G. (2003). Six3 repression of Wnt signaling in the anterior neuroectoderm is essential for vertebrate forebrain development. Genes Dev *17*, 368-379.

Lahav, R., Ziller, C., Dupin, E., and Le Douarin, N.M. (1996). Endothelin 3 promotes neural crest cell proliferation and mediates a vast increase in melanocyte number in culture. Proc Natl Acad Sci USA *93*, 3892-3897.

Lang, D., Lu, M.M., Huang, L., Engleka, K.A., Zhang, M., Chu, E.Y., Lipner, S., Skoultchi, A., Millar, S.E., and Epstein, J.A. (2005). Pax3 functions at a nodal point in melanocyte stem cell differentiation. Nature *433*, 884-887.

Lavado, A., Lagutin, O.V., and Oliver, G. (2008). Six3 inactivation causes progressive caudalization and aberrant patterning of the mammalian diencephalon. Development *135*, 441-450.

Le Douarin, N.M., Calloni, G.W., and Dupin, E. (2008). The stem cells of the neural crest. Cell cycle (Georgetown, Tex) *7*, 1013-1019.

Le Douarin, N.M., Creuzet, S., Couly, G., and Dupin, E. (2004). Neural crest cell plasticity and its limits. Development *131*, 4637-4650.

Lee, G., Chambers, S.M., Tomishima, M.J., and Studer, L. (2010). Derivation of neural crest cells from human pluripotent stem cells. Nat Protoc *5*, 688-701.

Lee, G., Kim, H., Elkabetz, Y., Al Shamy, G., Panagiotakos, G., Barberi, T., Tabar, V., and Studer, L. (2007). Isolation and directed differentiation of neural crest stem cells derived from human embryonic stem cells. Nat Biotechnol *25*, 1468-1475.

Lee, G., Papapetrou, E.P., Kim, H., Chambers, S.M., Tomishima, M.J., Fasano, C.A., Ganat, Y.M., Menon, J., Shimizu, F., Viale, A.*, et al.* (2009). Modelling pathogenesis and treatment of familial dysautonomia using patient-specific iPSCs. Nature *461*, 402-406.

Lee, G., Ramirez, C.N., Kim, H., Zeltner, N., Liu, B., Radu, C., Bhinder, B., Kim, Y.J., Choi, I.Y., Mukherjee-Clavin, B.*, et al.* (2012). Large-scale screening using familial dysautonomia induced pluripotent stem cells identifies compounds that rescue IKBKAP expression. Nat Biotechnol *30*, 1244-1248.

Levenberg, S., Golub, J.S., Amit, M., Itskovitz-Eldor, J., and Langer, R. (2002). Endothelial cells derived from human embryonic stem cells. Proceedings of the National Academy of Sciences of the United States of America *99*, 4391-4396.

Lewis, J.L., Bonner, J., Modrell, M., Ragland, J.W., Moon, R.T., Dorsky, R.I., and Raible, D.W. (2004). Reiterated Wnt signaling during zebrafish neural crest development. Development *131*, 1299-1308.

Li, B., Kuriyama, S., Moreno, M., and Mayor, R. (2009). The posteriorizing gene Gbx2 is a direct target of Wnt signalling and the earliest factor in neural crest induction. Development *136*, 3267-3278.

Li, L., Fukunaga-Kalabis, M., Yu, H., Xu, X., Kong, J., and Herlyn, J.T.L.A.M. (2010). Human dermal stem cells differentiate into functional epidermal melanocytes. Journal of Cell Science.

Li, W., Rusiniak, M.E., Chintala, S., Gautam, R., Novak, E.K., and Swank, R.T. (2004). Murine Hermansky-Pudlak syndrome genes: regulators of lysosome-related organelles. BioEssays : news and reviews in molecular, cellular and developmental biology *26*, 616-628.

Li, X.-J., Du, Z.-W., Zarnowska, E.D., Pankratz, M., Hansen, L.O., Pearce, R.A., and Zhang, S.-C. (2005). Specification of motoneurons from human embryonic stem cells. Nature biotechnology *23*, 215-221.

Light, W., Vernon, A.E., Lasorella, A., Iavarone, A., and LaBonne, C. (2005). Xenopus Id3 is required downstream of Myc for the formation of multipotent neural crest progenitor cells. Development *132*, 1831-1841.

Lin, J.Y., and Fisher, D.E. (2007). Melanocyte biology and skin pigmentation. Nature *445*, 843-850.

Linker, C., Bronner-Fraser, M., and Mayor, R. (2000). Relationship between gene expression domains of Xsnail, Xslug, and Xtwist and cell movement in the prospective neural crest of Xenopus. Developmental biology *224*, 215-225.

Linker, C., and Stern, C.D. (2004). Neural induction requires BMP inhibition only as a late step, and involves signals other than FGF and Wnt antagonists. Development *131*, 5671-5681.

Lister, J.A., Robertson, C.P., Lepage, T., Johnson, S.L., and Raible, D.W. (1999). nacre encodes a zebrafish microphthalmia-related protein that regulates neural-crest-derived pigment cell fate. Development *126*, 3757-3767.

Löhle, M., Hermann, A., Glass, H., Kempe, A., Schwarz, S.C., Kim, J.B., Poulet, C., Ravens, U., Schwarz, J., Schöler, H.R.*, et al.* (2012). Differentiation efficiency of induced pluripotent stem cells depends on the number of reprogramming factors. Stem Cells *30*, 570-579.

Lowry, W.E., Richter, L., Yachechko, R., Pyle, A.D., Tchieu, J., Sridharan, R., Clark, A.T., and Plath, K. (2008). Generation of human induced pluripotent stem cells from dermal fibroblasts. Proc Natl Acad Sci USA *105*, 2883-2888.

Luo, R., Gao, J., Wehrle-Haller, B., and Henion, P.D. (2003a). Molecular identification of distinct neurogenic and melanogenic neural crest sublineages. Development *130*, 321-330.

Luo, T., Lee, Y.-H., Saint-Jeannet, J.-P., and Sargent, T.D. (2003b). Induction of neural crest in Xenopus by transcription factor AP2alpha. Proc Natl Acad Sci USA *100*, 532-537.

Luo, T., Matsuo-Takasaki, M., and Sargent, T.D. (2001). Distinct roles for Distal-less genes Dlx3 and Dlx5 in regulating ectodermal development in Xenopus. Mol Reprod Dev *60*, 331-337.

Luo, T., Matsuo-Takasaki, M., Thomas, M.L., Weeks, D.L., and Sargent, T.D. (2002). Transcription factor AP-2 is an essential and direct regulator of epidermal development in Xenopus. Developmental biology *245*, 136-144.

Lutzner, M.A., Lowrie, C.T., and Jordan, H.W. (1967). Giant granules in leukocytes of the beige mouse. J Hered *58*, 299-300.

Lwigale, P.Y., Conrad, G.W., and Bronner-Fraser, M. (2004). Graded potential of neural crest to form cornea, sensory neurons and cartilage along the rostrocaudal axis. Development *131*, 1979-1991.

Maehr, R., Chen, S., Snitow, M., Ludwig, T., Yagasaki, L., Goland, R., Leibel, R.L., and Melton, D.A. (2009). Generation of pluripotent stem cells from patients with type 1 diabetes. Proc Natl Acad Sci USA *106*, 15768-15773.

Maherali, N., Sridharan, R., Xie, W., Utikal, J., Eminli, S., Arnold, K., Stadtfeld, M., Yachechko, R., Tchieu, J., Jaenisch, R.*, et al.* (2007). Directly reprogrammed fibroblasts show global epigenetic remodeling and widespread tissue contribution. Cell stem cell *1*, 55-70.

Mansouri, A., Pla, P., Larue, L., and Gruss, P. (2001). Pax3 acts cell autonomously in the neural tube and somites by controlling cell surface properties. Development *128*, 1995-2005.

Marchant, L., Linker, C., Ruiz, P., Guerrero, N., and Mayor, R. (1998). The inductive properties of mesoderm suggest that the neural crest cells are specified by a BMP gradient. Dev Biol *198*, 319-329.

Maroof, A.M., Brown, K., Shi, S.-H., Studer, L., and Anderson, S.A. (2010). Prospective isolation of cortical interneuron precursors from mouse embryonic stem cells. J Neurosci *30*, 4667-4675.

Martin, G.R. (1981). Isolation of a pluripotent cell line from early mouse embryos cultured in medium conditioned by teratocarcinoma stem cells. Proc Natl Acad Sci USA *78*, 7634-7638.

Mascré, G., Dekoninck, S., Drogat, B., Youssef, K.K., Broheé, S., Sotiropoulou, P.A., Simons, B.D., and Blanpain, C. (2012). Distinct contribution of stem and progenitor cells to epidermal maintenance. Nature *489*, 257-262.

Mayor, R., Guerrero, N., and Martínez, C. (1997). Role of FGF and noggin in neural crest induction. Dev Biol *189*, 1-12.

Mayor, R., Morgan, R., and Sargent, M.G. (1995). Induction of the prospective neural crest of Xenopus. Development *121*, 767-777.

McKeown, S.J., Lee, V.M., Bronner-Fraser, M., Newgreen, D.F., and Farlie, P.G. (2005). Sox10 overexpression induces neural crest-like cells from all dorsoventral levels of the neural tube but inhibits differentiation. Dev Dyn *233*, 430-444.

McLarren, K.W., Litsiou, A., and Streit, A. (2003). DLX5 positions the neural crest and preplacode region at the border of the neural plate. Developmental biology *259*, 34-47.

Meier, F., Nesbit, M., Hsu, M.Y., Martin, B., Van Belle, P., Elder, D.E., Schaumburg-Lever, G., Garbe, C., Walz, T.M., Donatien, P.*, et al.* (2000). Human melanoma progression in skin reconstructs : biological significance of bFGF. The American Journal of Pathology *156*, 193-200.

Meijer, L., Flajolet, M., and Greengard, P. (2004). Pharmacological inhibitors of glycogen synthase kinase 3. Trends Pharmacol Sci *25*, 471-480.

Ménasché, G., Pastural, E., Feldmann, J., Certain, S., Ersoy, F., Dupuis, S., Wulffraat, N., Bianchi, D., Fischer, A., Le Deist, F.*, et al.* (2000). Mutations in RAB27A cause Griscelli syndrome associated with haemophagocytic syndrome. Nature Genetics *25*, 173-176.

Menendez, L., Yatskievych, T.A., Antin, P.B., and Dalton, S. (2011). Wnt signaling and a Smad pathway blockade direct the differentiation of human pluripotent stem cells to multipotent neural crest cells. Proceedings of the National Academy of Sciences of the United States of America *108*, 19240-19245.

Meulemans, D., and Bronner-Fraser, M. (2002). Amphioxus and lamprey AP-2 genes: implications for neural crest evolution and migration patterns. Development *129*, 4953-4962.

Milet, C., and Monsoro-Burq, A.H. (2012). Embryonic stem cell strategies to explore neural crest development in human embryos. Developmental biology.

Mizuseki, K., Kishi, M., Matsui, M., Nakanishi, S., and Sasai, Y. (1998). Xenopus Zic-related-1 and Sox-2, two factors induced by chordin, have distinct activities in the initiation of neural induction. Development *125*, 579-587.

Monsoro-Burq, A.-H., Fletcher, R.B., and Harland, R.M. (2003). Neural crest induction by paraxial mesoderm in Xenopus embryos requires FGF signals. Development *130*, 3111-3124.

Monsoro-Burq, A.-H., Wang, E., and Harland, R. (2005). Msx1 and Pax3 cooperate to mediate FGF8 and WNT signals during Xenopus neural crest induction. Developmental Cell *8*, 167-178.

Moretti, A., Bellin, M., Welling, A., Jung, C.B., Lam, J.T., Bott-Flügel, L., Dorn, T., Goedel, A., Höhnke, C., Hofmann, F.*, et al.* (2010). Patient-specific induced pluripotent stem-cell models for long-QT syndrome. N Engl J Med *363*, 1397-1409.

Morgan, R., and Sargent, M.G. (1997). The role in neural patterning of translation initiation factor eIF4AII; induction of neural fold genes. Development *124*, 2751-2760.

Motohashi, T., Aoki, H., Yoshimura, N., and Kunisada, T. (2006). Induction of melanocytes from embryonic stem cells and their therapeutic potential. Pigment Cell Res *19*, 284-289.

Mummery, C., Ward-van Oostwaard, D., Doevendans, P., Spijker, R., van den Brink, S., Hassink, R., van der Heyden, M., Opthof, T., Pera, M., de la Riviere, A.B.*, et al.* (2003). Differentiation of human embryonic stem cells to cardiomyocytes: role of coculture with visceral endoderm-like cells. Circulation *107*, 2733-2740.

Nagai, T., Aruga, J., Minowa, O., Sugimoto, T., Ohno, Y., Noda, T., and Mikoshiba, K. (2000). Zic2 regulates the kinetics of neurulation. Proc Natl Acad Sci USA *97*, 1618-1623.

Nagle, D.L., Karim, M.A., Woolf, E.A., Holmgren, L., Bork, P., Misumi, D.J., McGrail, S.H., Dussault, B.J., Perou, C.M., Boissy, R.E.*, et al.* (1996). Identification and mutation analysis of the complete gene for Chediak-Higashi syndrome. Nat Genet *14*, 307-311.

Nakagawa, M., Koyanagi, M., Tanabe, K., Takahashi, K., Ichisaka, T., Aoi, T., Okita, K., Mochiduki, Y., Takizawa, N., and Yamanaka, S. (2008). Generation of induced pluripotent stem cells without Myc from mouse and human fibroblasts. Nat Biotechnol *26*, 101-106.

Nakata, K., Koyabu, Y., Aruga, J., and Mikoshiba, K. (2000). A novel member of the Xenopus Zic family, Zic5, mediates neural crest development. Mech Dev *99*, 83-91.

Nakata, K., Nagai, T., Aruga, J., and Mikoshiba, K. (1997). Xenopus Zic3, a primary regulator both in neural and neural crest development. Proc Natl Acad Sci USA *94*, 11980-11985.

Nakata, K., Nagai, T., Aruga, J., and Mikoshiba, K. (1998). Xenopus Zic family and its role in neural and neural crest development. Mech Dev *75*, 43-51.

Nakayama, A., Nguyen, M.T., Chen, C.C., Opdecamp, K., Hodgkinson, C.A., and Arnheiter, H. (1998). Mutations in microphthalmia, the mouse homolog of the human deafness gene MITF, affect neuroepithelial and neural crest-derived melanocytes differently. Mech Dev *70*, 155-166.

Nguyen, T., Novak, E.K., Kermani, M., Fluhr, J., Peters, L.L., Swank, R.T., and Wei, M.L. (2002). Melanosome morphologies in murine models of hermansky-pudlak syndrome reflect blocks in organelle development. J Invest Dermatol *119*, 1156-1164.

Nguyen, V.H., Schmid, B., Trout, J., Connors, S.A., Ekker, M., and Mullins, M.C. (1998). Ventral and lateral regions of the zebrafish gastrula, including the neural crest progenitors, are established by a bmp2b/swirl pathway of genes. Developmental biology *199*, 93-110.

Nichols, J., and Smith, A. (2009). Naive and Primed Pluripotent States. Cell stem cell *4*, 487-492.

Niclis, J.C., Trounson, A.O., Dottori, M., Ellisdon, A.M., Bottomley, S.P., Verlinsky, Y., and Cram, D.S. (2009). Human embryonic stem cell models of Huntington disease. Reprod Biomed Online *19*, 106-113.

Nishimura, E.K., Jordan, S.A., Oshima, H., Yoshida, H., Osawa, M., Moriyama, M., Jackson, I.J., Barrandon, Y., Miyachi, Y., and Nishikawa, S.-i. (2002). Dominant role of the niche in melanocyte stem-cell fate determination. Nature *416*, 854-860.

Nissan, X., Larribere, L., Saidani, M., Hurbain, I., Delevoye, C., Feteira, J., Lemaitre, G., Peschanski, M., and Baldeschi, C. (2011). Functional melanocytes derived from human pluripotent stem cells engraft into pluristratified epidermis. Proceedings of the National Academy of Sciences of the United States of America *108*, 14861-14866.

NIU, M.C. (1947). The axial organization of the neural crest, studied with particular reference to its pigmentary component. J Exp Zool *105*, 79-113.

Nordlund, J.J. (2007). The melanocyte and the epidermal melanin unit: an expanded concept. Dermatologic Clinics *25*, 271-281, vii.

O'Brien, E.K., d'Alençon, C., Bonde, G., Li, W., Schoenebeck, J., Allende, M.L., Gelb, B.D., Yelon, D., Eisen, J.S., and Cornell, R.A. (2004). Transcription factor Ap-2alpha is necessary for development of embryonic melanophores, autonomic neurons and pharyngeal skeleton in zebrafish. Developmental biology *265*, 246-261.

O'Rahilly, R., and Müller, F. (2007). The development of the neural crest in the human. J Anat *211*, 335-351.

Oh, J., Liu, Z.X., Feng, G.H., Raposo, G., and Spritz, R.A. (2000). The Hermansky-Pudlak syndrome (HPS) protein is part of a high molecular weight complex involved in biogenesis of early melanosomes. Hum Mol Genet *9*, 375-385.

Okita, K., Ichisaka, T., and Yamanaka, S. (2007). Generation of germline-competent induced pluripotent stem cells. Nature *448*, 313-317.

Okita, K., Nakagawa, M., Hyenjong, H., Ichisaka, T., and Yamanaka, S. (2008). Generation of mouse induced pluripotent stem cells without viral vectors. Science *322*, 949-953.

Opdecamp, K., Nakayama, A., Nguyen, M.T., Hodgkinson, C.A., Pavan, W.J., and Arnheiter, H. (1997). Melanocyte development in vivo and in neural crest cell cultures: crucial dependence on the Mitf basic-helix-loop-helix-zipper transcription factor. Development *124*, 2377-2386.

Osawa, M., Egawa, G., Mak, S.-S., Moriyama, M., Freter, R., Yonetani, S., Beermann, F., and Nishikawa, S.-I. (2005). Molecular characterization of melanocyte stem cells in their niche. Development *132*, 5589-5599.

Otto, A., Schmidt, C., and Patel, K. (2006). Pax3 and Pax7 expression and regulation in the avian embryo. Anat Embryol *211*, 293-310.

Padgett, G.A., Reiquam, C.W., Gorham, J.R., Henson, J.B., and O'Mary, C.C. (1967). Comparative studies of the Chediak-Higashi syndrome. Am J Pathol *51*, 553-571.

Papanayotou, C., Mey, A., Birot, A.-M., Saka, Y., Boast, S., Smith, J.C., Samarut, J., and Stern, C.D. (2008). A mechanism regulating the onset of Sox2 expression in the embryonic neural plate. PLoS Biol *6*, e2.

Papapetrou, E.P., Lee, G., Malani, N., Setty, M., Riviere, I., Tirunagari, L.M.S., Kadota, K., Roth, S.L., Giardina, P., Viale, A.*, et al.* (2011). Genomic safe harbors permit high β-globin transgene expression in thalassemia induced pluripotent stem cells. Nat Biotechnol *29*, 73-78.

Park, G.T., and Morasso, M.I. (2002). Bone morphogenetic protein-2 (BMP-2) transactivates Dlx3 through Smad1 and Smad4: alternative mode for Dlx3 induction in mouse keratinocytes. Nucleic Acids Res *30*, 515-522.

Park, I., Arora, N., Huo, H., Maherali, N., Ahfeldt, T., Shimamura, A., Lensch, M., Cowan, C., Hochedlinger, K., and Daley, G. (2008a). Disease-Specific Induced Pluripotent Stem Cells. Cell.

Park, I., Lerou, P., Zhao, R., Huo, H., and Daley, G. (2008b). Generation of human-induced pluripotent stem cells. Nat Protoc *3*, 1180-1186.

Park, I.-H., Zhao, R., West, J.A., Yabuuchi, A., Huo, H., Ince, T.A., Lerou, P.H., Lensch, M.W., and Daley, G.Q. (2008c). Reprogramming of human somatic cells to pluripotency with defined factors. Nature *451*, 141-146.

Pastural, E., Barrat, F.J., Dufourcq-Lagelouse, R., Certain, S., Sanal, O., Jabado, N., Seger, R., Griscelli, C., Fischer, A., and de Saint Basile, G. (1997). Griscelli disease maps to chromosome 15q21 and is associated with mutations in the myosin-Va gene. Nature Genetics *16*, 289-292.

Patthey, C., Gunhaga, L., and Edlund, T. (2008). Early development of the central and peripheral nervous systems is coordinated by Wnt and BMP signals. PLoS ONE *3*, e1625.

Pickering, S.J., Minger, S.L., Patel, M., Taylor, H., Black, C., Burns, C.J., Ekonomou, A., and Braude, P.R. (2005). Generation of a human embryonic stem cell line encoding the cystic fibrosis mutation deltaF508, using preimplantation genetic diagnosis. Reprod Biomed Online *10*, 390-397.

Pingault, V., Bondurand, N., Kuhlbrodt, K., Goerich, D.E., Préhu, M.O., Puliti, A., Herbarth, B., Hermans-Borgmeyer, I., Legius, E., Matthijs, G.*, et al.* (1998). SOX10 mutations in patients with Waardenburg-Hirschsprung disease. Nature Genetics *18*, 171-173.

Pla, P., Solov'eva, O., Moore, R., Alberti, C., Kunisada, T., and Larue, L. (2004). Dct::lacZ ES cells: a novel cellular model to study melanocyte determination and differentiation. Pigment Cell Res *17*, 142-149.

Placantonakis, D.G., Tomishima, M.J., Lafaille, F., Desbordes, S.C., Jia, F., Socci, N.D., Viale, A., Lee, H., Harrison, N., Tabar, V.*, et al.* (2009). BAC transgenesis in human embryonic stem cells as a novel tool to define the human neural lineage. Stem Cells *27*, 521-532.

Planque, N., Raposo, G., Leconte, L., Anezo, O., Martin, P., and Saule, S. (2004). Microphthalmia transcription factor induces both retinal pigmented epithelium and neural crest melanocytes from neuroretina cells. The Journal of biological chemistry *279*, 41911-41917.

Pomp, O., Brokhman, I., Ben-Dor, I., Reubinoff, B., and Goldstein, R.S. (2005). Generation of peripheral sensory and sympathetic neurons and neural crest cells from human embryonic stem cells. Stem Cells *23*, 923-930.

Potterf, S.B., Furumura, M., Dunn, K.J., Arnheiter, H., and Pavan, W.J. (2000). Transcription factor hierarchy in Waardenburg syndrome: regulation of MITF expression by SOX10 and PAX3. Hum Genet *107*, 1-6.

Potterf, S.B., Mollaaghababa, R., Hou, L., Southard-Smith, E.M., Hornyak, T.J., Arnheiter, H., and Pavan, W.J. (2001). Analysis of SOX10 function in neural crest-derived melanocyte development: SOX10-dependent transcriptional control of dopachrome tautomerase. Dev Biol *237*, 245-257.

Rambhatla, L., Chiu, C.-P., Kundu, P., Peng, Y., and Carpenter, M.K. (2003). Generation of hepatocyte-like cells from human embryonic stem cells. Cell Transplant *12*, 1-11.

Raposo, G., and Marks, M.S. (2007). Melanosomes--dark organelles enlighten endosomal membrane transport. Nat Rev Mol Cell Biol *8*, 786-797.

Rashid, S.T., Corbineau, S., Hannan, N., Marciniak, S.J., Miranda, E., Alexander, G., Huang-Doran, I., Griffin, J., Ahrlund-Richter, L., Skepper, J.*, et al.* (2010). Modeling inherited metabolic disorders of the liver using human induced pluripotent stem cells. J Clin Invest *120*, 3127-3136.

Raya, A., Rodríguez-Pizà, I., Guenechea, G., Vassena, R., Navarro, S., Barrero, M., Consiglio, A., Castellà, M., Río, P., Sleep, E.*, et al.* (2009). Disease-corrected haematopoietic progenitors from Fanconi anaemia induced pluripotent stem cells. Nature.

Reedy, M.V., Faraco, C.D., and Erickson, C.A. (1998). The delayed entry of thoracic neural crest cells into the dorsolateral path is a consequence of the late emigration of melanogenic neural crest cells from the neural tube. Dev Biol *200*, 234-246.

Reid, K., Nishikawa, S., Bartlett, P.F., and Murphy, M. (1995). Steel factor directs melanocyte development in vitro through selective regulation of the number of c-kit+ progenitors. Dev Biol *169*, 568-579.

Reid, K., Turnley, A.M., Maxwell, G.D., Kurihara, Y., Kurihara, H., Bartlett, P.F., and Murphy, M. (1996). Multiple roles for endothelin in melanocyte development: regulation of progenitor number and stimulation of differentiation. Development *122*, 3911-3919.

Richmond, B., Huizing, M., Knapp, J., Koshoffer, A., Zhao, Y., Gahl, W.A., and Boissy, R.E. (2005). Melanocytes derived from patients with Hermansky-Pudlak Syndrome types 1, 2, and 3 have distinct defects in cargo trafficking. J Invest Dermatol *124*, 420-427.

Ring, D.B., Johnson, K.W., Henriksen, E.J., Nuss, J.M., Goff, D., Kinnick, T.R., Ma, S.T., Reeder, J.W., Samuels, I., Slabiak, T.*, et al.* (2003). Selective glycogen synthase kinase 3 inhibitors potentiate insulin activation of glucose transport and utilization in vitro and in vivo. Diabetes *52*, 588-595.

Ringholm, A., Klovins, J., Rudzish, R., Phillips, S., Rees, J.L., and Schiöth, H.B. (2004). Pharmacological characterization of loss of function mutations of the human melanocortin 1 receptor that are associated with red hair. J Invest Dermatol *123*, 917-923.

Saint-Jeannet, J.P., He, X., Varmus, H.E., and Dawid, I.B. (1997). Regulation of dorsal fate in the neuraxis by Wnt-1 and Wnt-3a. Proc Natl Acad Sci USA *94*, 13713-13718.

Saito, H., Yasumoto, K.-I., Takeda, K., Takahashi, K., Fukuzaki, A., Orikasa, S., and Shibahara, S. (2002). Melanocyte-specific microphthalmia-associated transcription factor isoform activates its own gene promoter through physical interaction with lymphoid-enhancing factor 1. The Journal of biological chemistry *277*, 28787-28794.

Sánchez-Martín, M., Pérez-Losada, J., Rodríguez-García, A., González-Sánchez, B., Korf, B.R., Kuster, W., Moss, C., Spritz, R.A., and Sánchez-García, I. (2003). Deletion of the SLUG (SNAI2) gene results in human piebaldism. Am J Med Genet A *122A*, 125-132.

Santagati, F., and Rijli, F.M. (2003). Cranial neural crest and the building of the vertebrate head. Nat Rev Neurosci *4*, 806-818.

Santiago, A., and Erickson, C.A. (2002). Ephrin-B ligands play a dual role in the control of neural crest cell migration. Development *129*, 3621-3632.

Sarangarajan, R., Budev, A., Zhao, Y., Gahl, W.A., and Boissy, R.E. (2001). Abnormal translocation of tyrosinase and tyrosinase-related protein 1 in cutaneous melanocytes of Hermansky-Pudlak Syndrome and in melanoma cells transfected with anti-sense HPS1 cDNA. J Invest Dermatol *117*, 641-646.

Sasai, N., Mizuseki, K., and Sasai, Y. (2001). Requirement of FoxD3-class signaling for neural crest determination in Xenopus. Development *128*, 2525-2536.

Sato, T., Sasai, N., and Sasai, Y. (2005). Neural crest determination by co-activation of Pax3 and Zic1 genes in Xenopus ectoderm. Development *132*, 2355-2363.

Sato-Jin, K., Nishimura, E.K., Akasaka, E., Huber, W., Nakano, H., Miller, A., Du, J., Wu, M., Hanada, K., Sawamura, D.*, et al.* (2008). Epistatic connections between microphthalmia-associated transcription factor and endothelin signaling in Waardenburg syndrome and other pigmentary disorders. FASEB J *22*, 1155-1168.

Sauka-Spengler, T., and Bronner-Fraser, M. (2008). A gene regulatory network orchestrates neural crest formation. Nat Rev Mol Cell Biol *9*, 557-568.

Schmid, B., Fürthauer, M., Connors, S.A., Trout, J., Thisse, B., Thisse, C., and Mullins, M.C. (2000). Equivalent genetic roles for bmp7/snailhouse and bmp2b/swirl in dorsoventral pattern formation. Development *127*, 957-967.

Seiberg, M., Paine, C., Sharlow, E., Andrade-Gordon, P., Costanzo, M., Eisinger, M., and Shapiro, S.S. (2000). The protease-activated receptor 2 regulates pigmentation via keratinocyte-melanocyte interactions. Exp Cell Res *254*, 25-32.

Selleck, M.A., and Bronner-Fraser, M. (1996). The genesis of avian neural crest cells: a classic embryonic induction. Proceedings of the National Academy of Sciences of the United States of America *93*, 9352-9357.

Selleck, M.A., García-Castro, M.I., Artinger, K.B., and Bronner-Fraser, M. (1998). Effects of Shh and Noggin on neural crest formation demonstrate that BMP is required in the neural tube but not ectoderm. Development *125*, 4919-4930.

Serbedzija, G.N., Bronner-Fraser, M., and Fraser, S.E. (1989). A vital dye analysis of the timing and pathways of avian trunk neural crest cell migration. Development *106*, 809-816.

Serbedzija, G.N., Fraser, S.E., and Bronner-Fraser, M. (1990). Pathways of trunk neural crest cell migration in the mouse embryo as revealed by vital dye labelling. Development *108*, 605-612.

Setty, S.R.G., Tenza, D., Truschel, S.T., Chou, E., Sviderskaya, E.V., Theos, A.C., Lamoreux, M.L., Di Pietro, S.M., Starcevic, M., Bennett, D.C.*, et al.* (2007). BLOC-1 is required for cargo-specific sorting from vacuolar early endosomes toward lysosome-related organelles. Mol Biol Cell *18*, 768-780.

Shin, M.K., Levorse, J.M., Ingram, R.S., and Tilghman, S.M. (1999). The temporal requirement for endothelin receptor-B signalling during neural crest development. Nature *402*, 496-501.

Shotelersuk, V., Dell'Angelica, E.C., Hartnell, L., Bonifacino, J.S., and Gahl, W.A. (2000). A new variant of Hermansky-Pudlak syndrome due to mutations in a gene responsible for vesicle formation. Am J Med *108*, 423-427.

Sieber-Blum, M. (1989). Commitment of neural crest cells to the sensory neuron lineage. Science *243*, 1608-1611.

Sieber-Blum, M., and Cohen, A.M. (1980). Clonal analysis of quail neural crest cells: they are pluripotent and differentiate in vitro in the absence of noncrest cells. Developmental biology *80*, 96-106.

Sieber-Blum, M., Grim, M., Hu, Y.F., and Szeder, V. (2004). Pluripotent neural crest stem cells in the adult hair follicle. Dev Dyn *231*, 258-269.

Sieber-Blum, M., and Hu, Y. (2008). Epidermal neural crest stem cells (EPI-NCSC) and pluripotency. Stem cell reviews *4*, 256-260.

Slominski, A., and Paus, R. (1993). Melanogenesis is coupled to murine anagen: toward new concepts for the role of melanocytes and the regulation of melanogenesis in hair growth. J Invest Dermatol *101*, 90S-97S.

Slominski, A., Tobin, D.J., Shibahara, S., and Wortsman, J. (2004). Melanin pigmentation in mammalian skin and its hormonal regulation. Physiol Rev *84*, 1155-1228.

Smith, J.W., Koshoffer, A., Morris, R.E., and Boissy, R.E. (2005). Membranous complexes characteristic of melanocytes derived from patients with Hermansky-Pudlak syndrome type 1 are macroautophagosomal entities of the lysosomal compartment. Pigment Cell Res *18*, 417-426.

Soldner, F., Hockemeyer, D., Beard, C., Gao, Q., Bell, G.W., Cook, E.G., Hargus, G., Blak, A., Cooper, O., Mitalipova, M.*, et al.* (2009). Parkinson's disease patient-derived induced pluripotent stem cells free of viral reprogramming factors. Cell *136*, 964-977.

Sonnenberg-Riethmacher, E., Miehe, M., Stolt, C.C., Goerich, D.E., Wegner, M., and Riethmacher, D. (2001). Development and degeneration of dorsal root ganglia in the absence of the HMG-domain transcription factor Sox10. Mech Dev *109*, 253-265.

Soo, K., O'Rourke, M.P., Khoo, P.-L., Steiner, K.A., Wong, N., Behringer, R.R., and Tam, P.P.L. (2002). Twist function is required for the morphogenesis of the cephalic neural tube and the differentiation of the cranial neural crest cells in the mouse embryo. Developmental biology *247*, 251-270.

Sottile, V., Thomson, A., and McWhir, J. (2003). In vitro osteogenic differentiation of human ES cells. Cloning Stem Cells *5*, 149-155.

Southard-Smith, E.M., Kos, L., and Pavan, W.J. (1998). Sox10 mutation disrupts neural crest development in Dom Hirschsprung mouse model. Nature Genetics *18*, 60-64.

Spritz, R.A., Chiang, P.W., Oiso, N., and Alkhateeb, A. (2003). Human and mouse disorders of pigmentation. Curr Opin Genet Dev *13*, 284-289.

Steel, K.P., Davidson, D.R., and Jackson, I.J. (1992). TRP-2/DT, a new early melanoblast marker, shows that steel growth factor (c-kit ligand) is a survival factor. Development *115*, 1111-1119.

Steingrímsson, E., Copeland, N.G., and Jenkins, N.A. (2004). Melanocytes and the microphthalmia transcription factor network. Annu Rev Genet *38*, 365-411.

Steventon, B., Araya, C., Linker, C., Kuriyama, S., and Mayor, R. (2009). Differential requirements of BMP and Wnt signalling during gastrulation and neurulation define two steps in neural crest induction. Development *136*, 771-779.

Steventon, B., and Mayor, R. (2012). Early neural crest induction requires an initial inhibition of Wnt signals. Developmental biology.

Stuhlmiller, T.J., and García-Castro, M.I. (2012). Current perspectives of the signaling pathways directing neural crest induction. Cell Mol Life Sci *69*, 3715-3737.

Sung, J.H., Meyers, J.P., Stadlan, E.M., Cowen, D., and Wolf, A. (1969). Neuropathological changes in Chédiak-Higashi disease. J Neuropathol Exp Neurol *28*, 86-118.

Suzuki, A., Ueno, N., and Hemmati-Brivanlou, A. (1997). Xenopus msx1 mediates epidermal induction and neural inhibition by BMP4. Development *124*, 3037-3044.

Svensson, P.J., Von Tell, D., Molander, M.L., Anvret, M., and Nordenskjöld, A. (1999). A heterozygous frameshift mutation in the endothelin-3 (EDN-3) gene in isolated Hirschsprung's disease. Pediatr Res *45*, 714-717.

Swank, R.T., Novak, E.K., McGarry, M.P., Rusiniak, M.E., and Feng, L. (1998). Mouse models of Hermansky Pudlak syndrome: a review. Pigment Cell Res *11*, 60-80.

Tachibana, M., Takeda, K., Nobukuni, Y., Urabe, K., Long, J.E., Meyers, K.A., Aaronson, S.A., and Miki, T. (1996). Ectopic expression of MITF, a gene for Waardenburg syndrome type 2, converts fibroblasts to cells with melanocyte characteristics. Nature Genetics *14*, 50-54.

Takada, S., Stark, K.L., Shea, M.J., Vassileva, G., McMahon, J.A., and McMahon, A.P. (1994). Wnt-3a regulates somite and tailbud formation in the mouse embryo. Genes Dev *8*, 174-189.

Takahashi, K., Tanabe, K., Ohnuki, M., Narita, M., Ichisaka, T., Tomoda, K., and Yamanaka, S. (2007). Induction of pluripotent stem cells from adult human fibroblasts by defined factors. Cell *131*, 861-872.

Takahashi, K., and Yamanaka, S. (2006). Induction of pluripotent stem cells from mouse embryonic and adult fibroblast cultures by defined factors. Cell *126*, 663-676.

Takeda, K., Yasumoto, K., Takada, R., Takada, S., Watanabe, K., Udono, T., Saito, H., Takahashi, K., and Shibahara, S. (2000). Induction of melanocyte-specific microphthalmia-associated transcription factor by Wnt-3a. J Biol Chem *275*, 14013-14016.

Takemoto, C.M., Yoon, Y.-J., and Fisher, D.E. (2002). The identification and functional characterization of a novel mast cell isoform of the microphthalmia-associated transcription factor. The Journal of biological chemistry *277*, 30244-30252.

Tassabehji, M., Read, A.P., Newton, V.E., Harris, R., Balling, R., Gruss, P., and Strachan, T. (1992). Waardenburg's syndrome patients have mutations in the human homologue of the Pax-3 paired box gene. Nature *355*, 635-636.

Teillet, M.A., and Le Douarin, N. (1970). [The migration of pigmentary cells studies by the method of heterospecific grafts of neural tube in bird embryo]. CR Hebd Seances Acad Sci, Ser D, Sci Nat *270*, 3095-3098.

Tesar, P.J., Chenoweth, J.G., Brook, F.A., Davies, T.J., Evans, E.P., Mack, D.L., Gardner, R.L., and McKay, R.D.G. (2007). New cell lines from mouse epiblast share defining features with human embryonic stem cells. Nature *448*, 196-199.

Theos, A.C., Berson, J.F., Theos, S.C., Herman, K.E., Harper, D.C., Tenza, D., Sviderskaya, E.V., Lamoreux, M.L., Bennett, D.C., Raposo, G.*, et al.* (2006). Dual loss of ER export and endocytic signals with altered melanosome morphology in the silver mutation of Pmel17. Mol Biol Cell *17*, 3598-3612.

Theos, A.C., Tenza, D., Martina, J.A., Hurbain, I., Peden, A.A., Sviderskaya, E.V., Stewart, A., Robinson, M.S., Bennett, D.C., Cutler, D.F.*, et al.* (2005). Functions of adaptor protein (AP)-3 and AP-1 in tyrosinase sorting from endosomes to melanosomes. Mol Biol Cell *16*, 5356-5372.

Thiery, J.P., Duband, J.L., and Delouvée, A. (1982). Pathways and mechanisms of avian trunk neural crest cell migration and localization. Developmental biology *93*, 324-343.

Thomas, A.J., and Erickson, C.A. (2008). The making of a melanocyte: the specification of melanoblasts from the neural crest. Pigment cell & melanoma research *21*, 598-610.

Thomas, A.J., and Erickson, C.A. (2009). FOXD3 regulates the lineage switch between neural crest-derived glial cells and pigment cells by repressing MITF through a non-canonical mechanism. Development *136*, 1849-1858.

Thomas, S., Thomas, M., Wincker, P., Babarit, C., Xu, P., Speer, M.C., Munnich, A., Lyonnet, S., Vekemans, M., and Etchevers, H.C. (2008). Human neural crest cells display molecular and phenotypic hallmarks of stem cells. Hum Mol Genet *17*, 3411-3425.

Thomson, J.A., Itskovitz-Eldor, J., Shapiro, S.S., Waknitz, M.A., Swiergiel, J.J., Marshall, V.S., and Jones, J.M. (1998). Embryonic stem cell lines derived from human blastocysts. Science *282*, 1145-1147.

Toma, J.G., Akhavan, M., Fernandes, K.J., Barnabé-Heider, F., Sadikot, A., Kaplan, D.R., and Miller, F.D. (2001). Isolation of multipotent adult stem cells from the dermis of mammalian skin. Nat Cell Biol *3*, 778-784.

Toma, J.G., McKenzie, I.A., Bagli, D., and Miller, F.D. (2005). Isolation and characterization of multipotent skin-derived precursors from human skin. Stem Cells *23*, 727-737.

Toro, J., Turner, M., and Gahl, W.A. (1999). Dermatologic manifestations of Hermansky-Pudlak syndrome in patients with and without a 16-base pair duplication in the HPS1 gene. Arch Dermatol *135*, 774-780.

Tosney, K.W. (1978). The early migration of neural crest cells in the trunk region of the avian embryo: an electron microscopic study. Developmental biology *62*, 317-333.

Tribulo, C., Aybar, M.J., Nguyen, V.H., Mullins, M.C., and Mayor, R. (2003). Regulation of Msx genes by a Bmp gradient is essential for neural crest specification. Development *130*, 6441-6452.

Tríbulo, C., Aybar, M.J., Sánchez, S.S., and Mayor, R. (2004). A balance between the anti-apoptotic activity of Slug and the apoptotic activity of msx1 is required for the proper development of the neural crest. Developmental biology *275*, 325-342.

Unternaehrer, J.J., and Daley, G.Q. (2011). Induced pluripotent stem cells for modelling human diseases. Philos Trans R Soc Lond, B, Biol Sci *366*, 2274-2285.

Urbach, A., Schuldiner, M., and Benvenisty, N. (2004). Modeling for Lesch-Nyhan disease by gene targeting in human embryonic stem cells. Stem Cells *22*, 635-641.

Valenzuela, R., and Morningstar, W.A. (1981). The ocular pigmentary disturbance of human Chédiak-Higashi syndrome. A comparative light- and electron-microscopic study and review of the literature. Am J Clin Pathol *75*, 591-596.

Van Den Bossche, K., Naeyaert, J.-M., and Lambert, J. (2006). The quest for the mechanism of melanin transfer. Traffic *7*, 769-778.

Van Gele, M., Dynoodt, P., and Lambert, J. (2009). Griscelli syndrome: a model system to study vesicular trafficking. Pigment Cell Melanoma Res *22*, 268-282.

Veeman, M.T., Slusarski, D.C., Kaykas, A., Louie, S.H., and Moon, R.T. (2003). Zebrafish prickle, a modulator of noncanonical Wnt/Fz signaling, regulates gastrulation movements. Curr Biol *13*, 680-685.

Vega, S., Morales, A.V., Ocaña, O.H., Valdés, F., Fabregat, I., and Nieto, M.A. (2004). Snail blocks the cell cycle and confers resistance to cell death. Genes Dev *18*, 1131-1143.

Verlinsky, Y., Strelchenko, N., Kukharenko, V., Rechitsky, S., Verlinsky, O., Galat, V., and Kuliev, A. (2005). Human embryonic stem cell lines with genetic disorders. Reprod Biomed Online *10*, 105-110.

Villanueva, S., Glavic, A., Ruiz, P., and Mayor, R. (2002). Posteriorization by FGF, Wnt, and retinoic acid is required for neural crest induction. Dev Biol *241*, 289-301.

Waddington, C.H. (1957). The strategy of the genes; a discussion of some aspects of theoretical biology. (New York, Macmillan).

Wakamatsu, Y., Endo, Y., Osumi, N., and Weston, J.A. (2004). Multiple roles of Sox2, an HMG-box transcription factor in avian neural crest development. Dev Dyn *229*, 74-86.

Wakamatsu, Y., Mochii, M., Vogel, K.S., and Weston, J.A. (1998). Avian neural crest-derived neurogenic precursors undergo apoptosis on the lateral migration pathway. Development *125*, 4205-4213.

Wang, S., Bates, J., Li, X., Schanz, S., Chandler-Militello, D., Levine, C., Maherali, N., Studer, L., Hochedlinger, K., Windrem, M.*, et al.* (2013). Human iPSC-Derived Oligodendrocyte Progenitor Cells Can Myelinate and Rescue a Mouse Model of Congenital Hypomyelination. Cell Stem Cell *12*, 252-264.

Warren, L., Manos, P.D., Ahfeldt, T., Loh, Y.-H., Li, H., Lau, F., Ebina, W., Mandal, P.K., Smith, Z.D., Meissner, A.*, et al.* (2010). Highly efficient reprogramming to pluripotency and directed differentiation of human cells with synthetic modified mRNA. Cell stem cell *7*, 618-630.

Wawersik, S., Evola, C., and Whitman, M. (2005). Conditional BMP inhibition in Xenopus reveals stage-specific roles for BMPs in neural and neural crest induction. Dev Biol *277*, 425-442.

Wehrle-Haller, B., and Weston, J.A. (1995). Soluble and cell-bound forms of steel factor activity play distinct roles in melanocyte precursor dispersal and survival on the lateral neural crest migration pathway. Development *121*, 731-742.

Wei, M.L. (2006). Hermansky-Pudlak syndrome: a disease of protein trafficking and organelle function. Pigment Cell Res *19*, 19-42.

Weidinger, G., Thorpe, C.J., Wuennenberg-Stapleton, K., Ngai, J., and Moon, R.T. (2005). The Sp1-related transcription factors sp5 and sp5-like act downstream of Wnt/beta-catenin signaling in mesoderm and neuroectoderm patterning. Curr Biol *15*, 489-500.

Wen-Jun, L., Hai-Yan, W., Wei, L., Ke-Yu, W., and Rui-Ming, W. (2008). Evidence that geniposide abrogates norepinephrine-induced hypopigmentation by the activation of GLP-1R-dependent c-kit receptor signaling in melanocyte. J Ethnopharmacol *118*, 154-158.

Wernig, M., Meissner, A., Foreman, R., Brambrink, T., Ku, M., Hochedlinger, K., Bernstein, B.E., and Jaenisch, R. (2007). In vitro reprogramming of fibroblasts into a pluripotent ES-cell-like state. Nature *448*, 318-324.

Westbroek, W., Adams, D., Huizing, M., Koshoffer, A., Dorward, H., Tinloy, B., Parkes, J., Helip-Wooley, A., Kleta, R., Tsilou, E.*, et al.* (2007). Cellular defects in Chediak-Higashi syndrome correlate with the molecular genotype and clinical phenotype. J Invest Dermatol *127*, 2674-2677.

Weston, J.A. (1991). Sequential segregation and fate of developmentally restricted intermediate cell populations in the neural crest lineage. Curr Top Dev Biol *25*, 133-153.

White, R.M., and Zon, L.I. (2008). Melanocytes in development, regeneration, and cancer. Cell stem cell *3*, 242-252.

Widlund, H.R., Horstmann, M.A., Price, E.R., Cui, J., Lessnick, S.L., Wu, M., He, X., and Fisher, D.E. (2002). Beta-catenin-induced melanoma growth requires the downstream target Microphthalmia-associated transcription factor. The Journal of Cell Biology *158*, 1079-1087.

Wiggan, O.N., Fadel, M.P., and Hamel, P.A. (2002). Pax3 induces cell aggregation and regulates phenotypic mesenchymal-epithelial interconversion. J Cell Sci *115*, 517-529.

Williams, D.E., de Vries, P., Namen, A.E., Widmer, M.B., and Lyman, S.D. (1992). The Steel factor. Developmental biology *151*, 368-376.

Willot, V., Mathieu, J., Lu, Y., Schmid, B., Sidi, S., Yan, Y.-L., Postlethwait, J.H., Mullins, M., Rosa, F., and Peyriéras, N. (2002). Cooperative action of ADMP- and BMP-mediated pathways in regulating cell fates in the zebrafish gastrula. Developmental biology *241*, 59-78.

Woda, J.M., Pastagia, J., Mercola, M., and Artinger, K.B. (2003). Dlx proteins position the neural plate border and determine adjacent cell fates. Development *130*, 331-342.

Woltjen, K., Michael, I., Mohseni, P., Desai, R., Mileikovsky, M., Hämäläinen, R., Cowling, R., Wang, W., Liu, P., Gertsenstein, M.*, et al.* (2009). piggyBac transposition reprograms fibroblasts to induced pluripotent stem cells. Nature.

Wong, C.E., Paratore, C., Dours-Zimmermann, M.T., Rochat, A., Pietri, T., Suter, U., Zimmermann, D.R., Dufour, S., Thiery, J.P., Meijer, D.*, et al.* (2006). Neural crest-derived cells with stem cell features can be traced back to multiple lineages in the adult skin. The Journal of Cell Biology *175*, 1005-1015.

Wu, J., Yang, J., and Klein, P.S. (2005). Neural crest induction by the canonical Wnt pathway can be dissociated from anterior-posterior neural patterning in Xenopus. Dev Biol *279*, 220-232.

Wu, X., Bowers, B., Wei, Q., Kocher, B., and Hammer, J.A. (1997). Myosin V associates with melanosomes in mouse melanocytes: evidence that myosin V is an organelle motor. J Cell Sci *110 (Pt 7)*, 847-859.

Wu, X., Rao, K., Bowers, M.B., Copeland, N.G., Jenkins, N.A., and Hammer, J.A. (2001). Rab27a enables myosin Va-dependent melanosome capture by recruiting the myosin to the organelle. J Cell Sci *114*, 1091-1100.

Wu, X.S., Masedunskas, A., Weigert, R., Copeland, N.G., Jenkins, N.A., and Hammer, J.A. (2012). Melanoregulin regulates a shedding mechanism that drives melanosome transfer from melanocytes to keratinocytes. Proceedings of the National Academy of Sciences of the United States of America *109*, E2101-2109.

Xiong, C., Xie, C.-Q., Zhang, L., Zhang, J., Xu, K., Fu, M., Thompson, W.E., Yang, L.-J., and Chen, Y.E. (2005). Derivation of adipocytes from human embryonic stem cells. Stem cells and development *14*, 671-675.

Xu, C., Police, S., Rao, N., and Carpenter, M.K. (2002a). Characterization and enrichment of cardiomyocytes derived from human embryonic stem cells. Circ Res *91*, 501-508.

Xu, J., Lamouille, S., and Derynck, R. (2009). TGF-beta-induced epithelial to mesenchymal transition. Cell Res *19*, 156-172.

Xu, R.-H., Chen, X., Li, D.S., Li, R., Addicks, G.C., Glennon, C., Zwaka, T.P., and Thomson, J.A. (2002b). BMP4 initiates human embryonic stem cell differentiation to trophoblast. Nature biotechnology *20*, 1261-1264.

Yamane, T., Hayashi, S., and Kunisada, T. (2002). Embryonic stem cells as a model for studying melanocyte development. Methods Mol Biol *185*, 261-268.

Yamane, T., Hayashi, S., Mizoguchi, M., Yamazaki, H., and Kunisada, T. (1999). Derivation of melanocytes from embryonic stem cells in culture. Dev Dyn *216*, 450-458.

Yang, G., Li, Y., Nishimura, E.K., Xin, H., Zhou, A., Guo, Y., Dong, L., Denning, M.F., Nickoloff, B.J., and Cui, R. (2008). Inhibition of PAX3 by TGF-beta modulates melanocyte viability. Mol Cell *32*, 554-563.

Yasumoto, K.-I., Takeda, K., Saito, H., Watanabe, K.-I., Takahashi, K., and Shibahara, S. (2002). Microphthalmia-associated transcription factor interacts with LEF-1, a mediator of Wnt signaling. EMBO J *21*, 2703-2714.

Ye, L., Chang, J., Lin, C., Sun, X., Yu, J., and Kan, Y. (2009). Induced pluripotent stem cells offer new approach to therapy in thalassemia and sickle cell anemia and option in prenatal diagnosis in genetic diseases. Proc Natl Acad Sci USA.

Yoshida, H., Kunisada, T., Grimm, T., Nishimura, E.K., Nishioka, E., and Nishikawa, S.I. (2001). Review: melanocyte migration and survival controlled by SCF/c-kit expression. J Investig Dermatol Symp Proc *6*, 1-5.

Yoshida, H., Kunisada, T., Kusakabe, M., Nishikawa, S., and Nishikawa, S.I. (1996). Distinct stages of melanocyte differentiation revealed by anlaysis of nonuniform pigmentation patterns. Development *122*, 1207-1214.

Yu, J., Vodyanik, M.A., Smuga-Otto, K., Antosiewicz-Bourget, J., Frane, J.L., Tian, S., Nie, J., Jonsdottir, G.A., Ruotti, V., Stewart, R.*, et al.* (2007). Induced pluripotent stem cell lines derived from human somatic cells. Science *318*, 1917-1920.

Zhang, Q., Zhao, B., Li, W., Oiso, N., Novak, E.K., Rusiniak, M.E., Gautam, R., Chintala, S., O'Brien, E.P., Zhang, Y.*, et al.* (2003). Ru2 and Ru encode mouse orthologs of the genes mutated in human Hermansky-Pudlak syndrome types 5 and 6. Nature Genetics *33*, 145-153.

Zhao, H., Boissy, Y.L., Abdel-Malek, Z., King, R.A., Nordlund, J.J., and Boissy, R.E. (1994). On the analysis of the pathophysiology of Chediak-Higashi syndrome. Defects expressed by cultured melanocytes. Lab Invest *71*, 25-34.

Zhao, X., Li, W., Lv, Z., Liu, L., Tong, M., Hai, T., Hao, J., Guo, C., Ma, Q., Wang, L.*, et al.* (2009). iPS cells produce viable mice through tetraploid complementation. Nature.

Zhao, X.-Y., Lv, Z., Li, W., Zeng, F., and Zhou, Q. (2010). Production of mice using iPS cells and tetraploid complementation. Nat Protoc *5*, 963-971.

Zhou, H., Wu, S., Joo, J., Zhu, S., Han, D., Lin, T., Trauger, S., Bien, G., Yao, S., Zhu, Y.*, et al.* (2009). Generation of Induced Pluripotent Stem Cells Using Recombinant Proteins. Cell stem cell.

Zhou, Y., and Snead, M.L. (2008). Derivation of cranial neural crest-like cells from human embryonic stem cells. Biochem Biophys Res Commun *376*, 542-547.

Zwaka, T.P., and Thomson, J.A. (2003). Homologous recombination in human embryonic stem cells. Nature biotechnology *21*, 319-321.